Universitat de Girona

ABATEMENT OF SILOXANES IN SEWAGE BIOGAS:
COUPLING ADSORPTION AND BIOLOGICAL TREATMENTS

Eric Santos Clotas

Universitat de Girona

DOCTORAL THESIS

Abatement of siloxanes in sewage biogas: coupling adsorption and biological treatments

Eric Santos Clotas

2019

Universitat de Girona

DOCTORAL THESIS

Abatement of siloxanes in sewage biogas: coupling adsorption and biological treatments

Eric Santos Clotas

2019

Supervised by:

Dr. Maria J. Martin   Dr. Alba Cabrera Codony   Dr. Joaquim Comas Matas

Thesis submitted in fulfilment of the requirements for the degree of Doctor from the University of Girona

Doctoral Programme in Water Science and Technology

MARIA J. MARTIN SÁNCHEZ

Professora titular del Departament d'Enginyeria Química, Agrària i Tecnologia Agroalimentària de la Universitat de Girona i, Investigadora del grup de recerca Laboratori d'Enginyeria Química i Ambiental (LEQUIA).

ALBA CABRERA i CODONY

Professora associada del Departament d'Enginyeria Química, Agrària i Tecnologia Agroalimentària de la Universitat de Girona i, Investigadora post-doctoral del grup de recerca Laboratori d'Enginyeria Química i Ambiental (LEQUIA) de la Universitat de Girona.

JOAQUIM COMAS i MATAS

Professor titular del Departament d'Enginyeria Química, Agrària i Tecnologia Agroalimentària de la Universitat de Girona i, Investigador Sènior de l'Institut Català de Recerca de l'Aigua (ICRA).

Certifiquem:

Que el graduat en Ciències Ambientals Eric Santos Clotas ha dut a terme sota la nostra direcció el treball titulat *Abatement of siloxanes in sewage sludge: coupling adsorption and biological* treatments que es presenta en aquesta memòria, la qual constitueix la seva Tesi per optar al Grau de Doctor per la Universitat de Girona.

A Girona, 12 Juny de 2019

Dra. Maria J. Martin Sánchez   Dra. Alba Cabrera i Codony   Dr. Joaquim Comas i Matas

Acknowledgments

Tot aquest camí va començar un dia normal i corrent quan vaig rebre la trucada d'un número desconegut "Bon dia soc la Maria Martin, professora de la UdG". Després de 4 anys, finalment em trobo escrivint aquest "capítol" de la tesi, el que genera més expectativa. I no puc començar-lo d'altra manera que donant les gràcies a qui em va confiar tirar endavant amb la beca i no haver perdut la paciència durant aquest 4 anys, gràcies Maria. I també agrair a en Quim, per haver-me ajudat en tot el possible i co-dirigit aquesta tesi.

Aquest recorregut l'he compartit sencer, ja sigui presencialment o via Skype (gairebé 365 skypes), amb la última incorporació en la direcció d'aquesta tesi. Alba, gràcies per tot. Des dels moments cantant al laboratori, les estones mirant m/z en els cromatogrames, comprovar l'estat dels reactors abans de marxar (tú estás bien?), moments de coffee+piti, i un llarguíssim etcètera. De moment aquí no s'acaba, encara ens queda el congrés de la IWA!

Encara que durant el meu primer any de tesi estaves perdut per França, vas venir per aportar-me positivisme i el teu suport tècnic en els salts de secció, encapçalaments i peus de pàgina d'aquesta tesi. Va no, també pels dinars, sopars, cafès i birres, gràcies per escoltar-me i pels teus consells, gràcies Hèctor. No me n'oblido dels que sempre heu estat a prop durant aquest camí. Per quan entres al despatx i em desconcentres, gràcies per això i pel (pocs) runnings, Kudos for Sebas. Alexandra, gràcies per sempre escoltar-me i tirar-me flors sempre, per les converses sobre GOT, entre d'altres series, i per aportar la teva bogeria al despatx, blessed be the fruit. Natasa, my sunshine, you're such an amazing person, it was so great to have you here. You left a massive mark not only in Girona but also in Lloret. Also, to Igor, thank you for all the moments shared here and for being such a wonderful host in Ljubljana.

Gràcies també a tot l'Equip LEQUIA que he conegut durant aquests 4 anys: Suquet, Galizia, Anfruns, Ramiro, Gaetan, Teresa, Laura, Pau, Tico, Narcís, Elena, Anna, Zuzanna. Des de la planta subterrània de l'Aulari Comú, gràcies Adela i Maria, que allà amagades feu tot el possible perquè les comandes tirin endavant, perquè assistim a congressos, i el llarg i indispensable suport que potser no us ho comuniquem gaire però realment valorem molt. I sempre fent quilòmetres per Montilivi ajudant a tothom qui ho demana o necessita, gràcies a la Rustu i la Nuri per tot. Aprofito l'avinentesa també per demanar-vos perdó per tot el material agafat sense permís. També a les reunions amb Frederic i Ellana, que esperem que s'acabin traduint en uns quants articles.

Voldria donar les gràcies a en Gigi, qui em va presentar el món de la recerca per primera vegada obrint-me les portes de l'ICRA i deixant-me fer les pràctiques en empresa i el TFG amb en Jason. També a la Eliza, l'Anna i la Neus, amb qui vaig compartir moments de tot tipus.

Els qui vau acompanyar-me durant els 4 anys de carrera. Per una banda als hippies d'ambientals; Ester, Jofre, Marina, Enric i Oriol, pels moments pre- i post-exàmens, pels treballs grupals fets a deshores, per les excursions a abraçar arbres. Per altra banda, als de la Familia Risk: Irene, Marc, Joan, Mireia, Carla, Pau, Edu, Mercè, Xevi i Jordi, per les estones de botifarra (entre d'altres jocs), per Amsterdam, per les setmanes santes, estius i findes random a Sant Antoni menjant bikinis i bueno... what happened in St Antoni stays in St Antoni. Al conjunt d'aquest paràgraf, gràcies pels dijous universitaris. Ja ho he dit! No me n'oblido dels del màster: Bea, Carles, Albert, Sandra, Eliana Iván, Marc, Hilda i Angela. Gracias por todas las aventuras en las Fallas de Valencia, la escapada a Menorca, los barrancos en Huesca y los miles de planes que hicimos juntos. També a la Núria i Joan Dosta per deixar-me fer el TFM amb vosaltres i acabar publicant els resultats, el meu primer paper!

Pels que heu conviscut amb mi, literalment, durant aquests 4 anys: Albert, Marina, Marta i Núria. Pels sopars, celebracions múltiples, mojitades, etc. I gràcies també als de Figueres que, sobretot i sense voler-ho, m'heu ajudat a desconnectar de la tesi i passar-m'ho bé tot i algun que altre reject o resultats inesperats. Josep, Xampi, Izi, Albert, Mery, Cristina, Judit i Ester, gràcies per fer-me costat durant tants anys i tots els ànims.

I ja per acabar, l'agraïment majúscul li dec als de casa, la família. Als qui hi heu estat des del minut zero i mai heu dubtat de mi. Mama, Papa, Jordi, Martina, Iaies Maries i la resta de família en general, gràcies per formar part de mi i per haver-me facilitat el camí durant aquests 28 anys, els meus èxits són vostres. I als que ja no hi sou, als avis Enric i Santos, i a la tieta Roser i tiu Jaume, esteu sempre presents.

Table of Contents

List of Tables

Chapter 6: Performance of biotrickling filters for biogas purification

Chapter 7: Biogas treatment in membrane bioreactors

Chapter 8: Coupling adsorption and biofiltration for siloxane removal

List of Figures

Chapter 6: Performance of biotrickling filters for biogas purification

Chapter 7: Biogas treatment in membrane bioreactors

Chapter 8: Coupling adsorption and biofiltration for siloxane removal

Chapter 12: Appendices

List of Acronyms

AC: Activated carbon

AD: Anaerobic digestion

BE: Bed exhaustion

BET: Brunauer-Emmett-Teller equation

BT: Breakthrough

BTF: Biotrickling filter

BV: Bed volume

CAPEX: Capital expenditures

DA: Dubinin-Astakhov

DFT: Density functional theory

DR: Dubinin-Radushkevich

D3: Hexamethylcyclotrisiloxane

D4: Octamethylcyclotetrasiloxane

D5: Decamethylcyclopentasiloxane

D6: Dodecamethylcyclohexasiloxane

EBRT: Empty bed residence time

EC: Elimination capacity

ECS: Energy conversion system

EDSS: Environmental decision support system

EPS: Extracellular polymeric substances

EU: European Union

E_0: characteristic energy

FID: Flame ionization detector

GHG: Greenhouse gas

GC: Gas chromatography

HF: Hollow-fiber

ICE: Internal combustion engine

ICP: inductively coupled plasma

L: mean micropore size

L2: Hexamethyldisiloxane

L3: Octamethyltrisiloxane

L4: Decamethyltetrasiloxane

L5: Dodecamethylpentasiloxane

MBR: membrane bioreactor

MS: Mass Spectrometry

MW: Molecular weight

OES: Optical emission spectroscopy

OPEX: Operating expenditures

PAFC: Phosphoric acid fuel cell

PDMS: Polydimethylsiloxane

PhAC: Phosphoric activated carbon

PSD: Pore size distribution

RE: Removal efficiency

RH: Relative humidity

SAC: steam activated carbon

SEM: Scanning electron microscope

S_{BET}: specific surface area

S_{DR}: surface Dubinin-Radushkevich

SOFC: Solid oxide fuel cell

THF: tetrahydrofuran

TMS: Trimethylsilanol

TPD: Temperature-programmed desorption

VOC: Volatile organic compound

V_{TOT}: total pore volume

V_{me}: mesoporosity

$V_{\mu mi}$: microporosity

V_{mmi}: medium size micropore volume

WG: Waste gas

W_0: micropore volume

WWTP: Wastewater treatment plant

x/M: adsorption capacity ρ_{He}: real density

ρ_{ap}: apparent density

Publications and Communications

Journal publications resulting from this thesis:

- Competitive siloxane adsorption in multicomponent gas streams for biogas upgrading. Alba Cabrera-Codony, Eric Santos-Clotas, Conchi O. Ania, Maria J. Martin. Chemical Engineering Journal 344 (2018) 565-573

- Sewage biogas efficient purification by means of lignocellulosic waste-based activated carbons. Eric Santos-Clotas, Alba Cabrera-Codony, B. Ruiz, E. Fuente, Maria J. Martín. Bioresource Technology 275 (2019) 207-215

- Environmental Decision Support System for Biogas Upgrading to Feasible Fuel. Eric Santos-Clotas, Alba Cabrera-Codony, Alba Castillo, Maria J. Martín, Manel Poch, Hèctor Monclús. Energies 12(8) (2019) 1546

- Efficient removal of siloxanes and VOCs from sewage biogas by an anoxic biotrickling filter supplemented with activated carbon. Eric Santos-Clotas, Alba Cabrera-Codony, Ellana Boada, Frederic Gich, Raúl Muñoz, Maria J. Martin. *Submitted for publication*

- Beneficial aspects of coupling adsorption and biological technologies for siloxane abatement from biogas. Eric Santos-Clotas, Alba Cabrera-Codony, Maria J. Martin. *Prepared for submission*

Summary

The anaerobic digestion of organic matter in landfills and wastewater treatment plants (WWTP) leads to the formation of biogas that can be used in energy conversion systems for heat and electricity production, gas grid injection or as a vehicle fuel. Biogas is mainly composed by CH_4 (40-60%), CO_2 (40-55%) and other compounds in concentrations under 2% (e.g. H_2S, N_2). Moreover, it comprises a wide spectrum of trace pollutants including aromatic hydrocarbons, odour-causing terpenes, alkanes and siloxanes.

Siloxanes are a group of polymeric compounds of Si-O bonds with organic chains attached to the silicon atoms. Given their interesting physical and chemical properties, these compounds have been widely used in many industrial processes, and are present in cosmetics, detergents, shampoos and many more everyday products. In this sense, they end up in urban wastewater treatment plants, where some of them reach the anaerobic digesters and are volatilized into biogas. During the combustion reactions of biogas, volatile siloxanes are converted into microcrystalline silicon oxide leading to the abrasion of engine surfaces as well as the build-up of silica layers, which promotes serious damage to the gas conversion units.

The removal of siloxanes is mandatory for biogas-to-energy applications and the most widely used technology to reduce their concentration in biogas is adsorption onto activated carbon (AC). Siloxanes thermal desorption for AC regeneration has resulted unsuccessful due to the formation of higher molecular weight siloxanes, which are hardly desorbable. Therefore, the frequent exhausted material replacement and its disposal as hazardous waste increases the operational costs of this technology. Fuelled by the high costs and low sustainability of non-regenerative adsorption, this thesis aims at exploring different technologies as well as screening alternative activated carbons in order to improve the performance of the technologies to eliminate siloxanes from biogas.

The competitive adsorption of volatile organic compounds (VOC) and siloxanes into ACs of different sources and activation processes was studied in order to get a further insight in the mechanisms ruling the adsorption process in gas mixtures. For this purpose, 10 selected commercial materials were exhaustively characterized in terms of textural and chemical properties and were evaluated in dynamic competitive adsorption tests. Chemically ACs displayed higher adsorption capacities and selectivity for bulky siloxanes, being more convenient for biogas upgrading than steam ACs. Furthermore, the presence of moisture in the test gas was investigated, which promoted the formation of α-ω-silanediols, especially on phosphoric acid-activated carbons. In terms of biogas volume treated per volume of adsorbent

at the first siloxane breakthrough, phosphoric acid ACs were capable of treating higher number of bed volumes, reducing the costs associated to the adsorbent replacement.

Moreover, we evaluated the efficiency of sustainable ACs obtained from the valorisation of lignocellulosic waste in removing both siloxanes and volatile organic compounds. Pyrolyzed and non-pyrolyzed lignocellulosic residues generated in food and wood industries were used as precursor materials to obtain experimental adsorbents by chemical activation with several activating agents. The highest porosity was obtained in non-pyrolyzed residue activated by K_2CO_3 at 900 °C. The performance of the experimental materials was compared with that of commercial ACs in gas adsorption tests of siloxanes (D4 and L2) and VOC (toluene and limonene). The waste-based activated carbons developed proved to be more efficient for the removal of both siloxanes and VOCs than the commercial samples frequently used in WWTP in most of the conditions tested.

On the other hand, the biological removal of siloxanes (D4 and D5) and VOC (hexane, toluene and limonene) typically found in sewage biogas was investigated in a lab-scale biotrickling filter (BTF). The reactor was packed with lava rock and operated at empty bed residence times (EBRT) in the range 4-14.5 min in anoxic conditions. Toluene and limonene exhibited high elimination capacities and a complete removal even at the lowest residence time tested, whereas the abatement of siloxanes and hexane remained below 37%. The packing material was supplemented with 20% of activated carbon in order to increase the mass transfer of the most hydrophobic gas pollutants to the biofilm, which led to higher removal efficiencies for hexane and D5 while supporting complete limonene and toluene removals at a reduced EBRT.

Likewise, the capacity of polydimethylsiloxane membranes to separate the same pollutants as in the BTF was investigated. Gas-gas experiments revealed high transport efficiencies for most compounds from a polluted stream through the membrane towards a clean gas stream. The diffusion of the most hydrophobic pollutants (i.e. siloxanes and hexane) was challenged when clean water was circulated in the other side of the membrane regardless the gas residence time. Then, the performance of a hollow-fiber membrane bioreactor (HF-MBR) was explored for the abatement of such compounds under anoxic conditions. The biofilm grown in the liquid side of the membrane enabled a complete transference of toluene and limonene when the gas residence time was above 31.5 s. Hexane removal efficiency increased from 16 to 43% when gas residence times was incremented from 18 to 63 s. Contrarily, the removal of siloxanes did not show a significant enhancement with the gas residence time remaining below 21%.

Finally, the potentialities of the implementation of a BTF operated at different conditions coupled before the adsorption technology were evaluated as well as the use of ACs with

different characteristics and price. The capacity of a BTF to completely eliminate toluene and limonene as well as reduce siloxane concentration up to 40% led to significantly increase the adsorbent performance. The phosphoric acid wood-based AC reached 450 m^3 L^{-1} of synthetic biogas treated per bed volume, which corresponded to a 20-fold higher performance than current materials in adsorption filters. When carbon costs were taken into account, a steam-activated coal-based AC2 recorded the lowest operating costs according to its market price and siloxane adsorption capacity reaching 0.78 € (1000 $m^3_{treated}$)$^{-1}$.

Thus, coupling biotrickling filtration with adsorption into a steam-AC resulted in lower annual costs than adsorption alone due to the frequent replacements required when biogas was not pre-polished from other compounds.

Resum

La digestió anaeròbica de matèria orgànica en abocadors controlats i estacions depuradores d'aigües residuals (EDAR) provoca la formació de biogàs que es pot utilitzar en sistemes de conversió energètica per a la producció d'electricitat i calor, injecció a la xarxa de gas o com a combustible per a vehicles. El biogàs està compost principalment per CH_4 (40-60%), CO_2 (40-55%), i altres compostos en concentracions inferiors al 2% (per exemple, H_2S, N_2). A més, comprèn un ampli ventall de contaminants traça, incloent hidrocarburs aromàtics, terpens, alcans i siloxans.

Els siloxans són un grup de compostos polimèrics d'enllaços Si-O amb cadenes orgàniques unides als àtoms de silici. Degut a les seves interessants propietats físiques i químiques, aquests compostos s'han utilitzat àmpliament en molts processos industrials, trobant-se en cosmètics, detergents, xampús i molts més productes quotidians. Per aquest motiu acaben arribant a les estacions depuradores d'aigües residuals urbanes, on alguns siloxans arriben als digestors anaeròbics i es volatilitzen amb el biogàs. Durant les reaccions de combustió del biogàs, els siloxans es converteixen en micro-cristalls abrasius que malmeten les superfícies del motor, o s'acumulen en forma de capes de sílice, que finalment promouen greus danys a les unitats de conversió energètica.

L'eliminació de siloxans és obligatòria per les aplicacions energètiques del biogàs i la tecnologia més utilitzada per reduir la seva concentració en biogàs és l'adsorció en carbó activat (CA). La desorció tèrmica de siloxans per a la regeneració del CA no ha tingut resultats satisfactoris a causa de la formació de siloxans de pes molecular superior que no són fàcilment desorbibles. D'aquesta manera, el reemplaçament freqüent del material esgotat i el conseqüent tractament com a residu perillós augmenten els costos operatius. Degut als alts costos i la baixa sostenibilitat d'aquesta tecnologia, aquesta tesi pretén investigar diferents tecnologies i també explorar diferents carbons activats per eliminar siloxans del biogàs.

Així doncs, s'ha estudiat l'adsorció competitiva de compostos orgànics volàtils (COV) i siloxans en CA provinents de diferents fonts i processos d'activació. Amb aquesta finalitat, 10 materials comercials es van caracteritzar exhaustivament pel que fa a propietats texturals i químiques i es van avaluar en proves dinàmiques d'adsorció competitiva. Els carbons activats químicament van mostrar una major capacitat d'adsorció i selectivitat per als siloxans més grans, sent més convenients per a la millora del biogàs que els carbons activats amb vapor. A més, es va investigar la presència d'humitat en el gas matriu, la qual va promoure la formació d'α-ω-silanediols, especialment en carbons activats amb àcid fosfòric. Pel que fa al volum de biogàs

tractat per volum d'adsorbent en el trencament del primer siloxà, els carbons activats amb àcid fosfòric van ésser capaços de tractar un major nombre de volums de llit, reduint els costos associats al reemplaçament d'adsorbents.

També es va avaluar l'eficiència de CA sostenibles obtinguts a partir de la valorització de residus lignocel·lulòsics en l'eliminació de siloxans i COV. Els residus lignocel·lulòsics piròlitzats i no piròlitzats generats a les indústries alimentàries i de fusta es van utilitzar com a materials precursors per a l'obtenció d'adsorbents experimentals mitjançant activació química amb diversos agents activadors. La porositat més alta es va obtenir per residus no piròlitzats activats amb K_2CO_3 a 900 °C. El rendiment dels materials experimentals es va comparar amb el de CA comercials en proves d'adsorció de siloxans (D4 i L2) i COV (toluè i limonè). Els CA obtinguts a partir de residus van demostrar ser més eficients per a l'eliminació de siloxans i de COV que les mostres comercials en la majoria de les condicions estudiades.

D'altra banda, es va investigar l'eliminació biològica de siloxans (D4 i D5) i de COV (hexà, toluè i limonè), típicament presents en el biogàs de depuradora, en un biofiltre percolador de gasos a escala laboratori (BTF). El reactor es va empaquetar amb roca de lava i va operar a temps de residència (EBRT) en el rang de 4-14.5 min en condicions anòxiques. El toluè i el limonè van presentar elevades una eliminació completa fins i tot al menor temps de residència estudiat, mentre que la reducció de siloxans i hexà es va mantenir per sota del 37%. El material d'empaquetament es va complementar amb un 20% de carbó activat per augmentar la transferència de massa dels contaminants de gasos més hidròfobics, el que va suposar una major eficiència en l'eliminació d'hexà i D5, suportant simultàniament eliminacions completes de limonè i toluè a un EBRT reduït.

Paral·lelament es va investigar la capacitat de membranes de polidimetilsiloxà en la separació dels mateixos contaminants que al BTF. Els experiments gas-gas van revelar una gran eficiència de transport per a la majoria dels compostos des d'un flux contaminat a través de la membrana cap a un corrent de gas net. La difusió dels contaminants més hidròfobics (siloxans i hexà) es va dificultar quan es va fer circular aigua neta a l'altre costat de la membrana, independentment del temps de residència. A continuació, es va explorar el rendiment d'un bioreactor de membrana de fibres buides (HF-MBR) per reduir aquests compostos en condicions anòxiques. El biofilm cultivat al costat líquid de la membrana va permetre una eliminació completa de toluè i limonè a temps de residència superiors als 31.5 s. L'eficiència d'eliminació de l'hexà va augmentar del 16 al 43% quan els temps de residència de gas es va incrementar de 18 a 63 s. Per contra, l'eliminació de siloxans no va mostrar una relació significativa amb el temps de residència, mantenint-se per sota del 21%.

Finalment, es van avaluar les potencialitats d'implementació d'un BTF operant a diferents condicions abans de l'adsorció, així com l'ús de CA amb diferents característiques i preus. La capacitat d'un BTF per eliminar completament el toluè i el limonè així com reduir la concentració de siloxà fins a un 40%, va significar un augment notable en el rendiment de l'adsorbent. El carbó activat amb àcid fosfòric basat en fusta va assolir 450 m^3 L^{-1} de biogàs sintètic tractat per volum de llit, que corresponia a un rendiment 20 vegades més alt que l'assolit amb materials que s'utilitzen actualment en el tractament del biogàs. Quan es van tenir en compte els costos del carbó, un CA basat en carbó i activat per vapor va registrar els costos d'operació més baixos segons el seu preu de mercat i la seva capacitat d'adsorció de siloxà aconseguint 0.78 € (1000 m^3$_{tractats}$)$^{-1}$. L'acoblament d'un BTF amb l'adsorció en carbó activat per vapor va suposar uns costos anuals inferiors que considerant només l'adsorció, degut principalment als freqüents reemplaçaments necessaris quan el biogàs no s'havia polit prèviament d'altres compostos.

Resumen

La digestión anaerobia de la materia orgánica en vertederos y estaciones depuradoras de aguas residuales (EDAR) conduce a la formación de biogás que se puede usar en sistemas de conversión energética para la producción de calor y electricidad, inyección a la red de gas o como combustible para vehículos. El biogás está compuesto principalmente por CH_4 (40-60%), CO_2 (40-55%) y otros compuestos en concentraciones inferiores al 2% (por ejemplo, H_2S, N_2). Además, comprende un amplio espectro de contaminantes traza que incluyen hidrocarburos aromáticos, terpenos, alcanos y siloxanos.

Los siloxanos son un grupo de compuestos poliméricos de enlaces Si-O con cadenas orgánicas unidas a los átomos de silicio. Dadas sus interesantes propiedades físicas y químicas, estos compuestos han sido ampliamente utilizados en muchos procesos industriales, y por ello se encuentran en cosméticos, detergentes, champús y muchos más productos de uso diario. Por este motivo, terminan en plantas depuradoras de aguas residuales urbanas, donde algunos siloxanos llegan a los digestores anaeróbicos y se volatilizan con el biogás. Durante las reacciones de combustión del biogás, los siloxanos se transforman en microcristales abrasivos, que provocan la abrasión de las superficies del motor y la acumulación de capas de sílice, promoviendo un daño grave a las unidades de conversión energética.

La eliminación de siloxanos es obligatoria para las aplicaciones energéticas del biogás y la tecnología más utilizada para reducir su concentración en el biogás es la adsorción en carbón activado (CA). La desorción térmica de los siloxanos para la regeneración del CA ha resultado infructuosa debido a la formación de siloxanos de peso molecular más alto, que apenas son desorbibles. Por lo tanto, el reemplazo frecuente de material agotado y su tratamiento como residuo peligroso aumenta los costos operativos. En contemplación de los altos costes y la baja sostenibilidad de la adsorción no regenerativa, esta tesis tiene como objetivo explorar diferentes tecnologías, así como analizar diferentes carbones activados para la eliminación de los siloxanos del biogás.

Se estudió la adsorción competitiva de compuestos orgánicos volátiles (COV) y siloxanos en AC de diferentes fuentes y procesos de activación. Para este propósito, 10 materiales comerciales se caracterizaron exhaustivamente en términos de propiedades texturales y químicas, y se evaluaron en pruebas dinámicas de adsorción competitiva. Los carbones activados químicamente demostraron mayores capacidades de adsorción y selectividad para los siloxanos más grandes, siendo más convenientes para la purificación del biogás que los carbones activados mediante vapor. Además, se investigó la presencia de humedad en el gas

matriz, lo cual promovió la formación de α-ω-silanedioles, especialmente en los carbones activados con ácido fosfórico. En términos de volumen de biogás tratado por volumen de adsorbente a la ruptura del primer siloxano, las CA activados mediante ácido fosfórico fueron capaces de tratar un mayor número de volúmenes de lecho, reduciendo los costos asociados con el reemplazo del adsorbente.

También, evaluamos la eficiencia de CA sostenibles obtenidos a partir de la valorización de residuos lignocelulósicos en la eliminación de siloxanos y COV. Los residuos lignocelulósicos pirolizados y no pirolizados generados en las industrias de alimentos y madera se utilizaron como materiales precursores para obtener adsorbentes experimentales por activación química con varios agentes activadores. La mayor porosidad se obtuvo por un residuo no pirolizado activado con K_2CO_3 a 900 °C. El rendimiento de los materiales experimentales se comparó con el de CA comerciales en las pruebas de adsorción de siloxanos (D4 y L2) y COV (tolueno y limoneno). Los CA obtenidos a partir de residuos demostraron ser más eficientes para la eliminación de siloxanos y COV que las muestras comerciales en la mayoría de las condiciones estudiadas.

Por otro lado, la eliminación biológica de siloxanos (D4 y D5) y COV (hexano, tolueno y limoneno), típicamente presentes en el biogás de depuradora, se investigó en un biofiltro percolador de gases a escala laboratorio (BTF). El reactor se empaquetó con roca de lava y se operó a tiempos de residencia (EBRT) en el intervalo de 4-14.5 min en condiciones anóxicas. El tolueno y el limoneno mostraron altas capacidades de eliminación y una eficiencia de eliminación completa incluso en el tiempo de residencia más bajo, mientras que la reducción de siloxanos y hexano se mantuvo por debajo del 37%. El material de empaquetamiento se complementó con un 20% de carbón activado para aumentar la transferencia de masa los compuestos más hidrofóbicos, lo que llevó a una mayor eficiencia de remoción para el hexano y D5, manteniendo a la vez la eliminación completa de limoneno y tolueno a un EBRT reducido.

Paralelamente se investigó la capacidad de membranas de polidimetilsiloxano en la separación de los mismos contaminantes que en el BTF. Los experimentos gas-gas revelaron altas eficiencias de transporte para la mayoría de los compuestos desde una corriente contaminada a través de la membrana hacia una corriente de gas limpio. La difusión de los contaminantes más hidrofóbicos (siloxanos y hexano) se vio afectada cuando se circuló agua limpia en el otro lado de la membrana, independientemente del tiempo de residencia. Posteriormente, se exploró el rendimiento de un biorreactor de membrana de fibra hueca (HF-MBR) para la reducción de dichos compuestos en condiciones anóxicas. El biofilm crecido en el lado líquido de la membrana permitió una transferencia completa de tolueno y limoneno en tiempos de

residencia superiores a 31.5 s. La eficiencia de remoción de hexano aumentó de 16 a 43% cuando el tiempo de residencia se incrementó de 18 a 63 s. Por contra, la eliminación de siloxanos no mostró una relación significativa con el tiempo de residencia, manteniéndose por debajo del 21%.

Finalmente, se evaluaron las potencialidades de la implementación de un BTF operado en diferentes condiciones antes de un filtro adsorbente, así como el uso de CA con diferentes características y precios. La capacidad de un BTF para eliminar completamente tolueno y limoneno, así como para reducir la concentración de siloxano hasta en un 40%, llevó a un aumento notable en el rendimiento del adsorbente. El CA con base de madera activado con ácido fosfórico alcanzó 450 m^3 L^{-1} de biogás sintético tratado por volumen de lecho, lo que correspondió a un rendimiento 20 veces mayor que el de materiales que se utilizan actualmente en el tratamiento de biogás. Cuando se tuvieron en cuenta los costos del carbón, un CA con base de carbón i activado por vapor registró los costos operativos más bajos según su precio de mercado y su capacidad de adsorción de siloxano, que alcanzó 0.78 € (1000 m$^3_{tratados}$)$^{-1}$. El acoplamiento de un BTF con la adsorción en un CA activado con vapor resultó en costos anuales más bajos que la adsorción sola debido a los frecuentes reemplazos requeridos cuando el biogás no había sido pretratado de otros compuestos.

Chapter 1

INTRODUCTION

1.1   Biogas: a sustainable energy fuel

The accelerated consumption of finite energy resources, the impact linked to the production and use of traditional fuels, the power distribution, and the prices of the raw materials, confer to the renewable sources a rising importance in the energy policy of developed countries. The utilization of the energy from renewable resources is highly important in the energy and environmental policy strategy.

The biological degradation of organic substrates in the absence of oxygen leads to the formation of biogas. This process is commonly known as anaerobic digestion (AD), in which the organic matter undergoes four stages (hydrolysis, acidogenesis, acetogenesis and methanogenesis) being finally converted into CO_2 and CH_4 by different types of bacteria.

The climate and energy policies in the European Union (EU) have encouraged the development of biogas plants for energy conversion, given the economic advantages of power generation and environmental benefits provided by the anaerobic digestion. Most of the European biogas is converted into heat and/or electricity used to meet the local demand or to external users. Moreover, if biogas undergoes an upgrading process to biomethane it can be injected into the gas network or used as a vehicle fuel.

Agriculture and industrial residues, municipal organic waste and sewage sludge are the most common feedstocks for anaerobic digesters. The valorization of such residues is not only promoted by waste management strategies to produce renewable energies but also to assist environmental efforts to mitigate climate change. It is well-known that CO_2 accounts for a high percentage of all greenhouse gas emissions from human activities. CH_4, although accounting for a smaller portion of these emissions, has a global warming potential (GWP) around 25 times higher than carbon dioxide. Hence the necessity to collect and use biogas efficiently as an energy resource.

1.1.1   Biogas trends in Europe

The production of biogas in Europe has significantly increased since 2007 until 2016 (Figure 1.1). According to the last Biogas Barometer carried out by the EurObserv'ER in 2016 [1], biogas production hit more than 16 million tons of oil equivalent (Mtoe), and 62 TWh of

biogas electricity produced. The major contribution to the total biogas produced, which has presented a linear growth over time, is the represented as other biogases, including decentralized agricultural plants, municipal solid waste methanisation plants, industrial methanisation plants and centralized co-digestion. The contribution of biogas produced in landfills and wastewater treatments plants (sewage gas) has been almost constant up to date.

The number of plants within the European Union strongly increased during 2010-2012 almost doubling its number in 3 years. Although the origin of the biogas varies in each member state of the EU, this rapid growth was due to the increase in plants running on agricultural feedstocks. In 2015, almost 11000 out of the 16834 biogas plants in Europe (65%) were located in Germany, which made it the major biogas producer in the EU as observed in Figure 1.2.
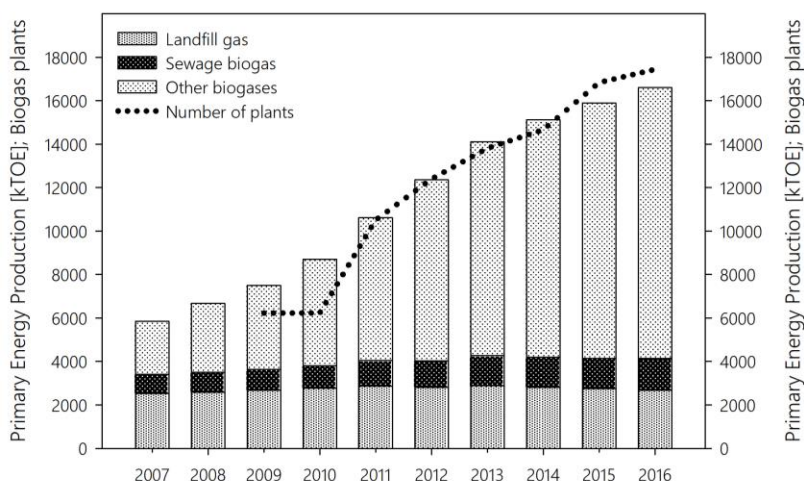
Figure 1.1 Evolution of the primary biogas production and the number of biogas plants in Europe from 2009 until 2016 [2]

Leading countries following Germany are the United Kingdom and Italy with biogas production above 2000 kTOE, and Czech Republic and France with productions higher than 600 kTOE. In most countries biogas is produced from the anaerobic digestion of agricultural wastes. Nevertheless, some countries obtain most of their biogas from landfills, as in the UK, Turkey, Spain, Portugal and Greece. Biogas from wastewater treatment plants prevails in countries like Poland and Sweden.
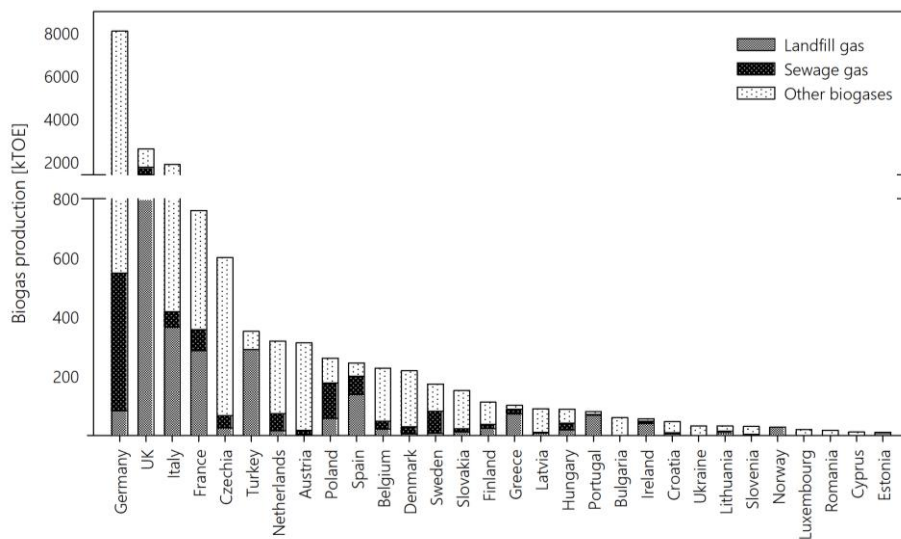
Figure 1.2 Primary energy production from biogas in European countries in 2016 [2]

1.2 Biogas composition

Biogas is a renewable fuel that can be used as an energy source for power and heat production. The main component of biogas is methane (40-70%) and its content determines the energetic value of the biogas produced. Methane is the energy source in biogas with a net calorific value of up to 7.5 kWh m^{-3}. However, as a result of the anaerobic digestions from which biogas is generated other compounds compose biogas (Table 1.1), and the composition of the final gas depends on the origin and characteristics of the substrate. In this sense, the other major compound in biogas is CO_2 (25-40%) followed by small amounts of other gases under 2% such as oxygen, hydrogen, nitrogen, ammonia and hydrogen sulphide. Trace concentrations of aromatic hydrocarbons and siloxanes are often present in biogases from anaerobic digesters in sewage plants as well as landfills. Papadias et al, (2011) reviewed published data and set up a database that included nearly 300 impurities found in biogas matrix.

Table 1.1 Composition of landfill and sewage digester biogases [3–6]

Composites/features	Units	Sewage digester biogas	Landfill biogas
CH_4	% by vol.	57-65	37-67
CO_2	% by vol.	34-38	24-41
O_2	% by vol.	<1	1-3
N_2	% by vol.	<1	5-15
H_2	% by vol.	<1	0-3
H_2S	ppm_v	0-4000	0-5400
NH_3	ppm_v	100	5
Halogenated compounds	ppm_v	<10	<100
Siloxanes	ppm_v	0-50	0-15
Relative humidity	%	100	100
Temperature	°C	36-60	0-25
Net calorific value	kWh Nm^{-3}	6-7.5	4.5-5.5

Most of these impurities may or must be removed depending on the final use of biogas (Table 1.2). H_2S, for instance, stresses corrosion in piping and equipment thus it needs to be removed prior to biogas combustion. Moreover, its combustion forms SO_2 that is emitted to the atmosphere and contributes to global warming. Common technologies for the abatement of H_2S include biological technologies (biofilters and biotrickling filters), absorption (scrubbers) and adsorption (activated carbon, activated alumina, silica gel and zeolites) [7]. On the other hand, siloxanes are considered one of the most harmful compounds in biogas even though their relatively low concentrations. They cause abrasion to the engines which makes their elimination mandatory [8].

Apart from heat and electricity generation, biogas can be directly injected to the gas grid or it can be used as a vehicle fuel. Depending on its final use, biogas treatment or further upgrading is required. Table 1.2 summarizes the main requirements based upon the energy conversion system (ECS) and the final use. The main ECS utilized for biogas within the EU are internal combustion engines (ICE), gas micro-turbines or large turbines, in which manufacturers dictate the biogas quality requirements. In the case of gas grid injection or usage as vehicle fuel, biogas needs to be upgraded to biomethane and a high quality must be ensured, which is subjected by national regulations.

Table 1.2 Concentration limits for different energy conversion systems or biogas uses [9–12].

Biogas final use/ECS	Type/manufacturer	Siloxane limit [mg m^{-3}]	H$_2$S tolerance [mg m^{-3}]
Internal combustion engine	Permissive ICE	30	695
	Restrictive ICE	12	70
Micro-turbine	Capstone®	0.03	6900
Fuel cells	PAFC	0.1	28
	SOFC	0.01	1.4
Stirling engine	Standard	No limit	1390
Grid injection	Spanish legislation	10	10

1.2.1 Siloxanes in biogas
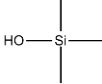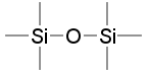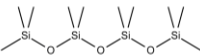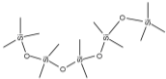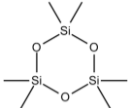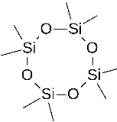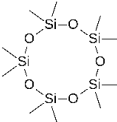
Siloxanes are a group of polymeric compounds of Si-O bonds with organic chains attached to the silicon atoms. Siloxanes have thermal stability, high flexibility, hydrophobicity and low surface tension that make them useful in many industrial processes or applications [13].

Given the wide range of applications, siloxanes can be found in cosmetics, detergents, shampoos and many more everyday products [14] ending up in urban wastewater treatment plants. Most of them are likely to volatise in the atmosphere and decompose, but some of them may remain in the wastewater adsorbed onto the extracellular polymeric substances (EPS) of the sludge flocs [15]. In this sense, siloxanes reach the anaerobic digesters where biogas is obtained and, due to the elevated temperatures, they are volatilized into the methane-rich gas. Commonly found siloxanes in biogas and some of their physicochemical properties are summarized in Table 1.3.

Siloxanes concentrations in biogas may differ depending on its source; landfill or anaerobic digester. Typical concentrations of this compounds in biogas are in the range 3-30 mg m^{-3} in landfill gas [15,16] and 10-240 mg m^{-3} in anaerobic digester gas [6,15,17].

During the combustion of biogas, present volatile siloxanes are converted into abrasive microcrystalline silica (SiO$_2$), which has properties similar to those of glass. More precisely, this residue deposition leads to the abrasion of engine surfaces and contributes to overheating motor sensitive parts as well as the build-up of silica layers. Overall, siloxanes inhibit heat conduction or lubrication thus promoting serious damage to the gas conversion unit [8].

Table 1.3 Frequent siloxanes detected in biogases and their properties

Compound (abbreviation)	Formula	MW [g mol⁻¹]	Boiling point [°C]	Vapour pressure [kPa]
Trimethylsilanol (TMS)		90	70	2.13
Hexamethyldisiloxane (L2)		162	107	4.12
Octamethyltrisiloxane (L3)		236	153	0.52
Decamethyltetrasiloxane (L4)		310	194	0.07
Dodecamethylpentasiloxane (L5)		384	230	0.009
Hexamethylcyclotrisiloxane (D3)		222	135	1.14
Octamethylcyclotetrasiloxane (D4)		297	176	0.13
Decamethylcyclopentasiloxane (D5)		371	211	0.02
Dodecamethylcyclohexasiloxane (D6)		445	245	0.003

1.3 Siloxanes removal: a technology overview

Non-regenerative adsorption is the most common technology applied to the removal of siloxanes from biogas. The majority of the patents found on this topic are based on the principle of adsorption and are not commercially available [18]. Nevertheless, several technologies can be found in the literature, most of them as end-of-pipe approaches.

1.3.1 Adsorption

Adsorption is the process in which atoms, ions or molecules from a gas or liquid (adsorbate) interact with the surface of a solid material (adsorbent). Adsorption may be classified as physisorption or chemisorption depending on the type of forces taking place between the adsorbate and the adsorbent. The forces participating in physical adsorption may be polarization forces, dispersive forces and dipole moment, where the adsorbate is retained due to weak van der Walls interaction. Chemisorption, on the other hand, involves transferring, exchanging or even sharing electrons leading to the formation of chemical bonds between adsorbates and adsorbent [19].

Conventional technologies used for siloxanes' abatement are based on adsorption on fixed beds of activated carbon. This technology consists on flowing the biogas through a fixed bed of activated carbon until the bed experiences breakthrough (Figure 1.3). Then, a second bed starts adsorbing while the saturated bed is replaced with fresh adsorbent material. Among other parameters, the performance of adsorption will depend on the type of adsorbent used. More precisely, the adsorbent's selectivity towards siloxanes will delimit the lifetime of the material before occurring breakthrough.
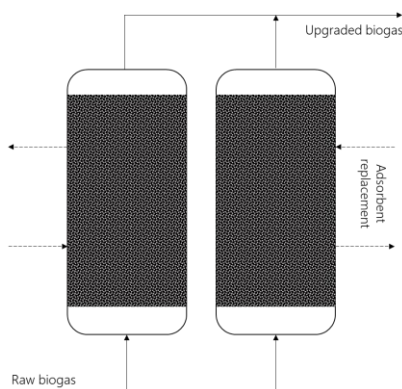
Figure 1.3 Non-regenerative adsorption on fixed beds

Activated carbon is the most widely used adsorbent support and its capacity to reduce siloxane concentration below 0.1 mg m^{-3} has been reported [18]. However, other inorganic materials have also been investigated such as silica gel, alumina and zeolites.

Several reports state that siloxanes' adsorption is affected by different parameters of the material such as its origin material, type of activation, BET surface area and porosity [20]. The main drawback of this technology is the high operational costs associated with the bed replacement. Siloxanes thermal desorption for AC regeneration has resulted unsuccessful due to the formation of higher molecular weight siloxanes (i.e. silicone polymers) which are hardly desorbable [21,22]. Cabrera-Codony et al. (2015) [23] investigated the regeneration of AC exhausted with siloxanes by means of advanced oxidation processes (O$_3$, H$_2$O$_2$) recovering up to 45% of the original capacity of the AC.

In the other hand, other inorganic silicon-based materials have been studied at laboratory scale, including silica gel, molecular sieves and zeolites (Figure 1.4).

Silica gel is an amorphous material with a polymeric structure of colloidal silicic acid being the general formula SiO$_2$·nH$_2$O. This material is commonly used as a desiccant due to its high affinity towards water. Thermal regeneration of spent silica gel is easily achieved due to a weaker adsorption force. Moreover, its regeneration has been observed to be more cost-effective than activated carbons [24]. Schweigkofler and Niessner (2001) reported siloxanes adsorption capacities up to 100 mg g^{-1} by silica gel. They also stated that the presence of humidity in the gas (>20% RH) greatly influenced the siloxanes uptake.

Zeolites are crystalline aluminosilicates with frameworks based on extensive three-dimensional networks of oxygen ions arranged tetrahedrally (AlO$_4$ or SiO$_4$) forming identical building unite cells. Zeolites have been widely employed for removing heavy metals from the environment, as catalysts in the petrochemical industry, reducing NOx emissions from vehicles and water purifications among many other applications. Some publications can be found in the literature addressing the removal of siloxanes.
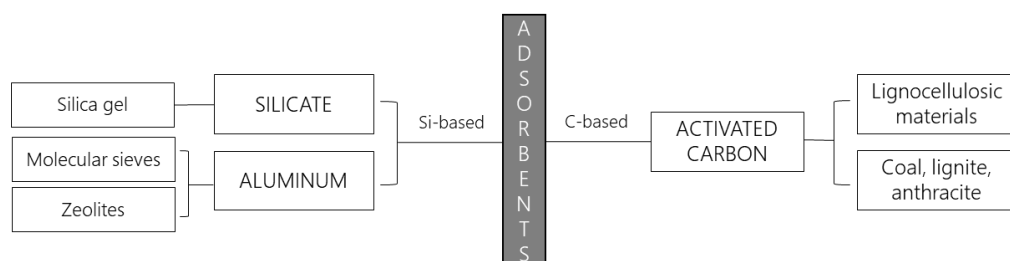
Figure 1.4 Adsorbents for siloxane removal in biogas upgrading

A review on the state-of-the-art of siloxanes adsorption onto various organic and inorganic adsorbents can be found in Table 1.4. It needs to be highlighted that most of these studies have been conducted at lab-scale with simple gas matrixes (i.e. dry N_2) and siloxanes concentrations well above the typical range in biogas. As a result of the high concentrations in the synthetic gas streams, high adsorption capacities have been reported, which is not later witnessed in real biogas facilities [12]. Sigot et al. (2014) [25] observed a 90% decrease in the D4 adsorption capacity of a silica gel when the inlet gas presented a 70% relative humidity. Water competition for the adsorption sites was also pointed out by Schweigkofler and Niessner (2001) [24]. The height-diameter ratio in the bed-dimensioning was also found to influence siloxanes' adsorption capacity [26].

1.3.2 Absorption (scrubbing)

Absorption has been widely applied in the removal of siloxanes from biogas. The principle of this technology consists in the mass transfer of a gas pollutant to a liquid absorbent. The polluted gas flows counter-current to the liquid absorbent solution (Figure 1.5) so the efficiency of this process relies on (i) the packing surface area, (ii) the contact time and (iii) the solubility of the pollutant in the absorbent solution. Absorption can be divided into chemical or physical depending on the nature of the absorptive agent applied.
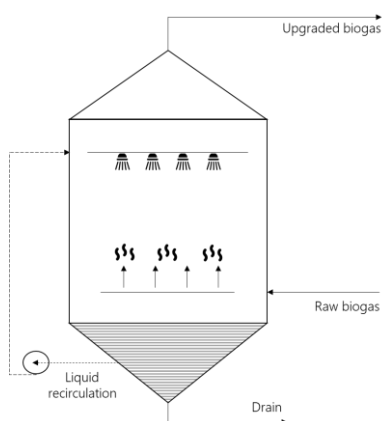
Figure 1.5 Chemical scrubber

Chemical absorption is referred when strong acids are used for the destruction of siloxanes and is associated to safety and corrosion concerns, which lead to higher costs [27]. Schweigkofler and Niessner (2001) reported siloxanes' elimination efficiencies of >95% and >65% with sulfuric acid and nitric acid, respectively, when temperature of the acids was

increased to 60ºC. Bases such as NaOH have been tested demonstrating poor efficiencies and producing carbonates that precipitates into the equipment [28].

Table 1.4 State-of-the-art on adsorbent materials for siloxane abatement.

Siloxane (gas matrix)	Concentration [ppm v/v]	Adsorbent	Capacity [mg g⁻¹]	Ref.
L2/D5 (dry N_2)	100-300	Silica gel	118/134	[29]
Siloxanes (sewage gas)		AC	20-50	
D3 (synthetic biogas)	Saturated	AC	570	[21]
		Silica gel	230	
		Zeolite	276	
D4/L2 (isotherms)	N/A	Zeolite DAY40	104-124	[30]
		Silica gel	77	
		Various ACs	300-400	
D4 (Langmuir isotherm)		Various ACs	198-459	[31]
D4	350	Various ACs	56-192	[32]
		Molecular sieve	4-77	
		Silica gel	104	
D4/D5 (dry N_2)	46/21	Zeolite	51/52	[33]
		Various ACs	150-531	
		Silica gel	230-240	
		Synthetic resin	200-530	
L2, D4 and D5 mixture (N_2)	N/A	Various ACs	155-307	[34]
		Silica gel	202	
		Alumina oxide	146	
D4	N/A	Various ACs	21-224	[35]
L2 (dry N_2)	20-300	AC	10-100	[36]
D4 (dry N_2)	1000	Various ACs	249-1732	[37]
D4 (synthetic biogas)	1,45	AC	897	[37]
D4	30	Silica gel	259	[25]
		AC	53	
		Zeolite	139	
D4	N/A	AC	856	[38]
		Polymer	2370	
D5 and D6 (N_2, toluene and limonene)	1-10	AC	120	[39]
		Molecular sieve	53	
		Silica gel	131	
D4	500	Silica gel	102-686	[40]
D4 (dry N_2)	170	Aluminosilicates	10-104	[41]
D4 (dry N_2)	250	Various Zeolites	11-143	[42]
D4 (dry N_2)	~600	Mesoporous aluminas	168	[43]

Physical absorption is associated to mere solubilization of the pollutant to the absorbent and later regeneration. Water, organic solvents or mineral oil are included in this type of adsorption. Polar organic solvents may be later regenerated by heating, stripping or desorption [8]. Water scrubbing is a common upgrading process simple and effective capable of remove corrosive compounds at relatively low costs. CO_2 and H_2S can be highly reduced from biogas due to their solubilities in water. However, low abatements have been reported for siloxanes considering their poor solubilities in water [44].

The most promising organic solvent for siloxanes removal from biogas is Selexol™, which is a polyethylene glycol dimethyl ether capable of removing not only siloxanes but also CO_2 and H_2S. Removal efficiencies up to 99% have been accomplished in a landfill biogas plant with adsorbent regeneration [16].

1.3.3   Deep chilling/condensation/refrigeration

Reducing the temperature of biogas is a simple and popular method commonly used for removing siloxanes as well as water from biogas. The objective of this unit is typically the elimination of water as pre-treatment prior to an activated carbon filter and so avoid the competition between water and siloxanes for the porous sites. Nevertheless, some reports have found that siloxanes can also be removed at different levels depending on the temperature achieved. Wheless and Pierce (2004) [16] reported moderate removal efficiencies of siloxanes ranging from 15 up to 50% when biogas was chilled to 5ºC, and advanced refrigeration to temperatures below -20 ºC accomplished 95% removal efficiencies.

The main disadvantage of this technology is the elevated costs due to the energetic requirements. Refrigeration systems for eliminating siloxanes have shown to be cost-effective when combined with activated carbon in plants generating high flow rates of biogas with high loads of siloxanes [27].

1.3.4   Membrane separation

The principle of this technology is the selective permeation of siloxanes by a solution diffusion mechanism through dense polymeric membranes [45]. Membranes are characterized by large surface areas for separation while occupying small volumes. They can be polymeric or inorganic materials, and the permeability and selectivity towards a specific compound will be determined by the pore size and molecular interactions [46].

Currently, biogas upgrading with membranes is applied in high pressure membrane systems (36 bar) with gas phases in both sides of the membrane, and in low-pressure systems (1 bar) where gas molecules diffuse through a microporous hydrophobic membrane and subsequently are solubilized in a liquid absorbent. Either way membranes require pre-treatment for the removal of harmful compounds such as H_2S (high concentrations) and halogenated compounds that can damage them. Membranes systems are commonly applied for the separation of CO_2, moisture and H_2S from methane [47].

Up to date only one report can be found in the literature for siloxanes abatement by means of membranes systems [48]. Ajhar et al. (2012) investigated the performance of polydimethylsiloxane (PDMS) membranes for the selective separation of several siloxanes (L2-L4, D3-D5) determining their permeability and selectivity towards methane. High siloxanes removal efficiencies (>80%) with ambient air as sweep gas were achieved.

In the other hand, membrane systems may be coupled to biological reactors, more precisely know as membrane bioreactors (MBR). These advanced membrane configurations have been widely implemented for wastewater treatment and many lab-scale experimental studies have been reported for waste gas treatment (MBRWG). This technology is based upon the gaseous pollutants diffusion through the membrane where the target pollutants are degraded into the biofilm grown to the membrane surface or the biomass suspended in the liquid phase [49,50]. In this sense, MBRWG are suitable for poorly water-soluble compounds that are hardly transferred with other biological technologies (i.e. biofilters or biotrickling filters). The transport of pollutants across the membrane is driven by the concentration gradient and therefore the capacity of the biomass to degrade the compounds transferred. It is also determined by the solubility and diffusivity of the compounds through the membrane.

Several laboratory scale studies have reported efficient removal capacities of a wide range of gaseous pollutants in MBRWG. An exhaustive review on this topic can be found elsewhere [50]. To the best of our knowledge no reports have been found for siloxanes abatement with this type of configuration.

1.3.5   Biological technologies

For many years polydimethylsiloxanes (PDMS) have been treated as non-biodegradable or even inert to living organisms due to their physicochemical properties [51]. In late 90s, some reports proved the biodegradability of many silicon-compounds by different kinds of bacteria

[52,53]. From 2008 on, scarce researchers have investigated the elimination of siloxanes in biological technologies, given their environmental and (often) economic advantages.

A biotrickling filter (BTF) consists in the biological treatment of a polluted gaseous stream through a packed bed with microorganisms grown attached to an inert support material often inorganic (e.g. ceramics, rocks, plastics, etc). Moreover, in order to provide the microorganisms with nutrients, a mineral solution is continuously irrigated (trickling solution) commonly in counter-current to the gas stream (Figure 1.6). In this sense, pollutants are firstly absorbed in the trickling solution and therefore degraded by the microbial consortium.

Biotrickling filters have been thoroughly explored specially in the removal of H_2S for biogas applications. A detailed review on the papers published regarding degradation of H_2S from biogas can be found elsewhere [54]. Given its high solubility, this pollutant can be easily eliminated by biofiltration even at low gas residence times (<10 s) and reach elimination capacities higher than 200 g m^{-3} h^{-1} [7,55].
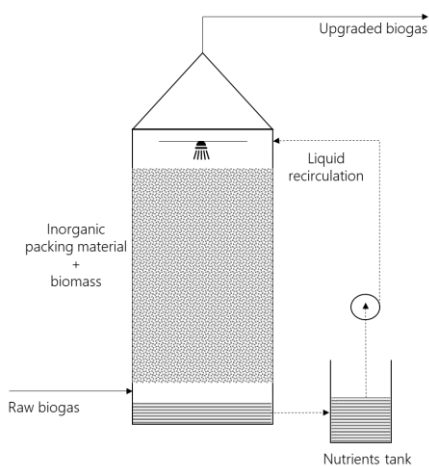
Figure 1.6 Biotrickling filter

This type of bioreactor has also been explored for odour abatement in WWTPs not only for treating H_2S but also VOCs such as BTEX and hexane among others. Biogas from anaerobic digesters in WWTPs and from landfills can also contain such compounds [56], though unlike siloxanes, they are not regarded as harmful for the energy conversion systems, so their removal is not often required.

Some researchers have investigated the removal of siloxanes by means of biotrickling filters. However, to our best knowledge and up till now, only four reports can be found in the literature and are summarized in Table 1.5.

All the four studies have been conducted in aerobic conditions and with different bacterial strains obtaining removal efficiencies from 10 up to 74%. Most of them concluded that low overall efficiencies were obtained due to mass-transfer limitations given the low water-solubility of siloxanes. Popat and Deshusses (2008) investigated siloxane D4 elimination through biofiltration under anaerobic and aerobic conditions. They did not observe much difference between both operation conditions, stating that a change in the electron acceptor (oxygen for nitrate or sulphate) did not affect significantly the reactor performance [57].

Table 1.5 Experimental studies on siloxanes removal from gas in BTFs

Reactor unit	Target	Conc. [mg m^{-3}]	EBRT [min]	RE [%]	EC [mg m^{-3} h^{-1}]	Ref.
Aerobic BTF (2 L) packed with Pall rings inoculated with *P. putida*. Co-current configuration.	D3	46-77	2.1 3.6	10 20	200	[58]
Aerobic BTF (4.4 L) packed with lava rock inoculated with P. aeruginosa. Counter-current.	D4	50	3.3 13.2	48 74	435 168	[59]
Aerobic and anaerobic (0.4 L) BTF packed with cattle bone and lava rock. Inoculum was activated sludge. Counter-current.	D4	45	5, 7.5 11, 16 19.5	10, 15 25,35 43	15 60	[57]
Aerobic BTF (2 L) packed with polypropylene rings. Phyllobacterium myrsincearum was isolated and enriched from AS and used as inoculum. Counter-current.	D4	50	24	60.2		[60]

Chapter 2

OBJECTIVES

Objectives

The general aim of the thesis is to improve the purification of biogas in terms of efficiency and sustainability, focusing on siloxane removal due to their hazardous nature towards energy applications. The specific objectives are listed below:

Enhance adsorption of siloxanes into activated carbons

- To assess the mechanisms of competitive adsorption of siloxanes in the presence of other biogas impurities:
    - The screening of a series of porous carbons for the removal of multicomponent mixtures of siloxanes and volatile organic compounds from biogas.
    - Understand the parameters ruling the co-adsorption of siloxanes and volatile organic compounds, and the competition between them during the adsorption process.
    - Investigate the influence of humidity in the gas matrix upon siloxanes adsorption.

- To decrease the environmental and economic costs of activated carbon by pursuing more sustainable precursor materials:
    - Obtain activated carbons from the valorisation of lignocellulosic waste as precursor material.
    - Evaluate the waste-based resulting adsorbents towards adsorption of siloxanes and VOCs.
    - Compare the performance of the lignocellulosic activated carbons with commercially available materials.

Explore the efficiency of different biotechnologies for the abatement of siloxanes

- In a biotrickling filter:
    - Investigate the anoxic biodegradation of siloxane D4 in a lab-scale biotrickling filter.
    - Study the co-treatment of siloxanes and other biogas impurities in the biotrickling filter as well as the influence of the empty bed residence time in order to optimize the performance of the system.
    - Study the role of an activated carbon layer at the top of the biotrickling filter aiming at enhancing the mass transfer of water insoluble siloxanes.

- In a membrane bioreactor:
    - Investigate the transport efficiency of siloxanes and volatile organic compounds through polydimethylsiloxane membranes in gas-gas experiments.
    - Evaluate the performance of a hollow-fibre membrane bioreactor inoculated with anaerobic digester sludge on the removal of siloxanes in the presence of VOCs.
    - Study the influence of the gas residence time in the membrane bioreactor upon the removal of the pollutants.
    - Assess the impact of different strategies regarding the final electron acceptor upon the performance of the reactor.

Towards coupling technologies

- To merge the knowledge obtained for evaluating the feasibility of coupling biotechnologies, particularly biotrickling filtration, to adsorption onto activated carbon in pursuance of decreasing operational costs associated with carbon frequent replacement and disposal of the spent waste generated.

Chapter 3

MATERIALS & METHODS

3.1   Test gas generation and analytical procedures

This section in the Materials & Methods Chapter aims to describe the procedures for generating the test gas in the different treatment technologies applied as well as the analytical methodologies, which are common methodologies in most of the chapters within the present dissertation.

3.1.1   Synthetic gas production

The generation of the polluted gases was carried out by infusing a liquid mixture of the target siloxanes and VOCs by a syringe pump (Harvard Apparatus) to a nitrogen stream (99.999%, Abelló Linde). N_2 was previously humidified in a water column and accurately regulated by a mass flow controller (Alicat Scientific). The resulting stream was mixed in four static mixers followed by a 1-L mixing chamber. Figure 3.1 shows the set-up for generating polluted streams.
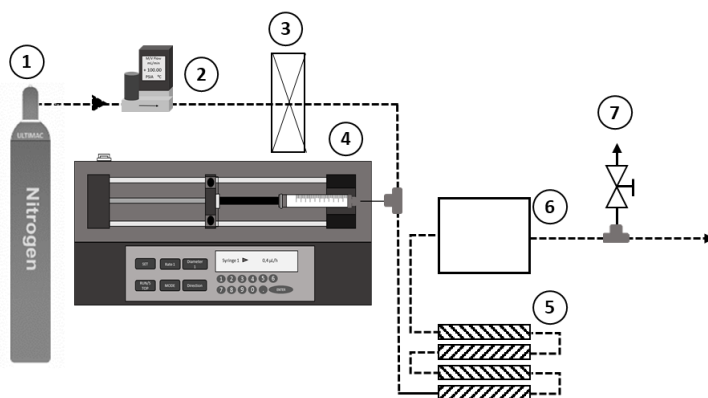
Figure 3.1 Gas generation setup. 1 N_2 bottle; 2 Mass flow controller; 3 Water column; 4 Syringe pump; 5 Static mixers; 6 Mixing chamber; 7 Feed gas sampling point.

The reagents used within this thesis to generate the polluted gases were purchased in liquid form; L2 (98.5 %), D4 (98 %) and D5 (97 %), toluene (99.8 %), n-hexane (98%), d-limonene (95 % purity) and tetrahydrofuran (THF, 99 %) from Sigma Aldrich (USA).

3.1.2   General analytical procedures

The composition of the target stream was analysed via a flow-through gas sampling valve in a gas chromatograph equipped with a flame ionization detector (GC-FID, 7589B Agilent Technologies) and a HP-5ms Ultra Inert capillary column (5%diphenyl-95%dimethylpolysiloxane, 30 m x 0.25 mm i.d. 0.25 µm thickness, Agilent Technologies).

The column oven temperature started from 60 °C (1 min), ramped to 120ºC at 30 °C min^{-1} before increasing to 150 at 10 °C min^{-1} and to 300ºC at 50ºC min^{-1}, held at this temperature for 3 min. The injector temperature was set at 240 °C with helium (99.99% Abelló Linde, Spain) at a split ratio 1:6. Calibration was carried out using external standards prepared in the above described continuous set-up.

3.2   Mineral medium preparation and analysis

The salts for preparing the mineral medium used in the bioreactors were obtained from PANREAC AppliChem with purities higher than 99 %. The synthetic mineral medium contained 1 g L^{-1} NaCl; 0.2 g L^{-1} MgSO$_4$·7H$_2$O; 0.02 g L^{-1} CaCl$_2$·2H$_2$O; 0.04 g L^{-1} NH$_4$Cl; 2 g L^{-1} NaNO$_3$; 1.16 g L^{-1} KH$_2$PO$_4$·H$_2$0; 4.76 g L^{-1} HEPES. pH was adjusted to 6.9 with NaOH 1 M.

NO$_3^-$, NO$_2^-$ and PO$_4^{3-}$ concentrations in the trickling solution of the BTF were analyzed in an Ion Chromatograph (Thermofischer, Dionex, IC5000) coupled with a conductivity detector.

Silicic acid was measured by means of a colorimetric test in which dissolved silicic acid reacted with ammonium molybdate under acid conditions producing the yellow complex molybdosilicate acid. Oxalic acid was added to avoid the formation of molybdophosphate acid and therefore the interference of phosphates. The absorbance of the resulting samples was measured at 410 nm in a spectrophotometer (3100PC, VWR, USA).

Total silica concentration was analyzed by means of inductively coupled plasma-optical emission spectroscopy (ICP-OES, Agilent 5100).

The biodegradation metabolites in the liquid solution were analyzed by GC-MS (7890B GC-5977B MS, Agilent Technologies). Silanediols determination procedure is reported elsewhere [42].

3.3   Adsorption onto activated carbons

This section aims to describe the materials and methods used within Chapters 4, 5 and 8.

3.3.1   Activated carbons

Experimental activated carbons

A set of four chemically activated carbons were obtained experimentally (Table 3.1). The activation procedure was the following: 3kg of lignocellulosic waste generated in a food industry were cleaned and dried at 60 °C. The resulting sample was grounded to a particle size below 5 mm. Part of the grounded sample was pyrolyzed in a tubular furnace Carbolite CTF 12/65/550. Pyrolysis conditions were selected according to previous experience [61,62] and were 150 mL min^{-1} of N$_2$ flow, a heating rate of 5 °C min^{-1} up to 750°C and maintained at this temperature for 60 min. Both the cleaned lignocellulosic waste and its pyrolyzed version were employed as precursors for the experimental activated carbons.

K$_2$CO$_3$ was the activating agent for the non-pyrolyzed samples (AC1 and AC2) and KOH (more reactive agent) for the pyrolyzed samples (AC3 and AC4). Prior to the activation process, the precursor and the activating agent were mixed in solid state in different ratios (0.5/1 and 1/1) as described in Table 3.1. The thermochemical process of KOH/K$_2$CO$_3$ activation was carried out in the aforementioned furnace at the activating temperature and nitrogen flow rate summarized in Table 3.1. After chemical activation the resulting adsorbents were washed with hydrochloric acid solution (5 M) and successively washed with deionized water (Milli-Q) for eliminating residual activation products that might block the obtained porosity. The last step consisted in drying the samples at 105 °C.

Commercial activated carbons

A set of 10 commercial activated carbons with different origin and varied textural and physicochemical properties (listed in Table 3.1) were selected for the removal of siloxanes and VOCs removal in competitive dynamic adsorption tests. The carbon adsorbents were supplied by Cabot (USA), CECA (France), Chemviron (Belgium), Desotec (Belgium), Ingevity (USA) and Jacobi (Sweden). The series of investigated adsorbents includes steam-derived activated carbons (samples denoted as SAC), and phosphoric acid activated carbons (samples denoted as PhAC). Among the samples, one of them is specifically commercialized for biogas treatment (sample denoted as SAC-2). These adsorbents differed in terms of origin, activation process undergone, pore structure and surface chemistry and therefore an extensive characterization

was carried out. Before use, pellets and granular carbons were ground and sieved to obtain a particle size between 212 and 425 µm.

Table 3.1 Activation conditions of the lignocellulosic-waste ACs and commercial samples.

Sample	Precursor	Activation	Activating agent/precursor weight ratio	Activation T [ºC]	N_2 flow rate [cm^3 min^{-1}]
Experimental					
AC1	LGC-W	K_2CO_3	1/1	850	150
AC2	LGC-W	K_2CO_3	0.5/1	900	150
AC3	P-LGC-W	KOH	0.5/1	900	150
AC4	P-LGC-W	KOH	1/1	900	150
Commercial					
PhAC-1	Wood	H_3PO_4	n.a.	n.a.	n.a.
PhAC-2	Wood	H_3PO_4	n.a.	n.a.	n.a.
PhAC-3	Wood	H_3PO_4	n.a.	n.a.	n.a.
PhAC-4	Wood	H_3PO_4	n.a.	n.a.	n.a.
PhAC-5	Wood	H_3PO_4	n.a.	n.a.	n.a.
SAC-1	Peat	Steam	n.a.	n.a.	n.a.
SAC-2	Anthracite	Steam	n.a.	n.a.	n.a.
SAC-3	Bituminous	Steam/N*	n.a.	n.a.	n.a.
SAC-4	Coal	Steam	n.a.	n.a.	n.a.
SAC-5	Coconut	Chemical	n.a.	n.a.	n.a.

*Impregnated / n.a. not available / LGC-W lignocellulosic waste / P pyrolyzed

3.3.2 Adsorbents characterization

Chemical characterization

The ash content and moisture of all the ACs was obtained following the UNE 32004 norm and the UNE 33002 norm, respectively. Therefore, samples were calcined in a muffle at a temperature of 815ºC for 1 hour in order to obtain the ash content. And the moisture of the sample was determined based on the weight loss after 1 h at 105 ºC. An elemental analysis was carried out using a LECO CHN-2000 equipment for determining the carbon, hydrogen and nitrogen contents, and a LECO S-144-DR instrument (LECO Corporation, USA) for analyzing the Sulphur content. The oxygen content was calculated as the difference to reach 100%.

Temperature-programed desorption (TPD) experiments were carried out by means of a DSC-TGA equipment (TA Instruments, SDT 2960 Simultaneous) coupled to a mass spectrometer (Thermostar Balzers, GDS 300 T3) to determine the oxygen-functional groups in the surface of the activated carbons [63]. The heating rate applied was 20 K min^{-1} up to 1000 ºC under a helium flow rate of 100 ml min^{-1} using ca. 10 mg of each sample.

In order to determine the pH_{slurry} of the ACs, ca. 500 mg samples were suspended in 25 mL of deionized water and left stirring for 24 h. The pH and conductivity of the supernatant was then measured with a Crison micro pH 2000 pHmeter. The supernatant phase was also analyzed with ion chromatography (Dionex ICS-500 DP) to determine the leached ions.

Scanning electron microscopy (SEM)

Prior to observation, all the samples were covered with iridium in order to reduce the charging of the materials and obtain improved pictures. A scanning electron microscope ZEISS DMS-942 (ZEISS, United States) equipped with an energy-dispersive X-ray analysis system (Link-Isis II) was used to examine the morphology of the materials.

Textural characterization

Helium pycnometry was carried out on a Micrometrics AccuPyc 1330 pycnometer in order to determine the real density (ρ_{He}) of the materials.

Adsorption-desorption equilibrium isotherms of N_2 at 77K and CO_2 at 273K were volumetrically obtained by a Micrometrics ASAP 2420 and a Quantachrome NOVA 4000 instrument. Prior to adsorption experiments for both gases, all the carbons were outgassed under vacuum at 120ºC overnight for the removal of moisture and other vapors and gases.

The specific surface area (S_{BET}) and the total pore volume (V_{TOT}) at a relative pressure of 0.99 were obtained by fitting the nitrogen adsorption data to the BET equation [64,65]. By applying the density functional theory (DFT) model to the N_2 isotherms, and assuming slit-shaped pore geometry [66], we obtained the pore size distribution; microporosity (V_{umi} <0.7 nm), medium size micropore volume (V_{mmi} 0.7-2 nm) and mesoporosity (V_{me} 2-50 nm).

On the other hand, the narrow microporosity was studied from the CO_2 adsorption isotherms. The micropore volume (W_0) and the characteristic energy (E_0) were calculated from the application of the Dubinin-Radushkevich equation (assuming the density of CO_2 adsorbed as 1.023 g cm^{-3} and the β parameter as 0.36). The Dubinin-Radushkevich surface (S_{DR}) was obtained from the micropore volume. The mean micropore size (L) was evaluated from the expression L = 10.8/(E_0 − 11.4) [67].

3.3.3   Target compounds

Due to the wide spectrum of pollutants found in biogases, a mixture of selected siloxanes and volatile organic compounds (VOCs) was investigated in this doctoral thesis. Their main

physicochemical properties are summarized in Table 3.2, while their molecular structures are shown in Figure 12.1. To calculate the critical diameter of the adsorbates -i.e. the diameter of the smallest cylinder inside which the molecule will fit [68]-, the Cartesian coordinates were obtained using Avogadro software. Principal component analysis was implemented using Matlab software to obtain the bounding box for the molecule system (Figure 12.2). Critical diameters were then computed as the second internuclear distance plus an estimate of the van der Waals radii of hydrogen (0.12 nm).

Table 3.2 Physicochemical properties of each compound in the test gas

Compound	Molecular formula	MW [g mol^{-1}]	Boiling point [ºC]	Critical diameter [nm]	Solubility* [mg L^{-1}]
L2	$C_6H_{18}OSi_2$	162.4	100	0.73	0.930
D4	$C_8H_{20}O_4Si_4$	296.6	175	1.08	0.056
D5	$C_{10}H_{30}O_5Si_5$	370.8	210	1.10	0.017
Toluene	C_7H_8	91.2	111	0.67	526
Limonene	$C_{10}H_{16}$	136.2	176	0.68	7.570
Hexane	C_6H_{14}	86.1	68	-	9.500

*In water at 25 ºC

3.3.4 Adsorption equilibrium experiments

The target compounds selected for carrying out the adsorption equilibrium experiments of this study (in Chapter 5) were toluene, limonene and the siloxanes D4 and L2. The adsorption experiments were carried out at room temperature (25 ± 2 ºC). The adsorption equilibrium of each compound was studied individually using 10-70 mg of powdered activated carbon in 20-cm^3 vials sealed with PTFE septa weighted by an analytical balance (XSR105 Mettler Toledo, USA). Liquid volumes of 4 µL of the target compound were successively injected on the vial and agitated in an orbital mixer for 24 h in a thermostatic chamber at 25 ºC to reach adsorption equilibrium. Preliminary tests showed that adsorption equilibrium was reached after 24 h (data not shown). After this time, the concentration of the target compound (C_e) in the vial headspace was analyzed by a gas chromatograph coupled to a mass spectrometry detector (7980B series GC-MSD, Agilent Technologies) and equipped with a PAL auto sampler system with a headspace tool, and a capillary column HP-5ms Ultra Inert (Agilent Technologies). Calibration was carried out diluting commercial standards of siloxanes (D4 and L2) and VOCs (toluene and limonene) in THF and injection to the 20-cm^3 vials.

The amount of target compound adsorbed at equilibrium, x/M (mg g^{-1}), was calculated by

$$x/M = \left(\frac{C_0 - C_e}{W}\right)V \qquad \text{Eq. 1}$$

where C_0 and C_e are the initial and equilibrium target concentrations (mg m^{-3}); W is the mass of carbon (g); and V is the volume of the vial (m^3). C_0 was calculated according to the amount of target compound injected on the 20-cm^3 vials, which was confirmed by weighing the vial before and after the liquid injection.

3.3.5   Multicomponent dynamic adsorption tests

Multicomponent dynamic adsorption tests, carried out in Chapter 4, were performed at room temperature (25 ± 2 °C), using ca. 250 mg of activated carbon packed in a glass fixed-bed column with an internal diameter of 7 mm. Bed heights ranged from 6 to 11 mm depending on the packing density of the tested adsorbent. The ratio of the column to particle diameter for this packed bed was around 20, considered to be large enough to eliminate the wall effects due to the near-wall lower packing density [69].

The generation of a multicomponent test-gas was achieved by following the procedure detailed in Section 3.1.1, excluding the water column to humidify the test gas. A mixture of the target pollutants was infused to a dry N_2 flow of 200 mL STP min^{-1} settled using a mass flow controller (Alicat Scientific) (Figure 3.2). The liquid mix was obtained using known amounts of siloxanes and VOCs. Their concentrations in a gas stream (detailed at the corresponding Results chapter) were proportionally higher than those found in real biogases [4], in order to obtain the breakthrough of the carbon beds in affordable experimental times, as well as simplified analytical procedures. The concentration of each compound in the outlet was continuously measured as described in Section 3.1.2.
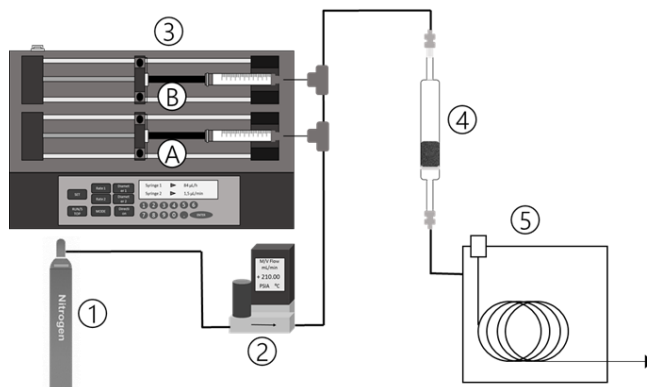
Figure 3.2 Set-up of the dynamic adsorption test: (1) Carrier gas (N$_2$); (2) Mass flow controller; (3) Syringe pump filled with a) target compounds mixture and b) DI water for wet tests; (4) fixed bed adsorbent; (5) GC-FID

Dynamic adsorption tests were carried out in a dry gas matrix and also in wet conditions by adding another syringe filled with distilled water and pumped to the N$_2$ gas at 1.5 µL min^{-1} so that the relative humidity in the test gas was around 25 ± 5 %, similar to real biogas content. The humidity content of the carrier gas was measured with an appropriate sensor (Testo 635). For each adsorption experiment, the adsorption column was operated until the compounds' outlet concentrations matched the inlet concentrations (i.e., bed exhaustion). Breakthrough curves were thus obtained by plotting the $c(t)/c_0$ vs. time where c_0 is the inlet concentration (mg m^{-3}) and $c(t)$ is the outlet concentration (mg m^{-3}) at a given time. The adsorption capacity of each activated carbon for every target compound (x/M, in mg of compound per gram of carbon adsorbent) was calculated as follows:

$$\frac{x}{M} = \frac{Q}{\omega}\left(c_0 t_s - \int_0^{t_s} c(t)dt\right) \qquad \text{Eq. 2}$$

where Q is the inlet flow (m^3 s^{-1}), ω is the adsorbent weight (g) and t_s is the bed exhaustion time (s).

3.3.6 Spent carbon analysis

The spent activated carbons after the dynamic adsorption tests (in Chapter 4) were analyzed to determine the formation of cyclic or lineal siloxanes and α-ω-silanediols (during the adsorption experiments) in the adsorbed phase. The concentration of these compounds was

measured following the analytical procedure indicated by Varaprath and Lehmann (1997) [70]. For this purpose, and in order to compare the activated carbons in the same conditions, the multicomponent adsorption tests were stopped after 30 min of run. Then, the spent carbon samples were suspended in 20 mL of anhydrous THF, vortexed for 2 min and shaken in an orbital mixer for 30 min. The resulting suspensions were centrifuged at 6000 rpm for 5 min (EBA 21, Hettich Zentrifugen) and the liquid phase was analyzed.

In adsorption equilibrium experiments at 25 °C (obtained in Chapter 5), a representative mass of 30 mg of powdered activated carbon samples were placed in 20-cm^3 vials and 6 μL of reagent D4 or L2 were injected through the septa of the vial. After 24 h of contact for adsorption/transformation to happen, 10 mL of THF were injected to the vials, vortexed for 2 min and shaken in an orbital mixer for 30 min. The resulting suspensions were filtered through 0.45 μm and the liquid suspensions were analyzed. Spent carbon experiments were performed in duplicate (error < 4%).

The analysis of the THF suspensions was carried out in a gas chromatograph coupled to a mass spectrometry detector (5977E series GC-MSD, Agilent Technologies) and equipped with a capillary column HP-5ms Ultra Inert (Agilent Technologies). Calibration was carried out using commercially available (Sigma Aldrich, USA) standards of cyclic siloxanes (D3, D4, D5), lineal siloxanes (L2, L3, L4, L5) and VOCs (toluene and limonene). The gas chromatograph was operated at 60 °C for 3 min, followed by a heating ramp of 20 K min^{-1} from 60 to 120 °C and 40 K min^{-1} until 250 °C. Retention time and analytical ions of the target compounds were previously reported [42].

3.3.7   Adsorption costs assessment

A biogas flowrate of 1000 m^3 h^{-1} containing average concentrations of VOCs (hexane, toluene and limonene) and siloxanes (D4 and D5) was set as biogas model to assess the capital (CAPEX) and operation cost (OPEX) of siloxane removal. Both CAPEX and OPEX calculations were estimated according to the literature revision [71,72]. Capital investments were annualized for a period of 10 years to calculate total annual costs of each scenario.

For scenarios coupling biotechnology and adsorption on activated carbons, the volume of the biotrickling filters was calculated following Eq. 3 according to the flowrate and EBRT set for S-B (1.5 min) and S-C (14 min).

$$V = F \times EBRT \qquad\qquad \text{Eq. 3}$$

where V is the reactor volume (m^3), F the biogas flowrate (m^3 h^{-1}) and EBRT is the empty bed residence time (h). Moreover, the scale up of larger bioreactor was calculated following the rule of six-tenths as in Eq. 4 [73].

$$C_B = C_A \left(\frac{V_B}{V_A}\right)^{\alpha} \qquad\qquad \text{Eq. 4}$$

where C refers to the equipment costs (€) and V to the volume of the reactors (m^3). α is the scale coefficient, which can vary from 0.3 to 0.9 in a wide range of equipment [73].

For the adsorption filter, the economic data referring to operational costs was estimated taking into account (i) the bed volumes obtained from the breakthrough curves, (ii) the density and (iii) price of each material. The CAPEX for the adsorption unit was estimated according to literature [54]. The prices for the ACs was stablished at 2, 4 and 7 € kg^{-1} for AC1, AC2 and AC3 respectively, according to personal communications with the corresponding manufacturers. Bed exhaustion of the carbon was considered for its replacement following a lead-lag configuration.

3.4   Biotrickling filtration

This section describes the reactor setup and defines the methodology followed in Chapter 6.

3.4.1   BTF inoculum

Anaerobic sludge from the mixed sludge anaerobic digester of the urban wastewater treatment plant of Rubí (Barcelona, Spain) was used as precursor inoculum in the biotrickling filter. The anaerobic sludge was centrifuged at 6000 rpm for 10 min and re-suspended in fresh synthetic mineral medium. This procedure was repeated several times in order to clean the sludge from dissolved organic matter. The BTF was first inoculated with 320 mL of anaerobic sludge and left recirculating for three days to promote biomass attachment to the lava rock. At day 43, the BTF was re-inoculated using a *Pseudomonas aeruginosa* strain isolated from anaerobic sludge samples by selective growth using the picking up method. The culture was incubated in liquid mineral salts medium containing D4 as a carbon source at 30 ºC and 125 rpm in an orbital shaker. After 72 hours, the inoculum was centrifuged and washed four times in mineral media without D4. The *P. aeruginosa* culture was finally re-suspended in 250 mL of synthetic mineral solution without residual organic compounds. The initial population density of *P. aeruginosa* culture was 4.06×10^6 cell mL^{-1}.

3.4.2 Experimental setup

A schematic of the lab-scale biotrickling filter setup designed and constructed for this study is shown in Figure 3.3. The reactor consisted of a cylindrical glass column with an inner diameter of 6 cm and a total height of 46 cm. The packing material consisted of inert lava rock of 8-12 mm particle size. Different empty bed residence times of 4.0, 7.3, 10.1 and 14.5 min were evaluated. The reactor was operated in a counter-current flow configuration. A trickling solution of synthetic mineral salt medium (described previously in Section 3.2) was continuously recirculated by a peristaltic pump (Watson Marlow, USA) from an external reservoir and sprayed through the top of the bed column at a rate of 47 cm h^{-1}. The total volume taking into account the piping as well as the reservoir accounted for roughly 400 cm^3. The trickling solution was renewed completely every 72 h (which represented a dilution rate of 0.3 days^{-1}). Anoxic conditions were provided during the whole operation of the BTF by supplementing the mineral medium with 2 g L^{-1} $NaNO_3$ (NO_3^- acting as the final electron acceptor).
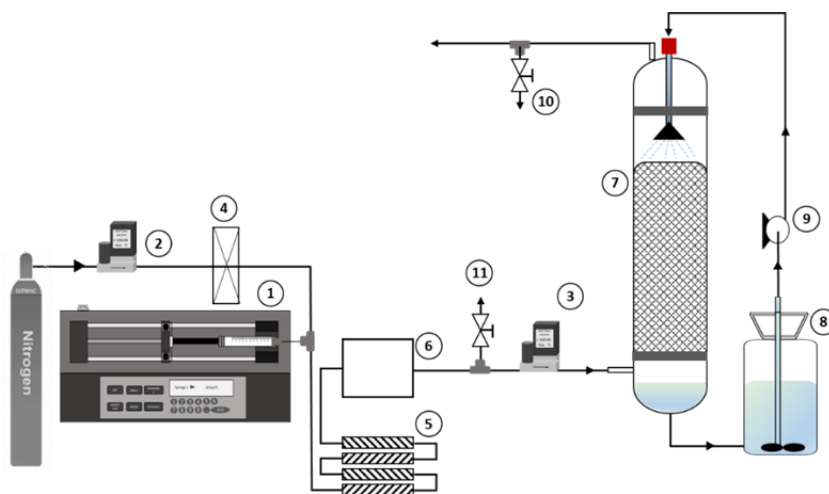
Figure 3.3 Schematic of the lab-scale BTF. 1 Syringe pump; 2 and 3 Mass flow controllers; 4 Humidifier; 5 Static mixers; 6 Mixing tank; 7 Bioreactor; 8 Nutrients tank; 9 Peristaltic pump; 10 and 11 sampling points.

The feed gas flow was accurately regulated by a mass flow controller (Alicat Scientific, USA) and was divided for the reactor inlet and a purge for analysis matters. The synthetic gas was composed by VOCs (hexane, toluene and limonene) and siloxanes (D4 and D5), the concentrations of which are latter described in the corresponding results chapter.

3.4.3 Operating conditions and process monitoring

The operation of the BTF was divided into four stages related to the carbon source provided in the gas stream and the type of packing material used in the BTF (Table 3.3). Stage I (days 0-42) operated with a N_2 stream containing D4 at 62 ± 2 mg m^{-3} supplied at an EBRT of 14.5 min. In stage II (days 43-152), a multicomponent mixture of siloxanes (D4 and D5) and VOCs (hexane, toluene and limonene) was supplied. These biogas pollutants were selected based on their occurrence in sewage biogas [6]. During stage II, the influence of the EBRT (14.5, 10.1, 7.3 and 4 min) on the removal efficiency and elimination capacity of the target biogas contaminants was tested. The higher EBRTs used in the present study compared to those reported in the literature were due to the anoxic conditions selected for biodegradation, which are needed to prevent biogas contamination with O_2 in case biogas is to be injected into natural gas grids. In stage III (days 153-186), 35 g of a commercial activated carbon in pellet size (2-3 mm particle size) were added at the top of the packed bed, which accounted for a layer of approximately 5 cm of packing bed. The AC selected was a wood-based chemically activated with H_3PO_4 (a.k.a. PhAC-1). It was selected due to its high siloxane adsorption capacity as well as its capacity to transform siloxanes into α-ω-silanediols in the presence of moisture (Chapter 4 and 5). Finally, the packing lava rock was removed from the column, and the biofiltration process was performed with the 5 cm layer of AC (introduced during Stage III) as the only packing bed (Stage IV, days 187-207). During stage II-4 and stage IV, the influence of the trickling solution irrigation on the performance of the BTF was evaluated by stopping (5 h) and re-starting the recirculation of the trickling solution. During these events, the outlet gas stream of the BTF was continuously monitored by GC-FID. An abiotic test was initially carried out to evaluate the physicochemical removal of siloxane D4 in the experimental set-up.

Table 3.3 Operating conditions of the BTF.

Stage		Period [days]	C-source	EBRT [min]	Packing media
I		0-42	D4	14.5	Lava rock
II	-1	43-85	Multicomponent	14.5	Lava rock
	-2	86-107	Multicomponent	10.1	Lava rock
	-3	108-128	Multicomponent	7.3	Lava rock
	-4	129-152	Multicomponent	4.0	Lava rock
III		153-186	Multicomponent	12.0	Lava rock + AC
IV		187-207	Multicomponent	2.0	AC

Multicomponent = Mixture of D4, D5, hexane, limonene and toluene

The composition of the inlet and outlet gas emission of the BTF was analyzed as explained in Section 3.1.2. Routine analysis of the inlet and outlet gas streams was performed in triplicate (coefficient of variation < 6%).

Silicic acid was measured by means of a colorimetric test in which dissolved silicic acid reacted with ammonium molybdate under acid conditions producing the yellow complex molybdosilicate acid. Oxalic acid was added to avoid the formation of molybdophosphate acid and therefore the interference of phosphates. The absorbance of the resulting samples was measured at 410 nm in a spectrophotometer (3100PC, VWR, USA). Total silica concentration was analyzed by means of inductively coupled plasma-optical emission spectroscopy (ICP-OES, Agilent 5100). Finally, the biodegradation metabolites in the trickling solution were analyzed by GC-MS (7890B GC-5977B MS, Agilent Technologies). Silanediols determination procedure is reported elsewhere [42]. Limonene metabolites were identified by GC-MS analysis by comparing the m/z of the metabolites with those in the NIST library, and by injecting pure reagents (if commercially available) for further confirmation.

On the other side, THF was used as solvent to extract polar and nonpolar species that remain adsorbed or biosorbed in the solid support and the biomass film.

3.4.4   SEM analysis

Samples of the lava rock and activated carbon were taken at different times for Scanning Electron Microscope (SEM) analysis in order to observe the biomass grown in the packed bed of the BTF. Biomass in the samples was fixed with 2.5% (wt/vol) glutaraldehyde in 0.1 M cacodylate buffer (pH 7.4) at 4°C for 4 h. Then, biomass samples were washed and dehydrated successively in ethanol, dried at the critical point CO_2 method (K 850 CPD, Emithech, Germany), and covered in carbon by the evaporation method with a turbo evaporator (K950, Emitrech, Germany). The analysis of the samples was carried out with a scanning electron microscope (S-4100 FE-SEM Hitachi, Japan). Digital images were collected and processed by Quartz PCI program.

3.5   Membrane separation

This present section defines the materials and methods employed in Chapter 7.

3.5.1 Gas abiotic experiments

Preliminary abiotic experiments were carried out with a polluted gas flowing through the lumen side (inside fibers) and clean gas through the shell side (outside membranes) as displayed in Figure 3.4. The feed gas flowing through the lumen side was set constant at 50 mL min^{-1} by a mass flow controller. On the other side of the fibers (shell side), a clean N2 stream was provided at rates ranging from 25 mL min^{-1} to 400 mL min^{-1} to give different shell-to-lumen flow ratios (0.5, 1, 2, 4 and 8).

The PDMS membrane module employed for the first set of experiments was the PermSelect PDMSXA-10 cm2 (MedArray Inc, USA). The module consisted of 30 parallel dense hollow fibers of 190 µm inner diameter and 300 µm outer diameter. The membrane area was roughly 10 cm^2 and the lumen priming volume 0.67 cm^3, so the gas residence time, considering that the lumen flow was set constant, accounted for 0.72 s.

For each experiment, the polluted gas was run overnight to reach steady state, due to possible adsorption of the compounds in the membrane fibers taking place.
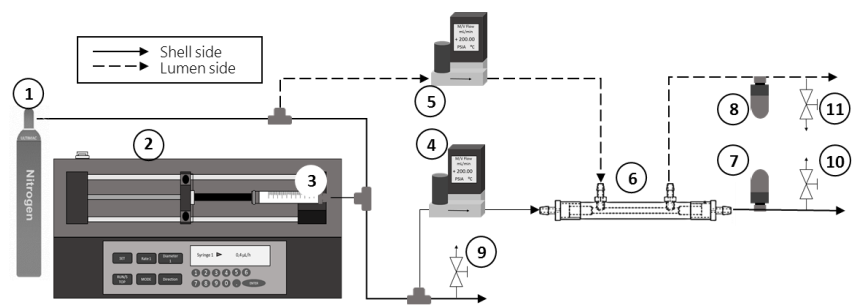
Figure 3.4 Membrane setup for gas-gas experiments: (1) N$_2$ cylinder; (2) Syringe pump; (3) 250-mL syringe with mixture; (4, 5) Mass Flow Controllers; (6) Hollow-fiber membrane (PDMSXA-10); (7, 8) Pressure transducers and (9, 10, 11) sampling ports for GC analysis.

3.5.2 Hollow-fiber membrane bioreactor setup

A schematic of the HF-MBR setup is shown in Figure 3.5. The reactor consisted in a commercial hollow-fiber module (PDMSXA-2500, PermSelect®, MedArrays Inc, USA) that consisted in 3200 hollow fibers of 190 and 300 µm inner and outer diameter, respectively. The total membrane area accounted for 2500 cm^2, the lumen-side priming volume of 21 cm^3 and the shell-side priming volume 26 cm^3. A synthetic polluted gas -containing VOCs (hexane, toluene and limonene) and siloxanes (D4 and D5)- was regulated by a mass flow controller and fed

through the lumen side of the membrane module. Through the shell side, a mineral medium with nutrients was recycled at 100 mL min^{-1} by a peristaltic pump (Watson Marlow, USA) from an external reservoir continuously agitated.
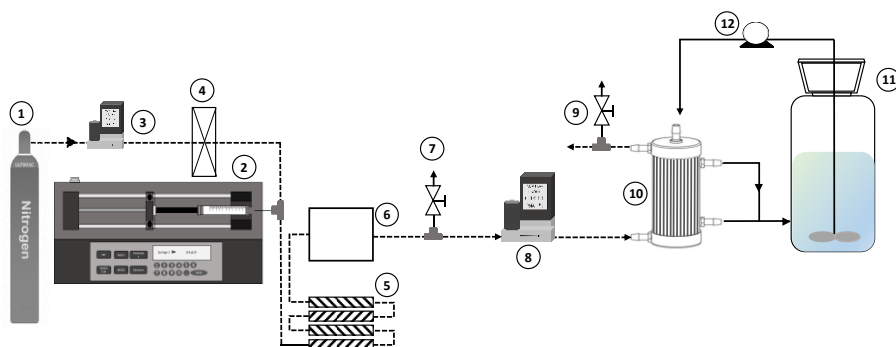
Figure 3.5 Schematic representation of the HF-MBR. 1 N2 bottle; 2 Syringe pump; 3 and 8 Mass flow controllers; 4 Water column; 5 Static mixers; 6 Mixing chamber; 8 and 9 Sampling points; 10 HF-MBR; 11 Nutrients reservoir; 12 Peristaltic pump.

HF-MBR Inoculum

Anaerobic sludge from the anaerobic digester of the urban wastewater treatment plant of Girona (Spain) was used as inoculum in the membrane bioreactor. In order to remove the dissolved organic matter from the sludge, the following procedure was carried out 3 times: centrifugation (EBA 21, Hettich Zentrifugen) at 10000 rpm for 10 min, pouring the remaining water and re-suspension with fresh mineral medium. The sludge was diluted to a final concentration of 4.2 g TSS L^{-1}, and 250 mL of the cleaned and diluted sludge were used as MBR inoculum.

Operating conditions

Before inoculating the HF-MBR, an abiotic mass transfer characterization of the target VOCs and siloxanes was conducted according to Lebrero et al., (2014) [74] at different gas residence times in an open. The polluted gas was supplied through the lumen side of the membrane regulated by a mass flow controller whereas a clean water flow was circulated at a constant flow of 100 mL min^{-1} through the shell side of the module. The abiotic transfer of the target pollutants vas evaluated at 9.6, 16, 24, 40 and 60 s of gas residence time.

Then, the membrane module was inoculated with 250 mL of the cleaned sludge corresponding to a concentration of 4.2 g TSS L^{-1} and operated at 18 s of gas residence time in the period 0-36 days (stage I) as detailed in Table 3.4, corresponding to a gas flow of 70 mL min^{-1}. The recirculating solution was renewed every 72 corresponding to a dilution rate of 0.3 d^{-1}. The

influence of the gas residence time on the removal of the target pollutants was evaluated by increasing it to 31.5 s (period II days 37-64) and 63 s (days 65-73). At day 73, an automatic injection of NO_3^- was started by infusing a solution of 200 g NO_3^- L^{-1} (provided by $NaNO_3$ of 99% purity) to the recirculation solution by means of a syringe pump (Harvard Apparatus) and the dilution rate of the recirculation solution was decreased to 0.1 d^{-1}. The infusion rate of the NO_3^- solution was started at 15 μL h^{-1} and adjusted when necessary. In the period 101-133, the gas residence time was decreased back to 18 s. A membrane cleaning was carried out at day 107 following the procedure described by Lebrero et al., (2014), which consisted in increasing the liquid recycling rate in order to slough off the biomass clogging. In stage IV the carrier gas was supplemented with 1% of O_2 at day 134 and was operated with NO_3^- and O_2 as final electron acceptors until day 152. Finally, from day 153 to 164, the reactor was operated with only O_2 and the automatic infusion of NO_3^- was stopped.

Table 3.4 Operating conditions of the HF-MBR.

Stage	Period [days]	EBRT [s]	Final e^- acceptor	Strategy
I	0-36	18	NO_3^-	Manual
II	37-64	31.5	NO_3^-	Manual
III	65-73	63	NO_3^-	Manual
	74-100	63	NO_3^-	Automatic
	101-133	18	NO_3^-	Automatic
IV	134-152	18	$NO_3^-+O_2$	Automatic
	153-164	18	O_2	Automatic

Analytical procedures

NO_3^- concentration in the recycling solution of the HF-MBR was analyzed by a Spectrophotometer (Cary3500, Agilent Technologies) following the Standard Methods. Biodegradation by-products in the trickling solution were analyzed by Gas Chromatography coupled to a Mass Spectrometry detector (GC-MS, 7890B-5977B, Agilent Technologies) and α-ω-silanediols determination was carried out following the procedure reported by Cabrera-Codony *et al.*, (2017) [42].

CO_2 in the effluent of the HF-MBR was analyzed by means of a gas sampling valve in the GC-MS described above, by monitoring the ion with m/z 44. Calibration standards were prepared by diluting CO_2 (99.99%, Abelló Linde, Spain) to N_2 streams.

The performance of the HF-MBR was evaluated by the removal efficiency (RE) and the elimination capacity (EC) following Eq. 5 and Eq. 6, respectively. In order to evaluate the biological degradation, the carbon mineralization efficiency (CME) was defined as in Eq. 7.

$$RE\ (\%) = \left(\frac{C_0 - C_F}{C_0}\right) \times 100 \qquad\qquad \text{Eq. 5}$$

$$EC\ (g\ m^{-3}h^{-1}) = \left(\frac{(C_0 - C_F) \times Q}{V}\right) \qquad\qquad \text{Eq. 6}$$

$$CME\ (\%) = \left(\frac{C_{CO2}\ produced}{(C_{Hexane} + C_{Toluene} + C_{Limonene} + C_{D4} + C_{D5})\ removed}\right) x100 \qquad \text{Eq. 7}$$

Where C_0 and C_F are the target compound concentrations (g m^{-3}) in the inlet and outlet of the HF-MBR, Q is the gas flow (m^3 h^{-1}) and V the reactor volume (m^3).

RESULTS

Chapter 4

RESULTS I

Competitive siloxane adsorption in multicomponent gas streams

4.1   Background and objectives

Most studies on siloxanes adsorption at lab-scale using activated carbons report the removal of D4 and D5, correlating the accessibility and uptake of D4 and D5 with the textural properties of the activated carbons, i.e. surface area and pore volume [20,33]. However, to simulate a real application scenario it is necessary to consider mixed component streams, introducing the complexity of competitive adsorption. In this regard, volatile organic compounds (VOCs) - including limonene, toluene, xylenes or methylated benzene compounds- are found in a wide range of concentrations in biogas and may compete with siloxanes in the adsorption process [4,29]. There is scarce experimental work done on the adsorption of siloxanes in the presence of other trace compounds of biogas [22,39], thus, little is known about the competitive adsorption to understand the system for design purposes.

The objective of this study is the screening of a series of nanoporous carbons for the removal of multicomponent mixtures of siloxanes and VOCs from biogas. To understand the parameters ruling the coadsorption of these compounds, a set of ACs from different origin and activation process displaying a wide range of textural and chemical properties were used in multicomponent dynamic adsorption tests, in both dry and wet gas matrices.

4.2   Methodology

A set of 10 commercial activated carbons with different origin and varied textural and physicochemical properties were selected for the removal of siloxanes and VOCs removal in competitive dynamic adsorption tests. The series of investigated adsorbents includes steam-derived activated carbons (samples denoted as SAC), and phosphoric acid activated carbons (samples denoted as PhAC) and their origin and activation are detailed in Table 3.1 (Section 3.3). Among the samples, one of them is specifically commercialized for biogas treatment (sample denoted as SAC-2). An extensive characterization was carried out (detailed in Section 3.3.2).

In order to investigate their capacity for removing siloxanes, multicomponent dynamic adsorption experiments -in dry conditions and in the presence of humidity- were carried out according to Section 3.3.5 with the target compounds in Section 3.3.3. The catalytic activity of the materials was investigated by means of extraction with THF, as explained in Section 3.3.6.

4.3   Results

4.3.1   AC textural characterization

A thorough textural characterization of the investigated activated carbons was carried out by the analysis of the N_2 (Figure 4.1A,B) and CO_2 (Figure 4.1C,D) adsorption isotherms. Selected textural parameters obtained from different methods are summarized in Table 4.1. Inspection of the N_2 adsorption/desorption isotherms revealed a number of distinctive features in the carbons. For instance, SAC-1, SAC-2 and SAC-3 (later referred to as Group A) exhibited type Ia N_2 adsorption isotherm according to the IUPAC classification [75], characterized by a marked knee at low relative pressures and almost negligible hysteresis loops in the desorption branch. These are the typical porous features of highly microporous materials with a pore structure dominated by narrow micropores.
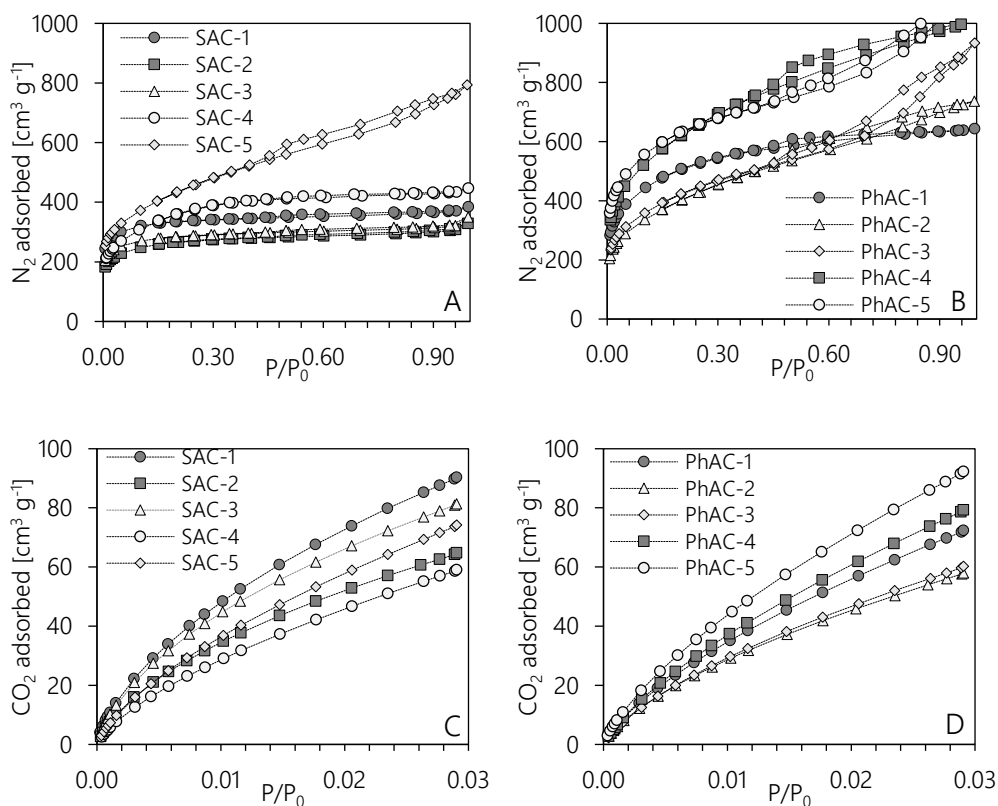
Figure 4.1 N_2 adsorption/desorption isotherms at 77 K: a) steam-AC, and b) H_3PO_4-AC. CO_2 adsorption isotherms at 273K obtained for c) steam-AC, and d) H_3PO_4-AC.

This was further confirmed by the CO_2 adsorption data (Figure 4.1C,D). In the case of carbon SAC-4 (Figure 4.1A) and PhAC-1 (Figure 4.1B), the knee of the isotherm is more open at low relative pressures (type Ib isotherm), indicating the presence of wider micropores. At converse, the nitrogen adsorption isotherms of samples SAC-5 (Figure 4.1A) as well as the rest of chemically activated carbons (ca. PhAC-2, PhAC-3, PhAC-4 and PhAC-5 in Figure 4.1B) showed more pronounced and gradually increasing slopes at relative pressures above 0.2 (still characteristic of type Ib isotherms), accompanied by well-defined hysteresis loops (type H4) typically reported for microporous activated carbons with a well-developed mesoporosity.

The analysis of the distribution of pore sizes was performed by the 2D-NLDFT-HS method applied to the N_2 adsorption isotherms corroborated these findings (Figure 12.3). As seen, the steam-activated carbons SAC-1, SAC-2 and SAC-3 showed distribution of pore sizes dominated by the micropores, with a large contribution of micropores below ca. 1 nm. In contrast, the pore size distribution (PSD) are broader and shifted towards pores of larger dimension for carbons SAC-4 and SAC-5, both showing an important contribution of wide micropores and small size mesopores (Figure 12.3). Similarly, the carbons obtained by phosphoric acid activation displayed wide distributions of pore sizes (Figure 12.3), with lower volumes in the primary micropore region (below ca. 1 nm) and higher volumes in the secondary micropores (ca. 1-2 nm) and mesopores region (2-50 nm).

Table 4.1 Packing density and main textural properties of the series of investigated ACs.

Sample	ρ_{ap} [g cm^{-3}]	S_{BET} [m^2 g^{-1}]	VDR$^a_{CO2}$ [cm^3 g^{-1}]	VDR$^b_{N2}$ [cm^3 g^{-1}]	V_{meso} ^{c} [cm^3 g^{-1}]	V_t^d [cm^3 g^{-1}]	micropores [%]
SAC-1	0.366	1114	0.35	0.43	0.03	0.48	93.7
SAC-2	0.356	909	0.26	0.34	0.05	0.42	87.7
SAC-3	0.490	970	0.31	0.36	0.04	0.43	90.3
SAC-4	0.332	1250	0.23	0.44	0.16	0.65	73.9
SAC-5	0.202	1530	0.29	0.46	0.56	1.10	45.4
PhAC-1	0.340	1737	0.29	0.58	0.25	0.91	70.0
PhAC-2	0.305	1082	0.23	0.38	0.64	1.07	37.3
PhAC-3	0.241	1567	0.24	0.35	0.96	1.41	33.6
PhAC-4	0.240	2170	0.32	0.62	0.76	1.51	44.9
PhAC-5	0.288	2190	0.35	0.70	0.77	1.58	47.3

[a] narrow micropores vol. obtained from the Dubinin-Radushkevich method applied to CO_2 adsorption data
[b] total micropore vol. obtained from the Dubinin-Radushkevich method applied to N_2 adsorption data
[c] obtained from 2D-NLDFT-Hs method applied to N_2 adsorption data
[d] obtained at relative pressure P/P_0 0.99

4.3.2 AC chemical characterization

To investigate the acidic/basic character of the ACs, the pH values of aqueous slurries of the carbons were measured (Table 4.2). As expected, the steam-activated carbons (series SAC) display a basic character with pH values ranging about 7.8-8.5; on the other hand, the chemically activated carbons (series PhAC) showed an acidic character, with pH values between 2 and 4 in the case of PhAC-2 and PhAC-4, and close to neutrality for the rest of the series. Low pH values are often reported for nanoporous carbons after activation using phosphoric acid, due to the difficulties in eliminating the activating agent remaining inside the nanopores [76]. Indeed, the ion analysis of the slurries revealed a high concentration of phosphates in the leachates of certain H_3PO_4- activated samples, such as PhAC-2. PhAC-1 leached also a remarkably high amount of PO_4^{-3}, neutralized by NaOH resulting in an almost neutral pH_{slurry}.

TPD-MS analysis was used to characterize the different O-containing surface groups of the studied activated carbons, whose nature and amount depend on the starting material and the activation treatment. Upon thermal treatment, CO_2 evolution results from the decomposition of carboxylic acid moieties at temperatures below 500 ºC, and/or lactone groups at above 600ºC. Phenols, ether and carbonyl/quinone-type groups (non-acidic ones) decompose as CO above 600 ºC [77]. Carboxylic anhydrides originate both a CO and CO_2 peak (Figure 12.4).

Table 4.2 pHslurry, relevant ions in the slurry, humidity content of the samples and amounts of CO and CO2 realized, obtained by integration of the areas under the TPD peaks of each AC.

	pH_{slurry}	Soluble PO_4^{-3} [mmol g^{-1}]	Soluble Na^+ [mmol g^{-1}]	Humidity [wt%]	CO [µmol g^{-1}]	CO_2 [µmol g^{-1}]
SAC-1	8.64	-	-	9.4	182	206
SAC-2	8.22	-	-	3.2	229	140
SAC-3	7.89	-	-	5.1	448	221
SAC-4	8.34	-	-	2.7	97	38
SAC-5	7.95	-	-	13.6	377	352
PhAC-1	6.51	10.7	14.4	8.8	2049	579
PhAC-2	2.23	17.9	0.4	12.0	2702	604
PhAC-3	6.08	1.4	1.8	5.2	1055	242
PhAC-4	4.67	2.8	2.9	7.0	2030	507
PhAC-5	7.35	0.8	1.8	7.6	2315	558

Table 4.2 shows the amounts of CO and CO_2 released, obtained by quantification of the TPD-MS profiles corresponding to the m/z 28 and 44, respectively. As seen, steam-ACs showed a low O-functionalization, in terms of low amount of CO and CO_2 releasing groups. This feature, along with the increasing pattern of the CO profiles above ca. 700 ºC is characteristic of hydrophobic activated carbons [78]. The CO_2-desorbing patterns of the PhAC series showed a broad peak between 300-550 ºC, attributed to the decomposition of carboxylic, lactone and

anhydride groups. It should also be noted that the TPD-MS measurements were performed in the as-received (i.e. non-dried) carbons. Therefore, a marked desorption peak for signal m/z 18 was observed at around 100 ºC for all the carbons, due to the removal of the moisture (Figure 12.4). Interestingly, the patterns of the profiles corresponding to H_2O and CO desorption peaks were similar above 450 ºC; this suggests that the high temperature m/z18 peaks may be originated from the condensation of neighbour –OH moieties.

The humidity content of the AC samples was determined by the loss of mass caused by dry N_2 flow during 5 h and verified by infrared moisture analyser (Table 4.2). As a general rule, higher humidity contents were obtained for the carbons prepared by phosphoric activation, which displayed higher amounts of O-containing functional groups, indicating the hydrophilic character of theses carbons with higher functionalization.

4.3.3   Multicomponent breakthrough curves

The dynamic competitive adsorption of the series of 10 commercial ACs for a gaseous mixture of siloxanes and VOCs (Table 3.2) was investigated. The breakthrough curves corresponding to the adsorption in the absence and the presence of moisture are shown in Figure 4.2, showing quite complex profiles. In general terms, the curves presented an S-shape profile characteristic of the adsorption of compounds with high affinity for the solid phase. However, the profiles of toluene, L2 and D4 are quite steep, as opposed to those of limonene and D5 showing a flatter shape, indicating some mass transfer resistance inside the micropores for the former (likely due to the larger dimensions of D5).

The breakthrough curves showed a different pattern depending on the nature of the compounds adsorbed, with a clear overshot (the outlet concentration, C, exceeds the feed concentration, C_0, for some period of time) for the adsorption of toluene, L2 and D4 from the mixture in most of the studied activated carbons. Such roll-up effect is characteristic of systems where the most weakly adsorbed compound of the mixture is displaced by the strongly bonded one along the length of the column [79].

The correlation of the adsorption patterns in the mixture and the characteristics of the activated carbons did not show a straightforward correlation. However, three distinct groups can be established upon further analysis of the breakthrough sequence and patterns. The first set of adsorbents (group A) comprises the steam activated carbons SAC-1, SAC-2 and SAC-3. As shown in Figure 4.2A (see also Figure 12.5), limonene was, by far, the compound removed to the highest extent, despite of its low concentration in the test gas. The other four components

in the mixture (i.e. toluene and the three siloxanes) broke through at t < 100 min, following the order: toluene ≈ L2 < D4 < D5. Furthermore, the profiles of toluene, L2 and D4 showed overshoots, indicating the displacement of these compounds upon the adsorption of D5 and/or limonene. Interestingly, these carbons showed PSD dominated of micropores with a minor contribution of mesopores (accounting for ca. 6, 12 and 10%, respectively).

SAC-4 and SAC-5 account for the second group (group B), showing the characteristic profiles exemplified in Figure 4.2B (see also Figure 12.5). Limonene was also the compound with the highest uptake; the profiles were spaced out compared to group A, with breakthrough times following the trend: toluene < L2 < D4 < D5 < limonene. At bed exhaustion, the amount of D5 adsorbed was higher than the other compounds (Figure 12.6). The profiles of toluene, L2 and D4 showed marked overshoots, being this effect more pronounced than in the case of group A, particularly for L2. Interestingly, carbons SAC-4 and SAC-5 showed a higher contribution of mesopores, and micropores of wider sizes compared to group A.

The third group of materials (group C) was composed by the PhACs, and all of them followed the common dynamic competitive adsorption pattern represented in Figure 4.2C (see also Figure 12.5). The weakest adsorbed compound was toluene, followed by L2, D4 and limonene. Again, the breakthrough curves show a clear roll-up behaviour due to the displacement promoted by D5 (the compound showing the highest retention time). In terms of porosity, these carbons presented the larger pore volumes and PSD of wide micro- and mesopores. Another important difference is the acidic character of these carbons and their higher functionalization (O-containing groups) compared to the carbons of groups A and B.

Interestingly, the adsorption capacities at bed exhaustion for each compound (Figure 12.6) were significantly higher for the series of chemically activated carbons (i.e., H_3PO_4-ACs) than those for the steam-activated ones, with total uptakes (x/M) of up to 1373 mg g^{-1}. Additionally, the amount of VOCs adsorbed at bed exhaustion represents less than 20% of the total x/M for all the carbons.
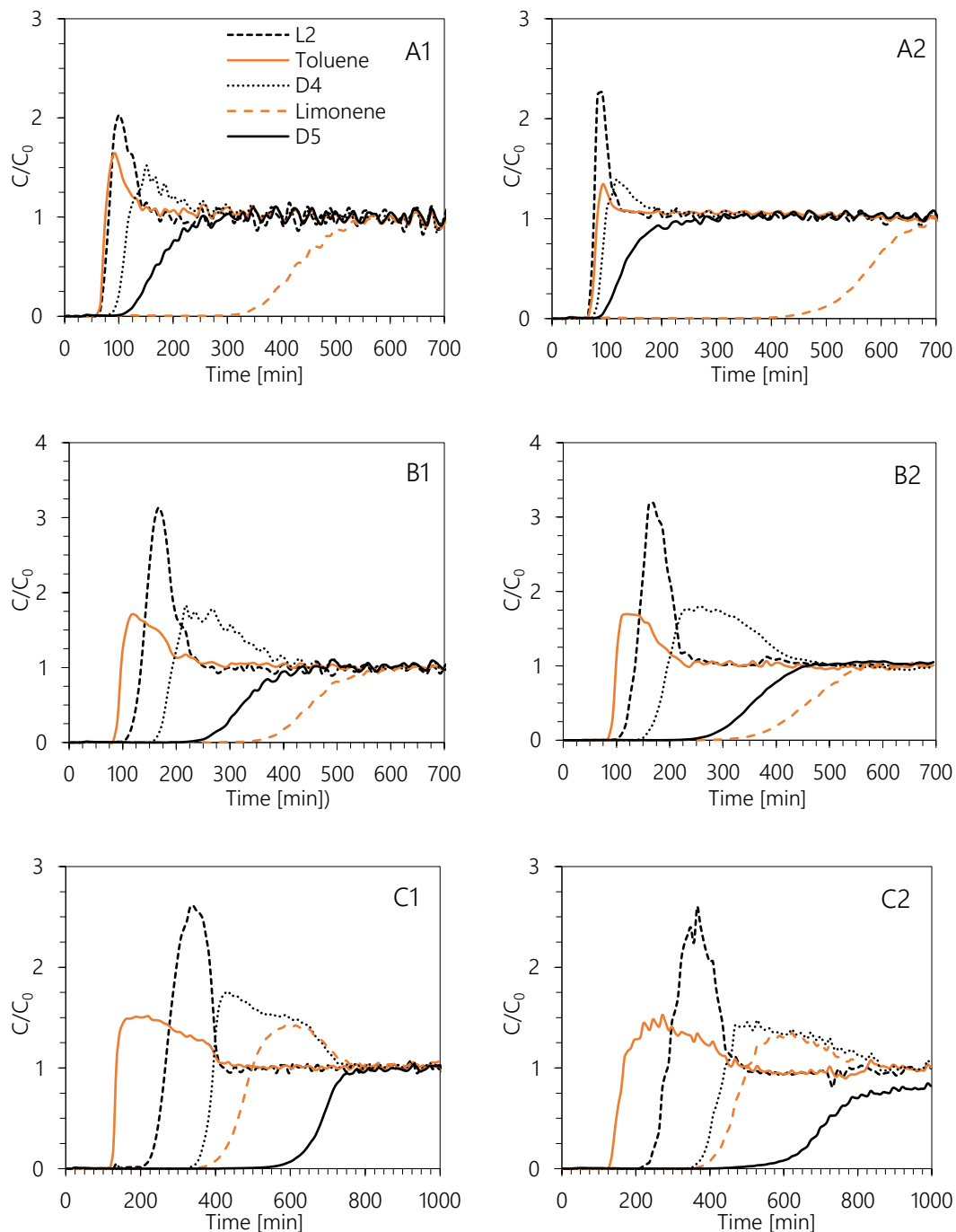
Figure 4.2 Multicomponent dynamic adsorption breakthrough curves obtained for a) Group A (SAC-1), b) Group B (SAC-4), c) Group C (PhAC-4). The first column corresponds to dry adsorption tests and the second column to the adsorption tests in presence of humidity.

4.3.4   Dynamic adsorption tests in the presence of humidity

The competitive adsorption of siloxanes and VOCs was further explored in the presence of humidity in the gas inlet. Deionized water was injected to the synthetic multicomponent test gas to simulate the 30% of relative humidity typically present in pre-dried biogas. Figure 4.2 shows the dynamic breakthrough curves corresponding to groups A, B and C. Data obtained for each AC are shown in Figure 12.7. For the series of steam-activated carbons (groups A and B), the presence of humidity in the gas feed induced small differences in their adsorptive behaviour; all the samples of the series displayed similar breakthrough profiles, with differences in the breakthrough times and adsorption capacities at bed exhaustion of up to 20%. It should also be pointed out that the siloxanes breakthrough time increased for the steam activated carbons with higher number of oxygen-functional groups (carbons SAC-1, SAC-3 and SAC-5), and decreased for SAC-2 and SAC-4.

On the other hand, significant changes were observed in the breakthrough curves of the PhACs measured in moisture conditions (Figure 4.2 C2). The breakthrough times of every compound were quite similar to those in dry tests (except for carbons PhAC-1 and PhAC-2), with the exception of D5. In the presence of moisture, the outlet concentration of compound D5 remained below the inlet concentration during the whole dynamic adsorption tests, for all the carbons of Group C. As seen in Figure 12.7, D5 outlet concentration stabilized at C/C_0 of around 0.8 for all the carbons after 1000 min of run, when dynamic tests where stopped. Consequently, the final uptake corresponding to bed exhaustion (x/M) could not be calculated for any H_3PO_4-AC.

4.3.5   Spent ACs extraction

To further understand the observed adsorption trends of the multicomponent mixture on the investigated carbons, the spent carbons samples (after the adsorption tests) were extracted in THF, so as to determine the nature of the compounds adsorbed inside the porosity of the activated carbons, as well as evaluating the overall mass balance. For these experiments and for comparison purposes, adsorption tests under both dry and moisture conditions were stopped after 30 min; when none of the compounds had broken through, thus the amount of siloxanes adsorbed on each carbon is the same, disregarding desorption due to competitive effects. The composition of the THF extracts was compared to a THF standard prepared with the same volume of multicomponent mixture injected to generate the test gas during 30 min (i.e. 42 µL), as shown in Figure 4.3A.

Higher molecular weight cyclic siloxanes than D4 and D5 (referred as Other cyclic in Figure 4.3) -i.e. dodecamethylcyclohexasiloxane (D6) and tetradecamethylcycloheptasiloxane (D7)- and small amounts of α-ω-silanediols (cited as Silanediols in Figure 4.3) were found in the THF extracts of the phosphoric activated carbons after 30 min of adsorption under both dry and wet conditions. Similar results have been observed upon the adsorption of D4 single component adsorption tests in a previous study [20]. Siloxane transformation was enhanced in the presence of water in the inlet gas, as shown in Figure 4.3B, with a higher amount of cyclic siloxanes, α-ω-silanediols and other lineal siloxanes than L2 (i.e. L3, L4, L5 and L6 referred as Other lineal in Figure 4.3) detected in the THF extracts. This corroborated that siloxanes undergo important modifications upon adsorption on chemically modified carbons of acidic nature at both dry and moisture conditions. On the other hand, fewer amounts of cyclic siloxanes of different molecular formulae were detected for the steam-activated carbons under dry conditions.
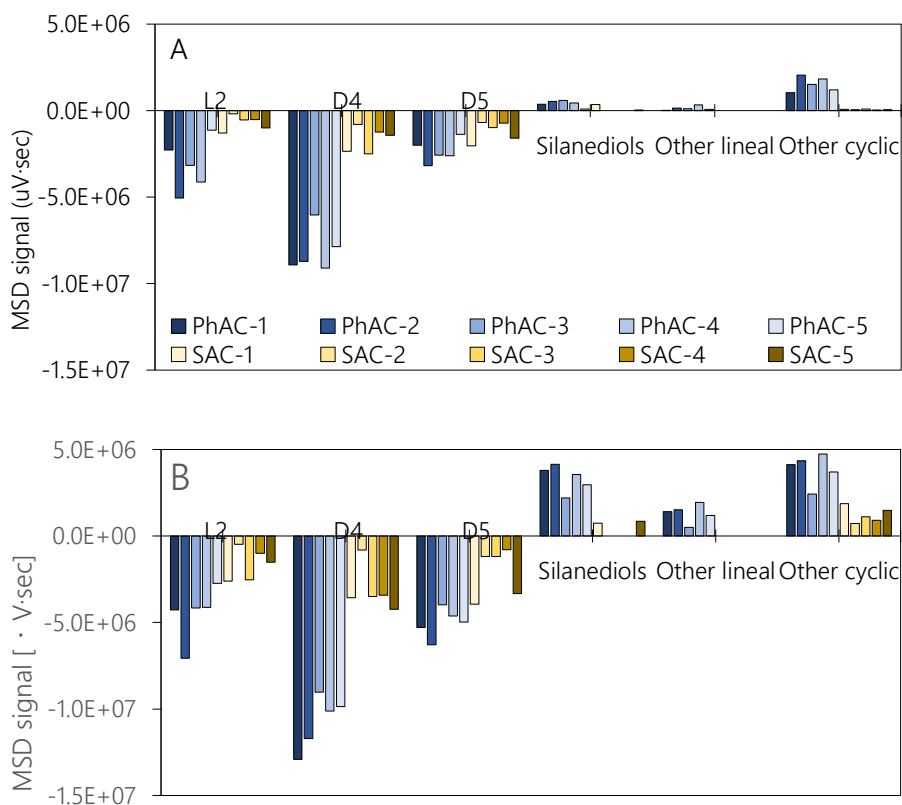
Figure 4.3 Amount of L2, D4 and D5 and other lineal siloxanes, other cyclic siloxanes and α-ω-silanediols extracted after 30 min adsorption tests in A) dry and B) wet conditions. Results expressed as MSD signal difference between the sample extraction and a THF standard.

4.3.6   Bed volume treated

Taking into account the great difference in the packing density (ρ_{ap}) of the ACs considered (see Table 4.1), the throughput given as number of bed volumes fed to the adsorber (BV) is a parameter frequently used in practice. The dimensionless parameter BV is defined as the volume of gas fed to the adsorber divided by the bed volume of the adsorber, according to Eq. 8

$$ \mathrm{BV} = \frac{V_W}{V_F} \qquad\qquad \text{Eq. 8} $$

where V_w is the volume of gas treated and V_F is the volume of the adsorbent bed.

Moreover, the performance of the adsorbents must be assessed at the first siloxane breakthrough, i.e. when the siloxane concentration after the adsorbent bed is under the limit tolerated by the energy conversion systems manufacturers. In the lab-tests performed, L2 and D4 are the first siloxanes that break up in all cases (see Figure 12.5). For comparison purposes, the breakthrough was established at 20 mg m^{-3}, which is in the range of the siloxane concentration limits reported, namely between 0.03 and 30 mg m^{-3} depending on the system and model [3]. Therefore, BV are calculated at L2 and D4 breakthrough respectively for each carbon (Figure 4.4), both in dry and wet adsorption tests. As seen, PhAC-2 (224 min), PhAC-4 (225 min) and PhAC-5 (225) presented the highest breakthrough times for the first siloxane (L2). The higher packing density of PhAC-2 leads to the highest number of bed volumes treated (55k BV) at L2 breakthrough at these dry conditions. The number of BV treated increased up to 83k at D4 breakthrough using PhAC-5, which is particularly important when dealing with biogas containing low L2 concentrations.
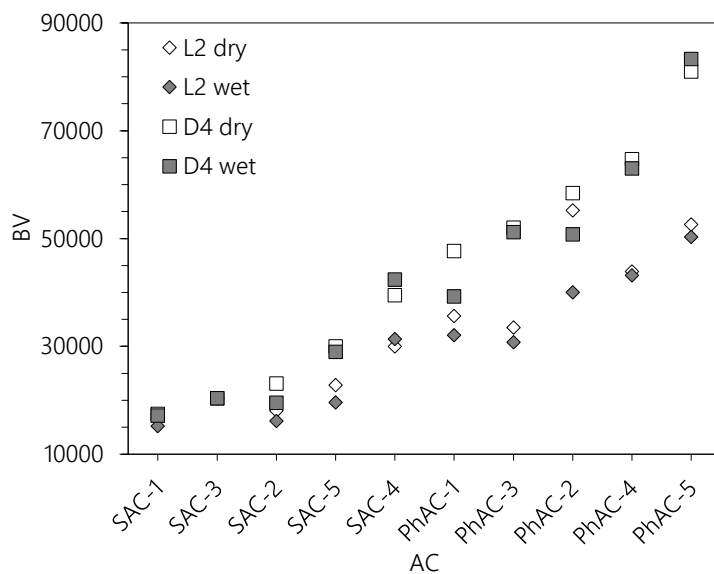
Figure 4.4 Multicomponent adsorption in N_2 dry matrix (empty symbols) vs in presence of 30% humidity (full symbols). Results expressed in BV treated at L2 (rhombs) breakthrough (C_{L2}=20 mg m^{-3}) and BV treated at D4 (squares) breakthrough (C_{D4}=20 mg m^{-3}).

4.4   Discussion

It is well-know that the adsorption of a given compound on activated carbons is governed by the textural and chemical features of the carbon adsorbent and the physicochemical features of the target compound, in terms of molecular size and weight, polarity, solubility and so forth [80]. For instance, matching the nanopore dimensions of a carbon adsorbent with those of the target gas molecule to be adsorbed usually increases the adsorption capacity, and results in stronger adsorption due to the increased adsorption potential between the pore walls and the retained compound (provided that size exclusion effects are discarded) [80–82]. Furthermore, it has been widely reported that the uptake of VOCs in activated carbons is governed by the volume of narrow micropores (i.e., pore width below 0.7 nm), while the adsorption strength increases with the molecular weight.

Considering this, the adsorption performance of the series of studied activated carbons towards the mixtures of siloxanes and VOCs will be discussed in terms of their differences in texture and composition. As a general rule, the uptakes of all the siloxane compounds is higher in the phosphoric activated carbons than in the steam-activated ones, which may be attributed to the basic character of the siloxanic Si-O-Si groups. The number of moles of each compound

adsorbed per surface unity is shown in Figure 12.8: higher number of moles of cyclic siloxanes (D4 and D5) were adsorbed per m^2 of BET surface area of phosphoric acid activated carbons, while steam activated carbons adsorbed more moles of VOCs. Also, cyclic siloxanes are preferentially adsorbed over linear ones (L2) at the conditions tested, where their competitive effects are increased by the different inlet concentration of each compound. Thus, no apparent lineal correlation between the carbon porosity and the uptake of the molecules adsorbed and later desorbed were observed, i.e. toluene and limonene (Figure 12.9) or L2 and D4 (Figure 12.10) while, a positive relation between the number of D5 moles adsorbed and the volume of pores was observed (Figure 4.5A) as well as the total adsorption capacity and pore volume (Figure 4.5B).
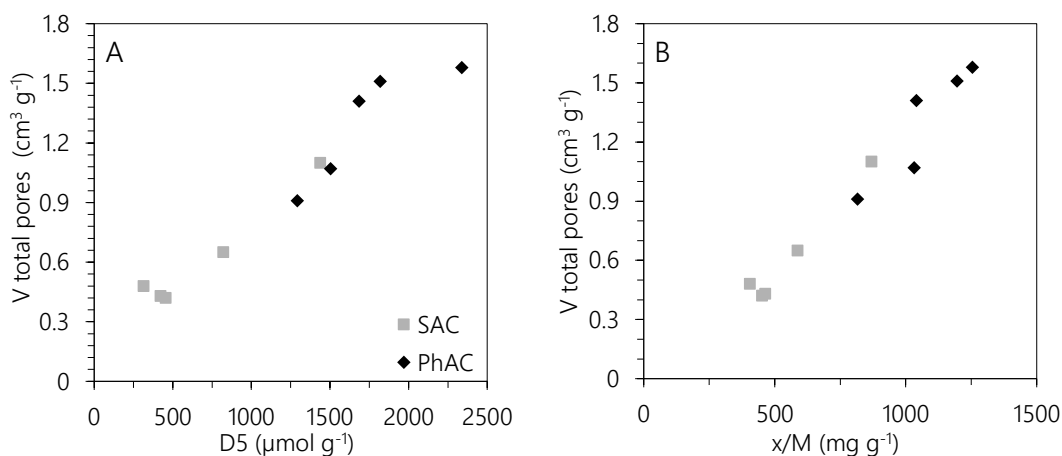
Figure 4.5 Relation between A) adsorption capacity of D5 (reported at bed exhaustion), and B) adsorption capacity (totality of compounds reported at bed exhaustion) with the textural properties of the ACs.

Furthermore, significant differences were obtained for the uptakes of the steam activated carbons. Indeed, in the case of group A (samples SAC-1, SAC-2 and SAC-3), the uptake followed the trend: limonene>toluene>D5>D4>L2, whereas for group B the trend was as follows: D5>limonene>toluene>D4>L2. Since both groups are characterized by a basic surface pH and low surface functionalization (Table 4.2), these differences may be explained in terms of their porous features. The porous features of carbons of group A are characterized by a distribution of micropores of small sizes with a minor contribution of mesopores. This would explain the smaller uptake of bulky D4 and D5 (critical diameters are 1.08 and 1.10 nm, respectively) compared to limonene and toluene. Among the adsorbate molecules with critical diameters under 0.8 nm, limonene molecular weight is the heaviest, resulting in the highest adsorption capacity. Carbons of the group B (SAC-4 and SAC-5) displayed a higher

contribution of larger pores (i.e., wide micropores and mesopores), that allows the access of D4 and D5. Thus, the adsorption capacity of both compounds increases, and the competitive effects between the different compounds in the mixture become stronger. Thus, toluene, L2 and D4 were displaced by the strongest adsorbed D5 and limonene. Additionally, data suggests no competitive adsorption between D5 and limonene.

On the other hand, for the phosphoric activated carbons (group C), the porosity is comprised of larger pore volumes and widths, thus the uptake of most compounds is larger than for groups A and B, being the effect more pronounced for D5 and D4. The weakest adsorbed compounds for these samples were toluene and L2; the sharp desorption profiles of toluene and L2 initiated at the same time that D4 was detected in the column outlet (Figure 4.2-C1). The L2 concentration profile levelled off at C/C_0 within a running time close to that of bed exhaustion for D4. For toluene, the ratio C/C_0 stabilizes at $C/C_0 = 1.1$, right after D4 breaks through, and this plateau lasted until limonene breakthrough. The D4 breakthrough curve also showed a wider and less stepped hump; the $C/C_0 = 1$ for D4 was achieved once the bed had reached the maximum adsorption capacity for D5. The two most efficiently removed compounds (i.e, limonene and D5) did not show any evidence for competitive adsorption.

Concerning the role of the surface chemistry of the activated carbons, it has been previously observed that the acidic sites on the AC's surface can promote bond cleavage of siloxanes leading to the formation of α-ω-silanediols that further condense to form other cyclic siloxanes [10]. Formation and detachment of α-ω-silanediols requires water, however the inherent moisture present in the carbons (Table 4.1) does not seem to play an important role on the adsorption tests carried out using dry gas, likely due to its relatively small amount (ca. 2.7-13.6 wt.%) and the drying impact of the gas stream upon adsorption. On the other hand, for the ACs of acidic nature characterized by high amounts of oxygen-functional groups, some polymerization occurs after 30 min of adsorption; this was corroborated by the higher molecular weight of the cyclic siloxanes and α-ω-silanediols extracted in these carbons.

When the adsorption tests were carried out under moisture conditions, there was a much higher availability of water, necessary for further polymerization. Thus, upon 30 min of adsorption in moisture conditions, the amount of other siloxane species detected in the extract increased for all the studied ACs (Figure 4.3); the effect was more pronounced for the phosphoric activated carbons, which are expected to retain higher amounts of water due to their increased hydrophilic character (provided by a higher amount of oxygen-functional groups). The coadsorption of the formed α-ω-silanediols -of smaller sizes than D4 and D5-, could enhance the siloxane uptake, as it has been reported for some zeolites [12]. Interestingly,

none of the newly formed compounds upon the hydrolysis and condensation of siloxanes were detected in the outlet gas during the adsorption tests, which suggests that they are strongly retained in the pores and/or bonded to the surface oxygen-functional groups of the carbons.

As above-mentioned, the D5 concentration at the end of adsorption runs under moisture conditions does not reach the inlet concentration for any of the carbons of the PhAC series; we also attribute this behaviour to the siloxane transformation reactions in the presence of water.

4.5   Final remarks

The porous features of the activated carbons were found to be responsible of VOCs and siloxanes uptake in competitive adsorption. Carbons presenting small size microporous distribution were more favorable for the adsorption of toluene and limonene than carbons that displayed a higher contribution of wider micropores and mesopores, which allow the access of bulky D4 and D5. Phosphoric acid activated carbons showed the larger pore volumes and width, leading to higher uptakes of the siloxane D4 and D5. However, L2 is completely desorbed after its breakthrough.

The presence of water increased the siloxane uptake of some activated carbons, leading to a higher number of BV treated. This was the case for carbon PhAC-5, which turned out to be the most suitable carbon adsorbent to remove siloxanes from wet gas. The use of phosphoric-activated carbons with a larger mesoporosity and medium-high packing densities increased the efficiency of siloxane removal, in terms of a higher number of BV treated. This is important since it would allow to reduce the costs associated to the adsorbent replacement, even if the average cost of phosphoric-activated carbons is higher (typically double) than that of steam-produced carbons.

Chapter 5

RESULTS II

Sustainable activated carbons from lignocellulosic waste

5.1 Background and objectives

Activated carbon (AC) is the most widely used adsorbent support in filters for biogas upgrading to remove siloxanes prior to biogas combustion. The major drawback of this technology is the high operational costs due to the carbon replacement when the adsorbent beds are exhausted [23]. Moreover traditional activated carbons are commonly produced from really expensive and non-renewable feedstocks such as coal, lignite or anthracite [83]. The current economic pressure over these materials has pushed the market to look for alternative precursors for producing activated carbon. Low-cost and sustainable bioresources like biomass residues have gained attention in the recent years.

The objective of the present work is to obtain activated carbons capable of removing siloxanes and volatile organic compounds (VOCs) from the valorisation of lignocellulosic waste as precursor material. The resulting materials will be evaluated in adsorption equilibrium experiments to compare their performance with the commercial ACs currently used for biogas upgrading and prove the efficiency of this residue valorisation.

5.2 Methodology

The experimental procedure for obtaining the lignocellulosic waste-based activated carbons is detailed in Section 3.3. The activation conditions for both the experimental and commercial samples as well as their origins are summarized in Table 3.1. The commercial activated carbons used in this chapter were also studied in Chapter IV but were named differently: AC5 (PhAC-1), AC6 (SAC-2) and AC7 (SAC-4).

The chemistry, texture and morphology of all materials were exhaustively characterized following the methodologies in Section 3.3.2. The capacity of the materials to adsorb both siloxanes (D4 and L2) and VOCs (toluene and limonene) was investigated through adsorption equilibrium experiments at 25 °C, as detailed in Section 3.3.4. Moreover, the siloxanes transformation reactions were studied in spent carbon analysis with THF, further explained in Section 3.3.6.

5.3 Results and discussion

5.3.1 Chemical characterization

The lignocellulosic waste used in the preparation of the activated carbons had a high carbon content (45.83%) and a low ash content (3.66%). After the pyrolysis process, the char obtained presented an increase in both parameters (82.15% and 8.10% carbon and ash content, respectively). Thus, both pyrolyzed and non-pyrolyzed samples presented a chemical composition, i.e. carbon content, appropriated to be used as precursors for obtaining activated carbon.

The elemental analysis and ash content of both the experimental and commercial activated carbons is presented in Table 5.1. The experimental carbons displayed higher carbon contents (>94% vs <90%) and lower ash content (<2% vs >7%) than the commercial ACs. Similar C contents have been reported for activated carbons obtained from the valorisation of other residues such as chestnut shells [84] and algae meal waste [61]. The commercial H_3PO_4-activated carbon AC5 stood out for its relatively low carbon (80.15%) and high hydrogen (2.31%) and oxygen (7.37%) contents among the rest of the materials. Nitrogen content was found greater for the experimental carbons (>1%) than the commercials (<0.7%), while sulphur content was under 0.5% for all the materials.

Table 5.1 Proximate and ultimate analysis of the activated carbons

Sample	Humidity[a]	Mass fraction (%), dry basis					
		Ash	C	H	N	S	O[b]
Experimental							
AC1	10.1	0.21	95.76	0.50	1.48	0.11	1.94
AC2	6.0	0.40	95.15	0.42	1.39	0.13	2.51
AC3	15.9	1.29	94.60	0.37	1.52	0.08	2.14
AC4	11.7	1.05	95.08	0.30	1.29	0.10	2.18
Commercial							
AC5	18.9	9.65	80.15	2.31	0.51	0.01	7.37
AC6	6.9	7.50	89.50	0.65	0.63	0.40	1.32
AC7	5.2	9.29	88.06	0.55	0.60	0.44	1.06

[a]Determined as-received
[b]Determined by difference

5.3.2   Textural characterization

N_2 and CO_2 adsorption isotherms are shown in Figure 5.1A and B, respectively. According to the IUPAC classification [75], AC5 and AC7 displayed a type Ib N_2 adsorption isotherm which indicated the predominance of wider micropores. [75], AC5 and AC7 displayed a type Ib N_2 adsorption isotherm which indicated the predominance of wider micropores. Moreover, AC5 presented a hysteresis cycle and a more defined slope from low relative pressures, which indicates the presence of mesopores. On the other hand, all the experimental materials and the commercial AC6 exhibited a type Ia N_2 adsorption isotherm, characteristic of materials dominated by narrow micropores. CO_2 adsorption isotherms further confirmed the high presence of narrow micropores within the experimental ACs.

The pore size distribution of the materials calculated by the DFT method is gathered in Table 5.2. These results show that, while most experimental materials are fundamentally microporous, the commercial ACs have lower contribution of narrow micropores. The greatest adsorption in medium micropores (V_{mmi}: volume corresponding to pore width 0.7-2 nm) is observed in the commercial AC5 and the experimental AC2. On the other hand, mesoporosity contribution, indicated by the hysteresis loop and steep slope in N_2 isotherm, is practically negligible in most samples except AC5. CO_2 adsorption data further confirmed that the experimental ACs had a major contribution of narrow micropores. From Table 5.2 it can be observed that AC4 was the most outstanding material in terms of narrow microporosity (0.73 cm^3 g^{-1}) and DR surface (1899 m^2 g^{-1}). Commercial samples had a clear minor contribution of such microporosity being the steam-activated coal-based AC7 the poorest material.
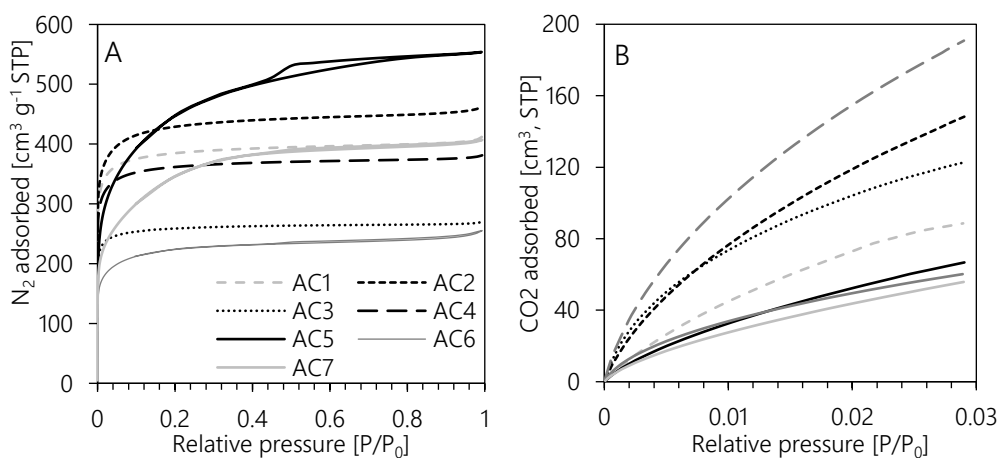
Figure 5.1 N_2 adsorption/desorption at 77K (A) and CO_2 adsorption isotherms at 273K (B) for the experimental (dashed lines) and commercial carbons (solid lines)

Table 5.2 Textural parameters of the materials

Sample	ρ_{He} [g cm^{-3}]	S_{BET} [m^2 g^{-1}]	V_{TOT} [cm^3 g^{-1}]	$^a V_{umi}$ [cm^3 g^{-1}]	$^b V_{mmi}$ [cm^3 g^{-1}]	$^c V_{me}$ [cm^3 g^{-1}]	W_0 [cm^3 g^{-1}]	S_{DR} [m^2 g^{-1}]	E_0 [KJ mol^{-1}]	L [nm]
	N$_2$ adsorption at 77K						CO$_2$ adsorption at 273K			
AC1	2.19	1512	0.63	0.26	0.22	0.02	0.42	1123	23.00	0.90
AC2	2.12	1668	0.70	0.25	0.28	0.03	0.63	1692	23.78	0.83
AC3	2.05	1025	0.40	0.22	0.11	0.00	0.45	1215	26.48	0.70
AC4	2.13	1419	0.57	0.24	0.21	0.01	0.73	1899	25.13	0.72
AC5	1.74	1659	0.86	0.09	0.36	0.28	0.26	683	24.61	0.82
AC6	2.15	862	0.39	0.10	0.17	0.03	0.21	560	26.90	0.70
AC7	2.31	1281	0.63	0.10	0.25	0.17	0.20	527	25.49	0.77

$^a V_{umi}$: ultramicropore volume (pore width <0.7 nm) / $^b V_{mmi}$: medium-micropore volume (pore width 0.7-2 nm) / $^c V_{me}$: mesopore volume (pore width 2-50 nm)

5.3.3 Effect of the activation conditions on the carbon development

In some cases, lignocellulosic wastes undergo a pyrolysis process for the production of other products such as liquid bio-oils and fuel gas. In these scenarios, the pyrolyzed waste is obtained as a char residue which can be regarded as a potential precursor material for activated carbon [85]. However, pyrolyzed waste presents an ordered structure that requires more reactive chemicals for its activation than non-pyrolyzed lignocellulosic waste.

Alkali activating agents K_2CO_3 and KOH have been widely used and reported in the activation of carbonaceous materials. They were selected in this study due to previous experience on the activation of lignocellulosic waste [86]. Generally, it is known that KOH is a more reactive agent than K_2CO_3 at a same activating temperature. For this reason, K_2CO_3 was the activating agent selected for the non-pyrolyzed samples (AC1 and AC2) and KOH for the pyrolyzed samples (AC3 and AC4).

The temperature in the activation process is a critical parameter in the development of the porosity. Ferrera-Lorenzo et al., (2014b) studied the temperature effect (500 ºC – 900 ºC) to activate a macro algae residue using KOH concluding that higher temperatures led to higher yields in this range. In the working conditions of this study, the non-pyrolyzed carbons activated with K_2CO_3 demonstrated higher BET surface area and total pore volume than the pyrolyzed materials. Within the pyrolyzed samples, which were activated at 900 ºC the textural development increased significantly with the KOH concentration (AC3<AC4). As a result of the pyrolysis prior to the activation process, the original structure of the biomass is highly preserved even at the highest KOH concertation used. SEM images of AC3 (Figure 5.2) show such preservation, which enables a more ordered development of the structure than those observed in other materials. Regarding the non-pyrolyzed samples, AC1 (1/1, 850°C), which was

obtained using a higher amount of activating agent than AC2 (0.5:1, 900°C), did not demonstrate a major textural development. Thus, temperature is critical in the activation of these samples. In the activation conditions of AC2, the largest mesoporosity was developed.

K_2CO_3 is an agent with a high capacity to react with the mineral matter of the biomass, leading to the formation of soluble compounds that will be removed during the post-cleaning step of the adsorbent. For this reason, the ash content of both AC1 and AC2 is the lowest of the set of carbons considered (Table 5.1). Accordingly, mineral matter (white shiny parts) cannot be observed in the SEM of AC1. On the contrary, AC6 is a commercial anthracite-based carbon physically activated with steam. Within this type of activation, the mineral matter remains in the resulting adsorbent material, as in the H_3PO_4-activated AC5, which is denoted by the ash content and the SEM images (Figure 5.2). Moreover, a major difference observed in the AC6 SEM captions in comparison with the other materials commented above, is the absence of cavities and channels. This fact might be indicative of a low porosity development, agreeing with the textural data in Table 5.2.
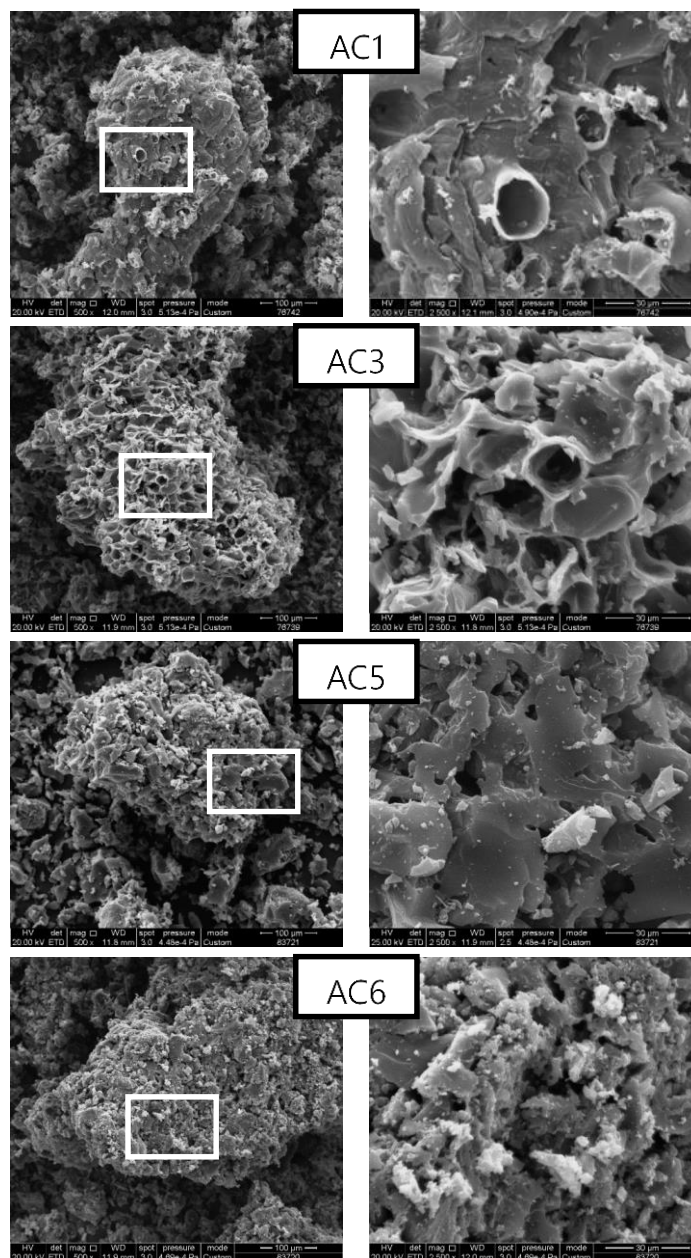
Figure 5.2 SEM pictures of two experimental (AC1 and AC3) and two commercial ACs (AC5 and AC6) at magnifications x500 (left side) and x2500 (right side).

5.3.4   Siloxanes and VOCs adsorption equilibrium at 25 ºC

Figure 5.3 shows the gas uptakes (x/M) obtained in static adsorption tests at different equilibrium concentrations (C_e) for both siloxanes (D4 and L2) and VOCs (toluene and limonene) for the whole set of carbons. In general terms, it can be observed that higher uptakes were achieved by lignocellulosic carbons rather than anthracite and coal-based materials. The best candidate adsorbing D4 was the commercial H_3PO_4-activated AC5, whereas the experimental material AC2 stood up in the adsorption of all the pollutants.
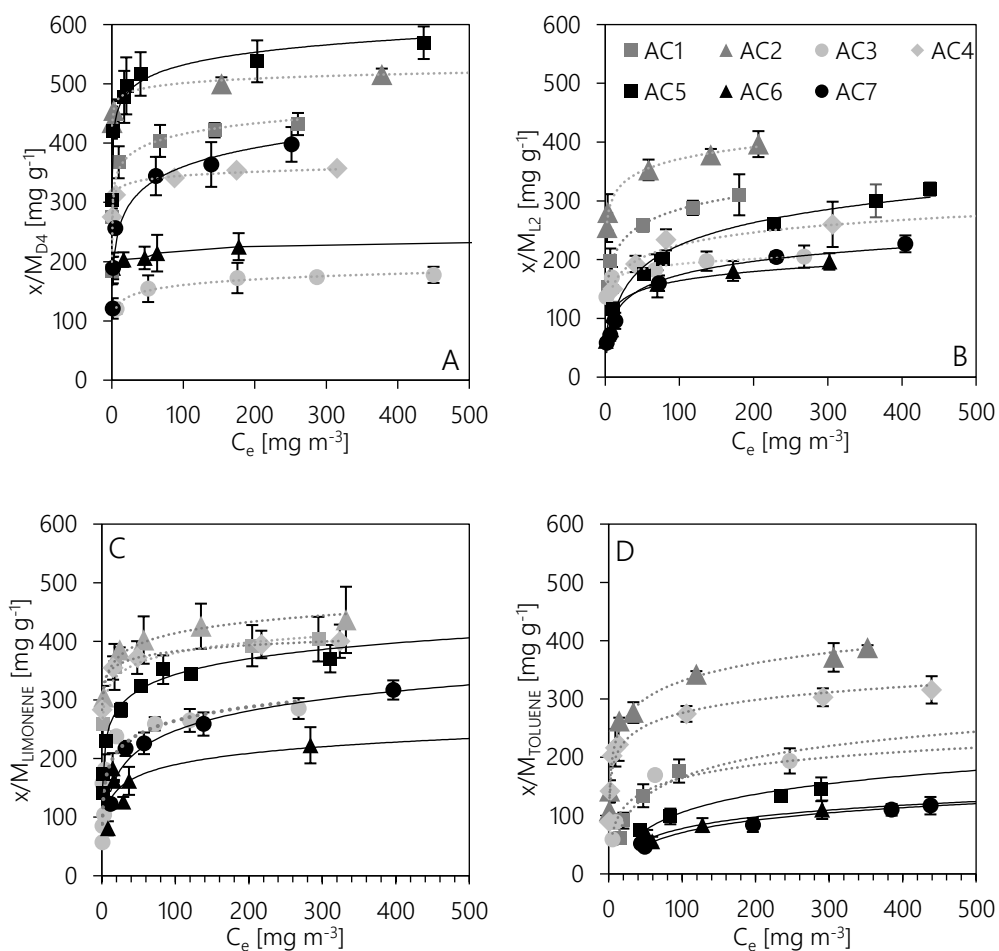
Figure 5.3 Gas uptake obtained at different equilibrium concentration (C_e) of (A) D4, (B) L2, (C) limonene and (D) toluene in static adsorption tests at 25 ºC and DA fitting (lines).

Adsorption characteristics were investigated by fitting the experimental data to three two-parameter models (Langmuir, Freundlich and Dubinin-Radushkevich) and to the three-

parameter Dubinin-Astakhov (DA) equation. The best fit was obtained with the latter, expressed as Eq. 9,

$$W = W_0 \cdot e^{\left[-\left(\frac{RT\ln\left(P_0/P\right)}{E}\right)^n\right]}$$
Eq. 9

where W is the mass of adsorbate adsorbed per mass of AC (mg g^{-1}), W_0 is the maximum mass of adsorbate adsorbed in the micropores (cm^{-3} g^{-1}), E is the adsorption energy (kJ mol^{-1}), T is the temperature (K), R the universal gas constant (0.008314 kJ K^{-1} mol^{-1}), P vapor pressure at saturation and P_0 adsorbate partial pressure (mm Hg), and n is an exponent that can range from 1 to 5 [88]. n parameter equal or above 3 represents molecular sieve carbons dominated by narrow micropores, whereas n values below 2 represent microporous carbons with wider pore size distribution [89,90]. DA fitting data is shown in lines in Figure 5.3. Maximum adsorption capacities (x/M) calculated for each adsorbate are presented in Table 5.3, together with the n, β and r^2 resulting from the DA fitting. L2 adsorption capacities calculated ranged from 220 (AC3) to 438 mg g^{-1} (AC2), while D4 ranged from 185 (AC3) to 577 mg g^{-1} (AC5). D4 presented the highest x/M from the compounds considered in this study, probably because it is the highest molecular weight molecule. Nam et al., (2013) reported similar adsorption capacities of siloxanes within adsorption equilibrium experiments fitted to Langmuir-Freundlich isotherm model using commercial activated carbons.

Table 5.3 Adsorption capacities (x/M, in mg g^{-1}), values of n and β determined by Dubinin-Astakhov equation and r^2 obtained from the model fitting.

| Pollutant	Parameter	AC1	AC2	AC3	AC4	AC5	AC6	AC7
L2	x/M*	359	438	220	321	394	255	314
	n	3.80	3.10	3.06	3.26	3.50	2.38	2.73
	β	1,57	1.32	1.69	0.97	1.44	1.50	1.57
	r^2	0.982	0.977	0.976	0.984	0.976	0.919	0.975
D4	x/M*	436	512	185	356	577	233	398
	n	2.93	3.26	2.94	2.36	2.44	2.08	5.71
	β	1.84	1.75	1.11	1.92	2.15	2.57	1.50
	r^2	0.996	0.899	0.997	0.941	0.994	0.893	0.962
Toluene	x/M*	374	417	255	318	343	192	268
	n	3.01	3.41	4.59	4.79	2.31	2.96	2.13
	β	1.00	1.00	1.00	1.00	1.00	1.00	1.00
	r^2	0.970	0.975	0.996	0.990	0.992	0.957	0.983
Limonene	x/M*	427	446	282	408	452	275	354
	n	2.53	3.11	3.93	2.13	2.04	2.33	3.51
	β	1.61	1.05	1.01	1.57	1.41	1.04	1.13
	r^2	0.988	0.997	0.943	0.989	0.988	0.936	0.967

β – Affinity coefficient (calculated from the adsorption energy in the DA equation E=βE$_0$) where toluene is taken as a reference compound assuming β$_{TOLUENE}$ = 1.

Thus, the highest x/M calculated for siloxanes corresponded to AC1, AC2 and AC5, all of them lignocellulosic-based activated carbons with chemical activation, and the performance of the experimental material AC was comparable in terms of efficiency to the best commercial carbon tested.

On the other hand, toluene capacities calculated range from 192 (AC6) to 417 mg g^{-1} (AC2), whereas limonene capacities range from 275 (AC6) to 446 mg g^{-1} (AC2). Toluene adsorption capacities ranging 62-183 mg g^{-1} have been reported from adsorption data fitted to Langmuir isotherm model of several commercial activated carbons [91]. Lillo-Ródenas et al., (2005) reported toluene adsorption capacities that are in good agreement with our study using experimental activated carbons impregnated with different chemicals. Hence, the experimental carbon AC2 resulted the carbon with the highest efficiency to remove VOCs of the set studied in this work.

5.3.5   Importance of the texture

We investigated the relationship of the adsorption capacities calculated by DA fitting (Table 5.3) with textural characterization (Table 5.2). In general terms, there was a positive correlation between the textural development of the carbons and their adsorption capacity for all adsorbates. Ultramicropore volume did not relate with the adsorption capacity for any of the compounds studied due to their molecular sizes, larger than ultramicropore width (<0.7 nm), which was observed by other studies working with D4 [20]. The best lineal correlations are shown in Fig. 3, i.e. total pore volume and the total micropore volume (V_{mi}).

As denoted by the different slopes in the lineal correlations obtained, experimental and commercial carbons showed different trends. Commercial activated carbons presented larger contribution of mesopores in their total porosity. While AC2 is the experimental sample with the most significant presence of mesopores, it was still lower than commercials.

D4 adsorption is known to occur within wide micropores and mesopores [33,34]. While L2 critical diameter is smaller, it is still preferently adsorbed in narrower mesoporosity (Cabrera-Codony et al., 2018). Thus, D4 and L2 adsorption capacities were correlated with the total volume of pores for the whole set of carbons (Figure 5.4A,C). When studying the effect of microporosity, experimental and commercial materials presented different correlations due to their difference on the mesoporosity contribution (Figure 5.4B,D).

On the other hand, adsorption of toluene and limonene is not ruled out by mesoporosity, but microporosity is the major contributor as pointed out in other studies [93]. Thus, similar tendency between the two groups of carbons regarding VOCs adsorption was found out when

considering micropore volume (Figure 5.4F,H), and it is observed that for the same total pore volume experimental samples performed the best (Figure 5.4E,G).
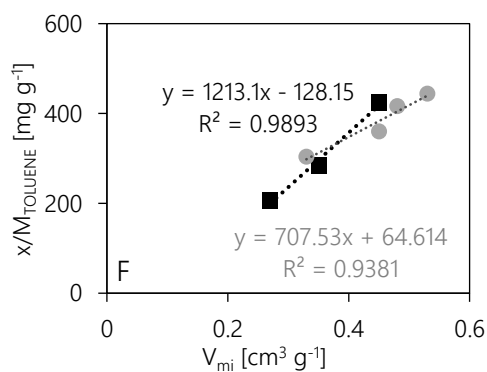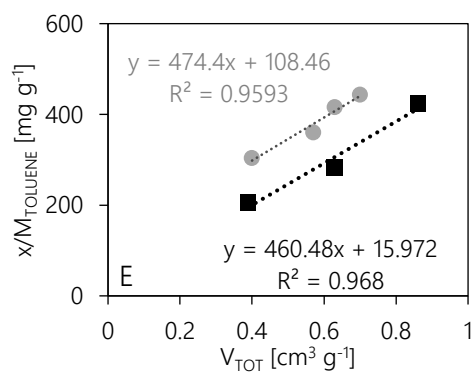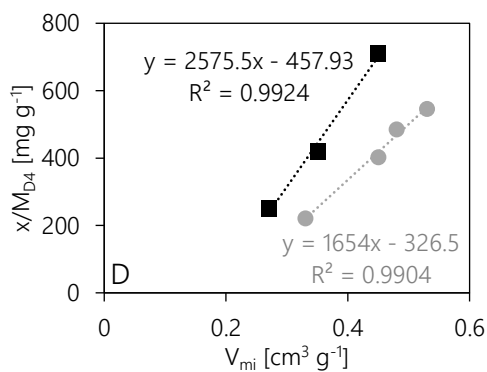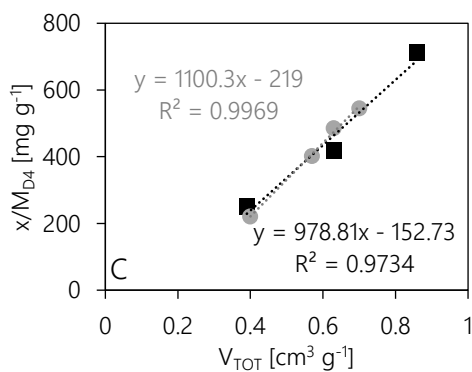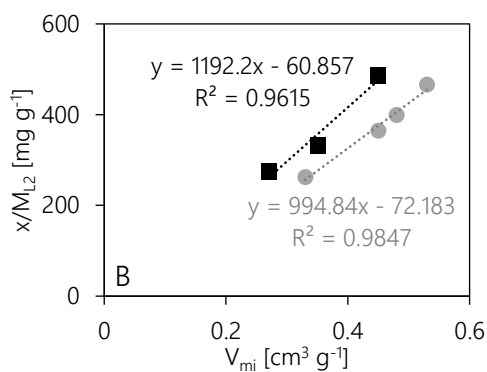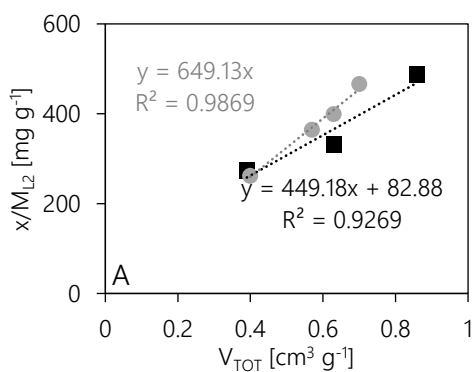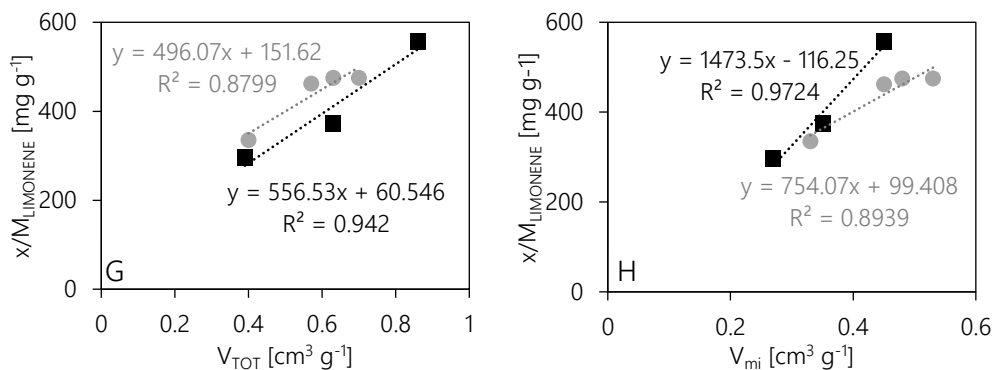
Figure 5.4 Relationships between total pore volume (V_{TOT}) and micropore volume (V_{mi}) with adsorption capacity of (A-B) L2, (C-D) D4, (E-F) toluene and (G-H) limonene (calculated on a dry basis by DA adjust). Gray circles represent experimental ACs and black squares commercial ACs

5.3.6   Siloxane transformation

It has been previously observed that the acidic sites on the activated carbons' surface may lead to the transformation of siloxanes into linear by-products, known as α-ω-silanediols [41,94]. We studied the catalytic activity of the samples towards D4 and L2 by extracting the adsorbed compounds and transformation products in THF suspensions.

In the extracts of the D4-spend carbon samples, other cyclic siloxanes (D5, D6 and D7) were found along with small amounts of α-ω-silanediols (Figure 5.5B). The highest D4 recoveries were found for the steam-activated carbons AC6 and AC7 reaching 94% in both cases. D4 hydrolysis and condensation reactions take place due to the oxygenated groups in the surface of the activated carbons [20]. In agreement with the elemental analysis (Table 5.1), AC6 and AC7 are the carbons with lowest oxygen content. On the contrary, a significant presence of α-ω-silanediols was found in the extract of the acid activated AC5, similar behaviour as those of the experimental ACs in this study.

On the other hand, in the THF extractions of L2-spend samples, no transformation products were found, and more than 85% of the L2 was recovered from most of the carbon samples (Figure 5.5A), denoting that L2 transformation reactions do not take place on the surface of the studied materials.
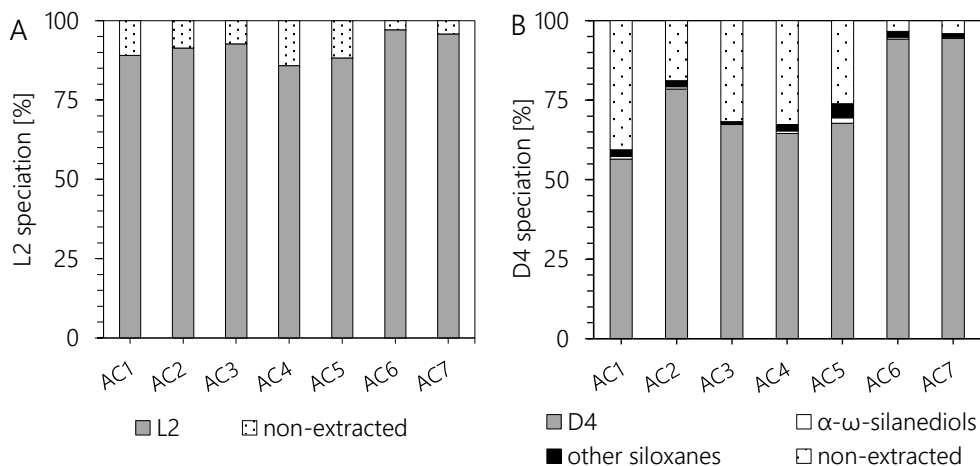
Figure 5.5 Percentage of A) L2 and B) D4 recovered or transformed to other siloxanes and α-ω-silanediols from THF extraction of spend samples. Non-extracted refers to the amount of siloxane adsorbed and not detected on the THF extracts.

5.4   Final remarks

The experimental carbons developed in this study performed better than commercial samples for the adsorption of L2 and toluene (up to 438 and 417 mg g^{-1}, respectively), and as good as the best commercial samples for limonene and D4. Thus, activation through K_2CO_3 of lignocellullosic wastes is an effective process for obtaining feasible adsorbents for biogas purification. Pyrolyzed samples activated by KOH led to carbons with lower porosities than non-pyrolyzed ones. Yet they presented performances comparable with steam ACs commercialized for biogas upgrading. AC4, activated using higher concentration of KOH presented a significant microporosity development, facilitating the uptake of VOCs.

Chapter 6

RESULTS III

Performance of biotrickling filters for biogas purification

6.1 Background and objectives

Biotrickling filtration (BTF) offers many advantages such as low pressure drops, simplicity in the operation and low operational costs, which make it more attractive and eco-friendlier than its physical-chemical counterparts and even than other biotechnologies (i.e. biofilters) [95]. Despite the advantages of BTFs, the number of publications investigating siloxane removal in BTFs is scarce and limited to a reduced number of siloxanes. The few studies reported in the literature demonstrated the biodegradability [96] of these compounds under aerobic conditions. However, the low concentrations of O_2 in biogas (if any at all), together with its associated explosion risk, have limited the use of aerobic biotechnologies in biogas upgrading applications. In addition, there is consistent evidence in literature demonstrating the capability of BTFs to treat VOC-laden emissions from the petrochemical industry using nitrate as an alternative electron acceptor [97–99].

The aim of the present work was to investigate the anoxic biodegradation of siloxanes (D4 and D5) in a lab-scale biotrickling filter. The ability of the BTF to treat other biogas impurities, i.e. volatile organic compounds such as hexane, toluene and limonene, was also assessed. The influence of the EBRT on siloxane and VOC removal performance, along with the beneficial role of activated carbon (AC) supplementation in the BTF (in order to enhance the mass transfer of biogas pollutants to the microbial community), were also investigated.

6.2 Methodology

The BTF set up, inoculum procedure and operating conditions (detailed in Table 3.3) as well as the analytical methodologies followed for the process monitoring are detailed in sections 3.4.1 to ¡Error! No se encuentra el origen de la referencia.. The concentration of the target compounds is found in Table 6.1.

Table 6.1 Concentration of the target pollutants in the feed gas of the BTF.

Pollutant	Hexane	Toluene	Limonene	D4	D5
Concentration [mg m^{-3}]	375 ± 18	24 ± 2	220 ± 11	54 ± 3	102 ± 5

6.3   Results and discussion

6.3.1   Lab-scale BTF start up

The experimental set-up was initially operated abiotically to assess the physico-chemical processes underlying D4 removal from the synthetic gas emission. The D4 concentration at the outlet of the BTF, which was measured by GC-FID after 72 h of abiotic operation, matched the inlet D4 concentration, which ruled out the occurrence of significant abiotic siloxane removal mechanisms. The low D4 aqueous solubility mediated a rapid equilibrium between the gas and liquid phases in the BTF, which explains the similar concentrations in the inlet and outlet emissions.

The lab-scale biotrickling filter was inoculated with anaerobic sludge from an urban wastewater treatment plant. D4 biodegradation under anoxic conditions in WWTPs was previously described [17], with microbial catalytic hydrolysis of cyclic siloxanes identified as one of the main degradation pathways. The system was run for 36 days at a D4 inlet load of 0.26 g m^{-3} h^{-1} (Stage I), which resulted in a steady state removal efficiency (RE) of 14%.

A sample of the bed material was collected to explore the biofilm grown in the lava rock used as packing material. SEM images revealed the presence of rod-shaped bacterial cells in the size range 1-3 μm attached on the surface of the packing rock. The population was not quantified, thought it could be observed that the lava rock structure was hardly noticed due to the high colonization of bacteria (Figure 6.1). A thorough microbial community analysis of the biofilm established in the BTF was recently reported by Boada et al., (2018) [100]. According to the gene sequencing analysis of the biofilm samples, species from the phylum *Proteobacteria* and *Actinobacteria* were identified, including *Rhodococcus* sp., *Methylibium* sp. and *Pseudomonas aeruginosa*. Of them, *P. aeruginosa* is a facultative anaerobe that can proliferate with nitrate as a terminal electron acceptor and has been described as a siloxane-biodegrading species capable of producing biosurfactant molecules [59,101,102].
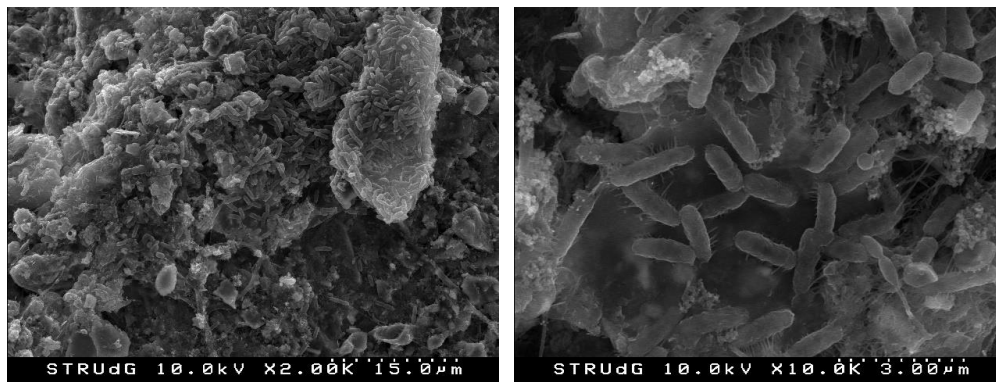
Figure 6.1 SEM photographs of the packing lava rock in the BTF after operating with D4 as carbon source.

6.3.2 BTF operation with multicomponent mixture (Stage II)

Based on the microbial analysis conducted in stage I, a concentrated culture of *P. aeruginosa* was used to re-inoculate the BTF at day 43 in order to boost the siloxane removal capacity of the system. The feed gas composition was switched to a multicomponent mixture of siloxanes (D4 and D5) and VOCs (toluene, limonene and hexane) typically found in sewage biogas [6]. Figure 6.2 plots the removal efficiency (RE) and the elimination capacity (EC) of the biogas contaminants during the entire operation. The system was operated at an EBRT of 14.5 min until day 86. The outlet concentrations of toluene and limonene during stage II-1 remained below the detection limit of the analytical method (0.5 mg m^{-3} for both compounds). Thus, a complete removal of both toluene and limonene was achieved almost immediately (Figure 6.2B and C, Stage II-1), which remained stable during the whole operation. Thus, the steady state elimination capacities accounted for 0.10 ± 0.002 and 0.83 ± 0.009 g m^{-3} h^{-1} for toluene and limonene, respectively. However, hexane EC during stage II-1 averaged 0.21 ± 0.02 g m^{-3} h^{-1}, which corresponded to a removal efficiency up to 14% (Figure 6.2A). *Pseudomonas* sp., the dominant specie in the biofilm community, was capable of degrading hexane to some extent, although this biodegradation was limited by pollutant mass transport as a result of its high Henry's law coefficient. On the other hand, the removal efficiency of the target siloxanes increased after 15 days of acclimation of the microbial communities to the multicomponent gas emission (Figure 6.2D and E days 55-70). Stable REs of 13% for D4 and 37% for D5 were achieved, which corresponded to ECs of 0.03 ± 0.009 and 0.14 ± 0.003 g m^{-3} h^{-1}, respectively. The EBRT was decreased to 10.1 min in Stage II-2 (days 86-107). The RE of toluene and limonene remained at ~100 % for both compounds, whereas their ECs increased to 1.19 ± 0.002 and 0.14

± 0.001 g m^{-3} h^{-1}, respectively. Hexane RE did not significantly vary, although its EC increased to 0.29 ± 0.003 g m^{-3} h^{-1}. On the other hand, the REs of D4 slightly decreased to 13 and 30%, while their ECs incremented up to 0.04 ± 0.004 and 0.16 ± 0.001 g m^{-3} h^{-1}. Interestingly, the capacity of the bioreactor to remove toluene and limonene was not hampered by a further decrease of the EBRT to 7.3 min in Stage II-3 (days 108-128), whose ECs were incremented up to 0.19 ± 0.002 g m^{-3} h^{-1} for toluene and 1.66 ± 0.001 g m^{-3} h^{-1} for limonene. The REs for hexane, D4 and D5 were slightly reduced to 11, 9 and 21%, respectively. The EC for hexane increased to 0.34 ± 0.005, while the EC of the two target siloxanes remained quite similar compared to the previous stage (0.04 ± 0.002 and 0.17 ± 0.001 g m^{-3} h^{-1} for D4 and D5, respectively). Finally, the EBRT was further decreased to 4 min in Stage II-4 (days 129-152). In this context, while toluene and limonene were still not detected in the outlet gas stream, hexane REs decreased to 8% (corresponding to an EC of 0.45 ± 0.004 g m^{-3} h^{-1}). The REs of D4 and D5 were also reduced, although their ECs increased up to 0.06 ± 0.009 g m^{-3} h^{-1} for D4 and 0.23 ± 0.003 g m^{-3} h^{-1}.

Overall toluene and limonene were completely eliminated regardless of the EBRT, exhibiting ECs of up to 3 ± 0.003 g m^{-3} h^{-1} and 0.35 ± 0.001 g m^{3} h^{-1}, respectively at the lowest EBRT (Figure 6.3). Hexane's removal efficiency remained stable over the tested range of EBRTs, with ECs up to 0.45 g m^{-3} h^{-1}. On the other hand, the decrease in the EBRT resulted in more remarkable decrease in the RE of D5 compared to D4, which also experienced an increase in ECs up to 0.23 ± 0.003 and 0.06 ± 0.009 g m^{-3} h^{-1}, respectively. The results obtained confirmed that the removal of the target compounds was correlated with their Henry's law constants, which pointed out that the performance of the BTF was limited by the mass transport of hexane, D4 and D5 from the gas to the microbial community.
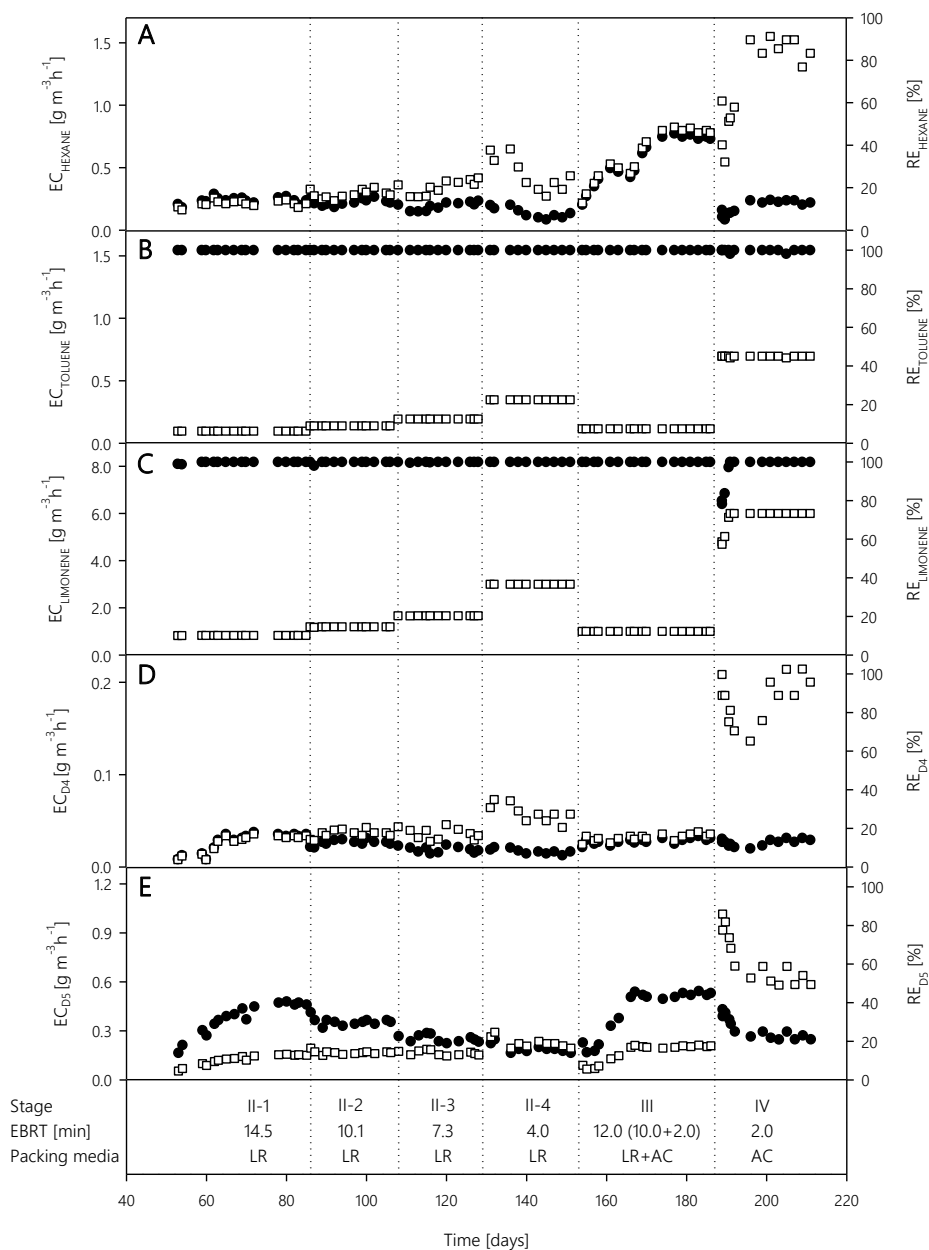
Figure 6.2 Time course of RE (●) and EC (□) of hexane (A), toluene (B), limonene (C), D4 (D), and D5 (E) in the BTF. Vertical dashed lines represent changes in the operation conditions: EBRT from 14.5>10.1>7.3>4 min, activated carbon addition (AC) and lava rock (LR) withdrawal.
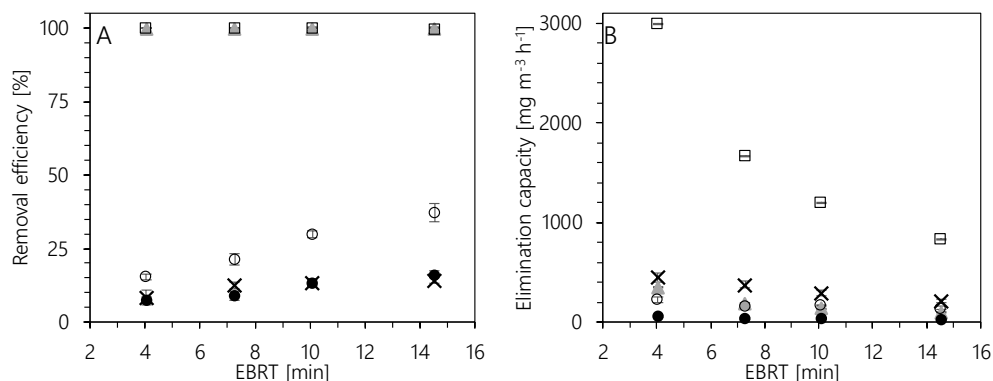
Figure 6.3 Effect of the EBRT on the removal efficiency (A) and elimination capacity (B) of D4 (●), D5 (O), toluene (▲), limonene (□) and hexane (x).

6.3.3 The role of activated carbon on the BTF performance (Stage III)

A layer of 5 cm of activated carbon was added at the top of the lava rock in the BTF by day 153 (Stage III) in order to improve the removal of siloxanes and hexane, which increased the EBRT up to 12 min. Some reports have pointed out the capability of the oxygen functional groups present in the surface of porous carbons to promote hydrolysis reactions leading to ring-opening and the formation of α-ω-silanediols [94,103], which are more water soluble compounds than cyclic methyl siloxanes. Thus, a phosphoric acid chemical activated carbon was chosen for this purpose according to previous investigations on siloxane adsorption [103].

Only hexane and the two target siloxanes were detected in the outlet of the BTF during stage III. The outlet concentration of the three compounds with the lowest REs rapidly dropped to negligible values when the activated carbon was added, likely due to physical adsorption (Figure 6.4). However, fast breakthrough curves were recorded until reaching the previous outlet concentration in approximately 250 min, which corresponded to the time required for the carbon layer to get completely wet. According to Chapter 4 and 5, the capacity of this carbon towards siloxanes was known to be higher than 170 mg Si g_{AC}^{-1}, therefore the breakthrough of the carbon layer in the present study was estimated to be reached in a period of time longer than 3 years. However, the rapid breakthrough curves herein obtained suggested that adsorption of both siloxanes and hexane in soaked activated carbon was negligible.

Interestingly, the beneficial role of activated carbon on hexane and D5 was evident after an acclimation period of 20 days (Figure 6.2 from day 170 on). Indeed, the removal efficiency of

hexane increased up to steady state values of 43 ± 2 %. Previous investigations on the biodegradation of hexane by *Pseudomonas aeruginosa* identified that mass transfer limited the performance of bioreactors, which encouraged the use of organic solvents to enhance the availability of this hydrophobic gas pollutant [104]. In this investigation, the mass transfer of hexane to the biofilm was thereby enhanced with the addition of activated carbon.

The impact of activated carbon addition on siloxane removal depended on the type of siloxane. Thus, while D4 removal efficiency remained stable at 16% during stage III, D5-REs gradually increased up to steady state values of 45%. D5 affinity for chemically activated carbons was found stronger than that of D4 and other siloxanes in Chapter 4, as well as its proneness to transformation into α-ω-silanediols in the presence of moisture. In this context, the higher degradation of D5 could be related to the activated carbon layer, which supported the ring-opening polymerization of siloxane D5 and its transformation into more water-soluble compounds (i.e. α-ω-silanediols), eventually enhancing their mass transfer towards the biofilm.
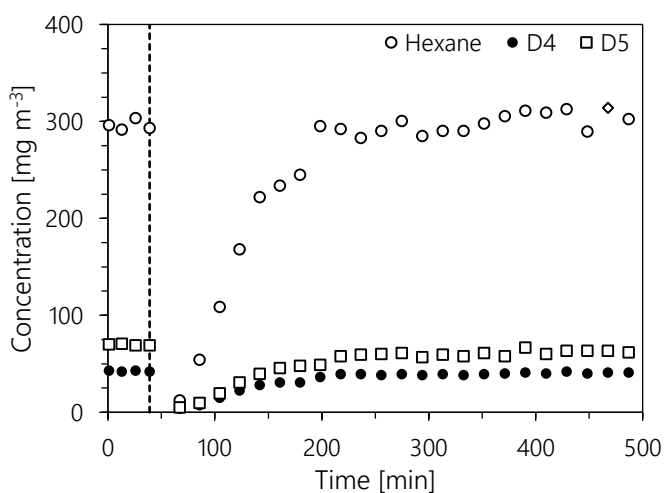
Figure 6.4 (A) Effect of the addition of AC at day 153 in Stage III (represented by the dashed line) on the outlet stream concentration of hexane (○), D4 (●) and D5 (□).

6.3.4   Activated carbon as biomass support

The activated carbon surface was analyzed at day 180 using scanning electron microscopy to observe the microbial population. SEM pictures (Figure 6.5B) revealed a carbon surface heterogeneously colonized by microorganisms, where the cracks and fissures in the rough surface of granular activated carbon served as effective spots for biofilm formation [105].
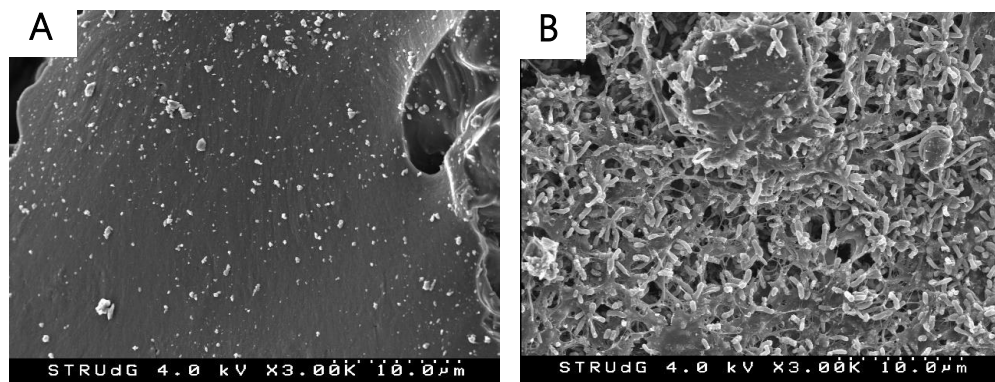
Figure 6.5 SEM photographs of the activated carbon (A) before and (B) after operating 30 days in the BTF within Stage III

Thus, after ensuring that biofilm was formed over the AC surface, the lava rock was completely removed from the reactor, which entailed that the 5 cm layer of activated carbon was the only packing material in the BTF and the EBRT decreased to 2 min (Stage IV). In this context, while toluene removal was complete, limonene RE decreased to 78% at the beginning of stage IV. This initial decrease in the RE of this monoterpene was likely mediated by the absence in the AC of a microbial community capable of degrading limonene, which was completely degraded throughout the lava rock layer during Stage II, and therefore prevented the exposure of the top AC-layer to limonene in Stage III. Thus, the microbial community already acclimated to limonene was also cleared from the BTF when removing the lava rock. However, the RE of limonene reached 100 % within the next 3 days from re-packing of the BTF, which highlighted the high robustness of the system and the rapid acclimation of the microbial community to VOCs. The lava rock evacuation and its associated decrease in the EBRT to 2 min resulted in a sharp decrease in D5 removal efficiency from 43% at the beginning of stage IV to steady stated values of 22. D5 abatement in the BTF during steady state was likely due to a combination of microbial degradation boosted by an enhanced siloxane adsorption and hydrolysis mediated by the activated carbon. Overall, the BTF packed with a thin layer of activated carbon (corresponding to an EBRT of 2 min) achieved comparable removal efficiencies to those recorded in the BTF packed with a 6 times larger of lava rock bed (Figure 6.3, EBRT 14.5 min). The AC was an effective packing material for cell attachment as well as an efficient packing material for the final polishing of biogas. This study also confirmed that a short bed of AC (i.e. low EBRT) would entail smaller bioreactor volume than the lava rock, which will significantly decrease the capital and operating cost of biogas.

6.3.5 Processes governing siloxane removal

In stages II and III the GC-MS analysis of the outlet gas did not detect significant amount of volatile metabolites. In this context, the trickling solution was analyzed to determine the presence of soluble transformation products during the operation with lava rock (Stage II-4) and lava rock and AC (Stage III). Acid silicic concentrations of 7.3 and 10.6 mg Si L^{-1} were recorded during stage II-4 and III, respectively. Moreover, GC-MS qualitative analysis revealed the presence of dimethylsilanediol (DMSD), tetramethyl-1,3-disiloxanediol and hexamethyl-1,5-trisiloxanediol (Table 6.2) in the trickling liquid of stage III. Only the first two silanediols compounds were identified at lower concentrations in the trickling solution during stage II-4. These results agree with the higher removal efficiency of D5 achieved under BTF operation with an activated carbon packed bed. This siloxane transformation products are formed by both i) bond cleavage of D4 and D5 through hydrolysis reactions promoted by AC's functional groups, and ii) biodegradation of larger α-ω-silanediols, D4 and D5. Thus, the higher concentration found was the consequence of both the AC catalytic activity and biodegradation, which would eventually support the hypothesis of the ability of ACs to catalyze the ring-opening of cyclic siloxanes and thus boost siloxane degradation. Since silanediols could not be quantified due to lack of commercial reagents, total Si analysis were performed by ICP-OES aiming at closing the Si mass balance. Si contents of 13.2 and 21.8 mg L^{-1} were obtained in the trickling solution of Stages II-4 and III, respectively. For the mass balance, it was taken into account that the liquid samples were collected after 3 days (when the recirculation media was replaced) and a total liquid volume of roughly 400 cm^3. The Si analyses accounted for a 22 and 36% of the total Si that entered the reactor and was found dissolved in the recirculation liquid of Stages II-4 and III, respectively. Moreover, according to the average REs obtained for both D4 and D5 in the different stages, a 74 and 65% of Si was found in the outlet emissions in Stage II-4 and III, respectively, which mostly completed the Si mass balance. The remaining percentage of Si to reach 100 was below 4% in both stages, which could be attributed to the inlet concentration stability as well as the accurate liquid volume in the system. In this context, siloxane removal was likely due to mainly biodegradation in stage II-4. In stage III biodegradation would still be the major process involved, though boosted by transformation reactions due to the AC surface, as observed with the higher presence of Silicon soluble species.

On the other hand, in stage IV the use of activated carbon as biomass support drastically increased the elimination capacity of siloxanes. Thus, the removal efficiency of the system remained stable despite the reduction of the EBRT from 14.5 min (Stage I) to 2 min. In order to get a further insight on the mechanisms governing siloxane removal, activated carbon

samples were collected at the end of Stage IV to analyze the compounds adsorbed or retained in the biofilm. THF extraction showed that the siloxane retained in the solid phase was in a concentration below the quantification limit (<0.5 mg m^{-3}). Considering the total volume of the packing material and the amount of siloxane circulated during the whole stage, both physicochemical adsorption and biosorption of siloxane removal could be ruled out.

While no volatile silicon byproducts were detected in the gas outlet, the CO_2 production during Stage IV was monitored. An average increase in the concentration of CO_2 up to 405 ppm$_v$ was detected, which corresponded to 21 g h^{-1} m$_{reactor}$$^{-3}$. This CO_2 production corresponded to an average pollutant mineralization of 80% considering both the siloxanes and VOCs removed. Such incomplete mineralization determined by the CO_2 analysis could be linked to the accumulation of methyl-siloxane by-products in the liquid phase as well as the growth of new biomass. Therefore, these results supported the hypothesis that biodegradation was the predominant process involved in the removal of VOCs and siloxanes.

6.3.6   Robustness evaluation of the BTF

In order to assess the impact of trickling solution dispersion on the performance of the BTF, the recirculation of the trickling solution was paused during periods of ca. 5 hours and re-started. While toluene and limonene were completely removed during the trickling dispersion period, both biogas pollutants were detected in the exhaust gas in the absence of irrigation likely due to the limitation in nitrate availability, which was the only final electron acceptor in the biodegradation process. Moreover, biodegradation metabolites from the incomplete mineralization of limonene were detected in the outlet emission. Figure 6.6 depicts the outlet/inlet areas ratios (C/C$_0$) for toluene, limonene and metabolites during the stop and resumption of the trickling solution. After 5 h of trickling solution shutdown, the C/C$_o$ ratios for toluene and limonene reached 0.7 and 0.46, while a complete removal of both pollutants and metabolites was recorded after the resumption of trickling dispersion. GC-MS analysis of the outlet gas in the absence of irrigation identified 2-carene and α-terpinene (Table 6.2) as the main metabolites released during the incomplete oxidation of limonene in the absence of NO$_3$$^{-}$. Moreover, a qualitative analysis by GC-MS of the trickling solution revealed traces of p-cymene, which could have also originated from the partial oxidation of limonene.

On the other hand, Figure 6.6B shows the performance of the BTF packed with activated carbon (stage IV) during an event of irrigation stoppage. During the 5-hour trickling solution shutdown, the removal efficiency of both toluene and limonene remained at 100 % and no

metabolite was detected in the outlet gas emission. It needs to be highlighted that, as visually noticed, the carbon layer remained highly humidified during period without irrigation, which was not observed during the same experiment with lava rock. This finding suggested that the porous AC was capable of retaining sufficient amount of trickling solution to provide the biofilm with the necessary compounds to maintain microbial activity during periods without irrigation. Using AC as packing material in anoxic BTF may guarantee a sustained electron acceptor availability to the biofilm compared to conventional packing media, which are dependent on stable irrigation conditions.
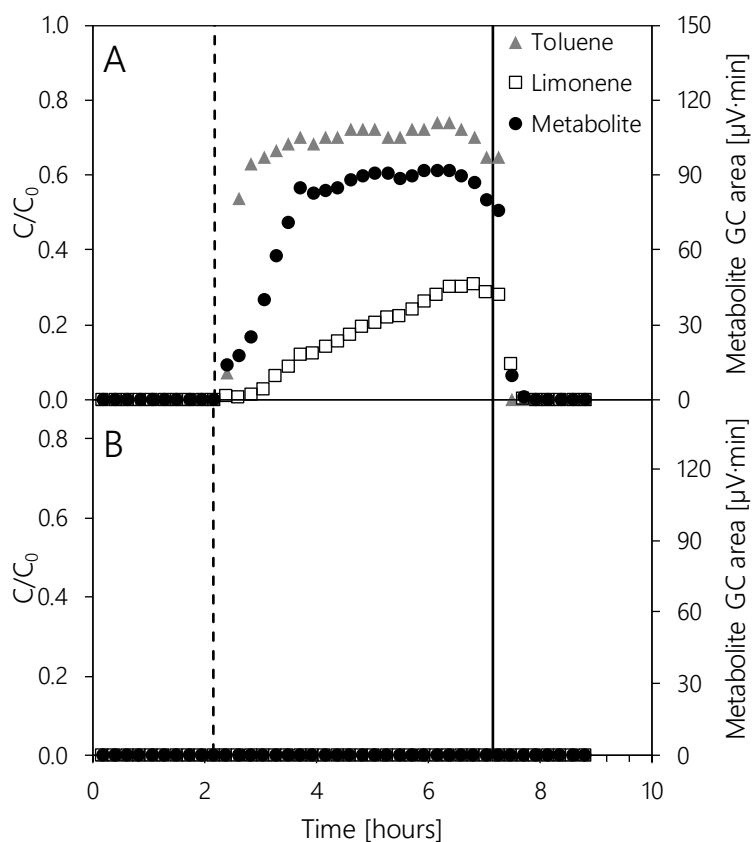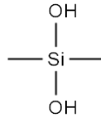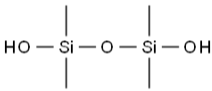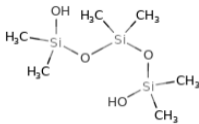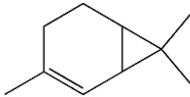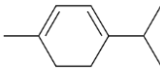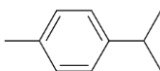
Figure 6.6 Time-course toluene (▲) and limonene (□) and the GC-FID response in area units of the metabolites in the outlet gas (●), vertical dashed lines indicate the stoppage of the trickling recirculation, and vertical solid lines display the re-start of the recirculation. Data corresponding to stage II-1 with lava rock as packing material (A) and stage IV with AC (B).

The results herein obtained also suggest that a supplementary adsorption treatment would be required for complete siloxanes removal. The complete removal achieved for the target VOCs

in the lava rock bed is particularly relevant since toluene and limonene are major competitors for adsorptive sites in current biogas adsorption technologies [94]. A complete VOC removal in an anoxic BTF prior a final adsorption polishing step, together with the partial siloxane biodegradation, might extend the lifetime of adsorption filters, which would ultimately decrease the operational costs of biogas upgrading.

Table 6.2 Metabolites identified by GC-MS during the BTF operation.

Metabolite [abbreviation]	MW [g mol^{-1}]	Chemical formula	Analytical ions m/z [abundance*]
Dimethylsilanediol [DMSD]	92.2		77 [99.9] 45 [14.6] 78 [6.6]
Tetramethyl-1,3-disiloxanediol	166.3		133 [99.9] 151 [71.2] 135 [22.6]
Hexamethyl-1,5-trisiloxanediol	240.5		207 [99.9] 208 [21.1] 209 [17.0]
2-carene	136.2		93 [99.9] 121 [96.8] 136 [66.9]
α-Terpinene	136.2		121 [99.9] 93 [84.7] 136 [42.6]
p-cymene	134.2		119 [99.9] 91 [34.7] 134 [23.8]

*Abundance – relative intensity of each ion peak in % to the maximum ion intensity

6.4   Final remarks

This chapter confirmed the potential of biotrickling filtration to remove siloxanes and VOC under anoxic conditions. Toluene and limonene were effectively degraded regardless of the EBRT tested. Siloxane D5 was more biodegradable than D4, with a removal efficiency of 37% at the longest EBRT tested. The use of activated carbon as packing material to overcome the mass transfer limitation encountered during the biodegradation of hexane, D4 and D5

supported an effective biomass growth, while promoting hydrolysis reactions leading to soluble silanediols. Furthermore, AC supplementation enabled BTF operation at reduced EBRTs, which would ultimately decrease the operating and investment cost of biogas upgrading. This study also demonstrated a high robustness towards variations in the EBRT and interruptions in the trickling solution dispersion.

Chapter 7

RESULTS IV

Biogas treatment in membrane bioreactors

7.1   Background and objectives

Membrane biofiltration is based on the transference of gas pollutants from one side of the membrane to the other side where a biofilm is grown over the membrane surface and is in contact with a mineral medium containing nutrients. Several membranes can be found commercially. Dense membranes are more selective but their capacity of diffusing the pollutants from one side to another will also depend on the solubility and diffusivity of the contaminant [50]. The driving force for the pollutants to permeate through the membrane depends on the concentration difference between both sides, which will therefore depend on the capacity of the microbial population to degrade the contaminants [106].

Membranes are capable of selectively permeate pollutants hardly transferred with other reactor configurations [107]. Few scientific papers can be found in the literature evaluating the treatment of VOC-laden gases at laboratory or pilot scale, such as toluene, benzene and hexane among others [74,108]. Considering biogas treatment, siloxanes permeation through PDMS membranes was evaluated with clean air in the other side of the membrane [45]. No reports are found for this issue by means of membrane bioreactors.

The aim of this study is to investigate the performance of a PDMS hollow-fibre membrane bioreactor inoculated with anaerobic digester sludge on the removal of siloxanes in the presence of VOCs.

7.2   Methodology

The hollow-fiber reactor membrane bioreactor set up, operation and inoculum procedures are detailed in Section 3.5. Firstly, it was operated with clean water to study the target pollutants transference from the lumen side (gas) towards the shell side (water). Then, it was inoculated with anaerobic digester sludge to investigate the degradation of both siloxanes and VOCs.

Table 7.1 Concentration of the target pollutants in the feed gas of the membrane reactors.

Pollutant	Hexane	Toluene	Limonene	D4	D5
Concentration [mg m^{-3}]	375 ± 18	24 ± 2	220 ± 11	54 ± 3	102 ± 5

7.3   Results and discussion

7.3.1   Abiotic diffusion of the pollutants

Towards clean air

The capacity of the PDMS membrane module to separate the target pollutants was investigated in gas abiotic experiments. Each target concentration was monitored in the feed gas and in both outlet streams (lumen and shell). The transport efficiency for each pollutant under different ratios is reported in Figure 7.1. Experiments were done by triplicate with a relative error below 5%. Similar experiments were carried out by Ajhar et al., (2012) [48] with gas polluted with cyclic and linear siloxanes, and high permeabilities for the siloxanes D4 and D5 were reported.

The transport efficiency of most compounds displayed a clear steep increase with the shell/lumen flow ratio as observed in Figure 7.1. Incrementing the flow of clean gas in the shell side distinctly boosted the transference of the target pollutants through the membrane. In the case of limonene and D5, their transport increased from 66.5 and 74.5% at the lowest ratio, respectively, up to 94.8 and 99.2 at the highest ratio 8. The transport of toluene and D4 went respectively from 55.2 and 51.4% up to 82.7 and 76.8% by increasing the shell/lumen ratio from 0.5 to 8. Contrarily, hexane was the compound with the lowest transport efficiencies, demonstrating a flat increase from 36.8 to 48% from 0.5 to 8 ratios.
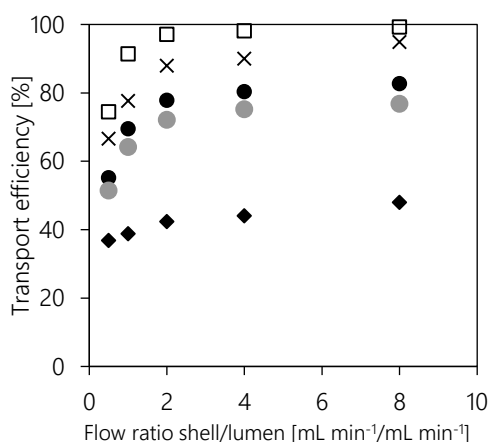

Figure 7.1 Toluene (●), limonene (□), hexane (♦), D4 (●) and D5 (×) transport efficiency through the membrane in (A) gas/gas experiments at different flow ratios (shell/lumen).

The transport efficiency of all pollutants, excluding hexane, through the membrane was above 50% even at the lowest shell/lumen ratio tested, demonstrating that operating at such a short residence time (i.e. 0.72 s), and with a low gas flow through the shell side, the target pollutants were successfully permeated through the membrane. Moreover, the diffusion of all compounds levelled off at a flow ratio of 2, where high transport efficiencies were already recorded, being 97.1, 87.9, 77.8 and 72.1% for limonene, D5, toluene and D4, respectively. Therefore, incrementing the shell flow from 100 up to 400 cm^3 min^{-1} did not significantly improve the pollutants transport.

Towards clean water

In order to approach a bioreactor configuration, in which a liquid media is found in one side of the membrane, the capacity of the contaminants to permeate from the lumen side towards water in the shell side was investigated. An open configuration with clean water continuously circulating through the membrane (water/gas) was set-up. The transport efficiency of each compound was evaluated at different gas residence time (9.6, 16, 24, 40 and 60 s) (Figure 7.2).

A noticeable linear increase in the transport efficiency with the residence time was observed specially for toluene, which was the compound with the highest water solubility. At 9.6 s its transport across the membrane was of 40% and it raised up to 84 and 93% when the gas residence time was increased to 40 and 60 s, respectively. Limonene had a definite increase from 28% at 9.6 s up to 53% at 60 s, although the improvement from 16 (39%) to 40 s (44%) was not significant, which might be explained by the relatively low solubility of limonene in water. For the same reason, D4, D5 and hexane, that are low water-soluble compounds, were less transported through the membrane than toluene and limonene. Maximum transport efficiencies for D4, D5 and hexane were 28, 37 and 21%, respectively, obtained at 60 s of residence time.

The PDMS membrane was capable of permeating both siloxanes in the abiotic gas experiments, but when water was present in the other side of the membrane, their diffusion was hampered due to their low solubility. In the case of hexane, a lower affinity with the membrane material than for the rest of pollutants was observed in the abiotic gas experiments, and the presence of a liquid media did not improve its permeation through the membrane, which is in good agreement with Lebrero *et al.*, (2014) [74]. In this sense, even the much higher residence time in comparison with the gas experiments, the transfer of the compounds was also related to their Henry's law coefficients.
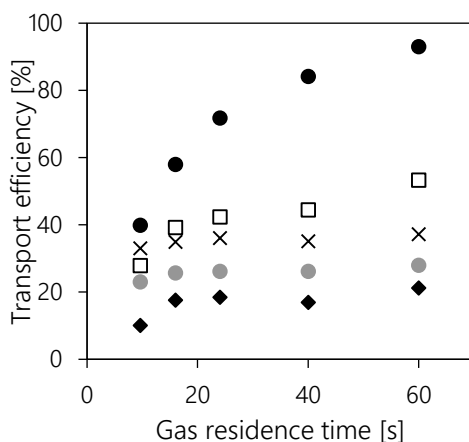
Figure 7.2 Toluene (●), limonene (□), hexane (♦), D4 (●) and D5 (×) transport efficiency through the membrane in water/gas tests at different EBRTs.

7.3.2   HF-MBR performance

Start-up of the HF-MBR

At the light of the results obtained in the abiotic tests, the HF-MBR was inoculated with anaerobic sludge from an urban WWTP and fed with the synthetic gas stream as in the abiotic experiments. The outlet of the membrane was monitored for evaluating the RE and EC of each target compound (Figure 7.4).

The reactor was initially operated at a gas residence time of 18 s, corresponding to the first period of operation (stage I, days 0-36). Steady state for toluene and limonene (Figure 7.4B and C) was achieved within 7-8 days reaching average REs of 52 ± 2 and 85 ± 3%, respectively, which corresponded to ECs of 2.4 ± 0.1 and 33.5 ± 1.2 g m^{-3} h^{-1}. In the abiotic experiments with a clean water stream circulating continuously, the transport efficiency of these target VOCs at 16 s of gas residence time was 39.2 and 57.9% for limonene and limonene. Therefore, the presence of a biofilm in the shell side of the membrane clearly promoted a higher elimination of these target VOCs. The degradation of these compounds favored their diffusion through the membrane, which led to higher REs. Hexane steady state was achieved after 15 days with an average EC of 2.1 g m^{-3} h^{-1} (corresponding to a RE of 4%). This compound abatement was expected to be lower than the other VOCs due to the low diffusion through the membrane previously observed in the abiotic experiments. Siloxanes removal efficiencies were found to be fluctuating from REs from 2 to 23% in the case of D5 (Figure 7.4E), and from 4 to 14% for D4 (Figure 7.4D). The lack of stability in the removal of siloxanes could be attributed to the

oscillating concentration of NO_3^- in the recirculation mineral medium, which acted as the final electron acceptor (Figure 7.5B).

The gas outlet of the membrane revealed the presence of CO_2, which was not detected in the feed gas. CO_2 was the final product resulting from the mineralization of the target pollutants being degraded by the biofilm in the shell side of the membrane. As observed in Figure 7.5, the carbon from the CO_2 recorded in the outlet emission did not fit in with the C degraded from the pollutants, being the latter slightly higher. The CME within this stage was roughly 60%, suggesting a partial oxidation and therefore an accumulation of byproducts resulting from the biodegradation of the target compounds. In this context, the presence of a byproduct was recorded in the outlet emission of the reactor, which was later identified as α-terpinene by means of GC-MS analysis and a match higher than 90% with NIST library. The occurrence of such byproduct was related to an incomplete oxidation of limonene, as suggested earlier in Chapter 6 in an anoxic biotrickling filter when the input of NO_3^- in the trickling solution was limited due to interruptions on the irrigation system.

Furthermore, GC-MS analysis of the recirculation solution revealed the presence of dimethylsilanediol, which could not be quantified due to the lack of pure commercial standards. Dimethylsilanediol has been reported to be one of the main metabolites of D4 [60]. Since no data was found in the literature assessing the biodegradation of D5, we suggest that the apparition of such metabolite could originate from the degradation pathway of both D4 and D5.

Influence of the gas residence time

In order to improve the abatement of the pollutants, the gas residence time was increased to 31.5 s in the second stage (stage II, days 37-64). The longer residence time led to a rapid increase in the RE of all the VOCs (Figure 7.4). Hexane reached a steady state RE of 30 ± 6% corresponding to an EC of 12.5 ± 1.2 g m^{-3} h^{-1}. Toluene gradually increased until its absence in the outlet gas stream (i.e. below the detection limit of the analytical method) at day 52, which indicated that it was completely transferred through the membrane and so eliminated up until 2.6 ± 0.3 g m^{-3} h^{-1}. Limonene displayed a similar trend but right the day after increasing the residence time its removal was already complete reaching an EC of 22.4 g m^{-3} h^{-1}. The removal of siloxanes increased up to REs 17 ± 6 and 21 ± 6% for D4 and D5, respectively, where the ECs accounted for 1.0 ± 0.2 and 2.5 ± 0.7 g m^{-3} h^{-1}. Even though a higher gas residence time was provided, the stability of the siloxanes' removal continued displaying ups and downs along the time-course of the reactor operation.

The gas residence time was further increased to 63 s in the third period (stage III, days 65-100). Toluene and limonene REs remained complete, as expected. while the RE of hexane increased up to 43 ± 7%, much higher than the diffusion recorded in the water abiotic tests. Average ECs within this were 1.3, 11.2 and 8.2 g m^{-3} h^{-1} for toluene, limonene and hexane, respectively. The abatement of siloxanes slightly decreased to 14 ± 4% for D4 and 17 ± 2% for D5. The CO_2 produced within this stage averaged 60 ± 7 g m^{-3} h^{-1} and a stable CME as high as 91 ± 6 % was registered, which suggested that pollutants were almost completely mineralized towards CO_2. This was confirmed by a low presence of α-terpinene and even its absence in the gas emission.

Overall, toluene and limonene were completely removed when the HF-MBR was operated at gas residence times longer than 18 s, although even at such short contact time removals were found above 80% for both pollutants. As regarded in Figure 7.3 the RE of these VOCs was positively influenced by increasing the gas residence time. The removal of hexane also appeared to be boosted with higher residence times from 17% at 18 s up to an average RE of 42% at 63 s. In the case of siloxanes, their removal did not display a significant correlation with the gas residence time, indicating that their diffusion through the membrane towards the liquid side was limited due to their hydrophobicity regardless the residence time. REs ranged 17-21 and 20-22% for D4 and D5, respectively.
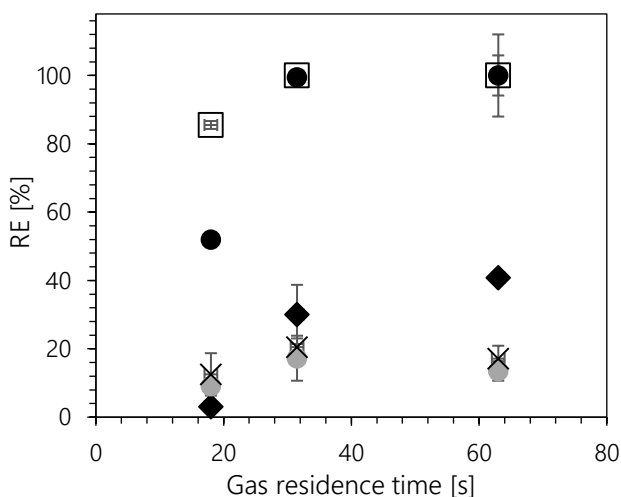

Figure 7.3 Influence of the gas residence time on the RE of hexane (♦), D4 (●), D5 (×), toluene (●) and limonene (□) at steady state

Strategies related to the final electron acceptor

During the operation of the HF-MBR in stages III and IV, different strategies were executed in order to enhance the performance and the stability of the system. Up until day 73, the nitrate input was carried out by replacing the mineral medium. Since a fluctuating NO_3^- concentration was observed (Figure 7.5B) in the mineral medium, an automatic injection of NO_3^- was started by means of a syringe pump. The concentration of NO_3^- was then maintained between 1.7 and 2.2 g L^{-1}, based on literature [97]. Moreover, the recycling solution replacement was decreased to a dilution rate of 0.1 d^{-1} to avoid so frequent washings of the biomass suspended in the recycling solution. Resulting from this strategy, a NO_3^- consume of roughly 50 mg $(L d)^{-1}$ (Figure 7.5B) supported an efficient removal of the VOCs and a less oscillating removal of siloxanes.

In stage IV (days 101-152) the gas residence time was decreased back to 18 s in order to evaluate the influence of the strategies over the removal of all the target pollutants, given the fact that toluene and limonene were already removed due to higher gas residence times. A sudden decrease in the performance of the HF-MBR occurred at day 104 due to membrane clogging. The clogging effect was most remarkably observed for both toluene and limonene, whose REs dropped to 24 and 30%, respectively. The membrane cleaning at day 108 allowed for the recovery of both target pollutants removal, which increased to average REs of 83 ± 12 and 94 ± 5%, clearly higher than those recorded in the first period that operated at the same gas residence time. Hexane removal was also achieved higher than in the first period, its RE increased from 5 to 21%. The performance of the HF-MBR towards siloxanes was more stable within this period with ECs of 1.7 ± 0.2 and 3.9 ± 0.7 g m^{-3} h^{-1}. The concentration of electron acceptor decreased after reducing the gas residence time to 18 s, so the NO_3^- infusion had to be adjusted due to an incremented consume of ca. 80 mg $(L d)^{-1}$.

Another strategy regarding the final electron acceptor was adopted at day 133 (days 134-152) and consisted in supplementing the gas matrix with a 1% of O_2, which is the common content of oxygen in biogas [109]. The RE of hexane stabilized at 14 ± 5%, slightly higher compared to the operation with NO_3^- alone. An enhanced RE was also observed for toluene, whose RE stabilized at 94 ± 3% and EC at 4.3 ± 0.2 g m^{-3} h^{-1}. For the rest of pollutants, no significant difference was distinguished when O_2 was incorporated. 79 ± 4, 15 ± 2 and 14 ± 2% steady state REs were recorded for limonene, D4 and D5 respectively, corresponding to ECs of 30.5 ± 1.5, 1.4 ± 0.2 and 2.6 ± 0.7 g m^{-3} h^{-1}.
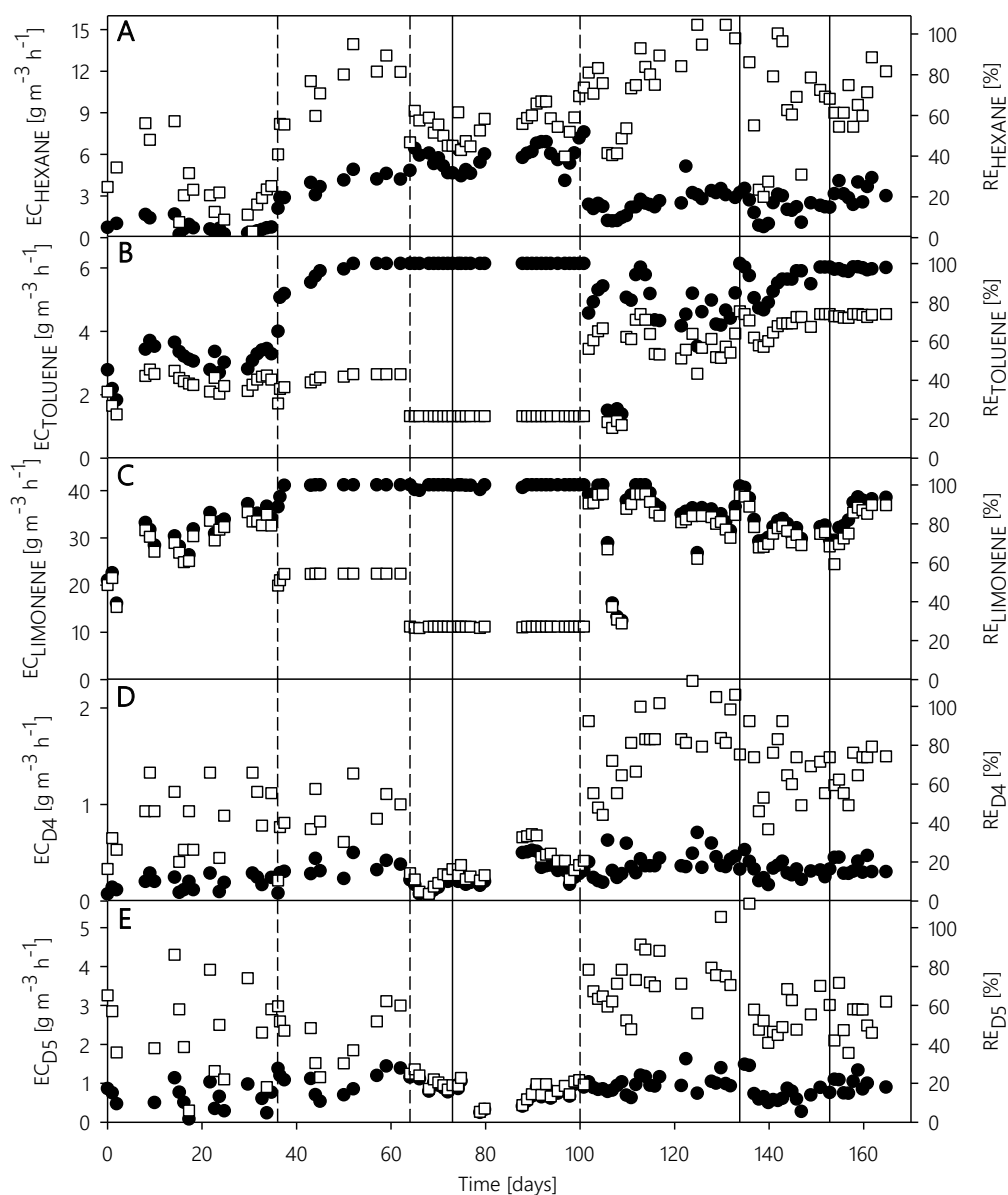
Figure 7.4 Removal efficiency (RE, ●) and elimination capacity (EC, □) of hexane (A), toluene (B), limonene (C), D4 (D) and D5 (E). Solid lined represent the strategies set for the electron acceptor (Automatic NO_3^- injection, 1% O_2 supply and NO_3^- injection stoppage).

The highest CO_2 production was recorded in this stage corresponding to an average 28 ± 6 g C m^{-3} h^{-1} (Figure 7.5A). However, the pollutants removal accounted for 45 ± 12 g C m^{-3} h^{-1}, giving a rough CME of 65 %, which was lower than in the previous stage. In this sense, a shorter residence time implied lower RE and therefore an incomplete oxidation of limonene towards CO_2, which was also observed in stage I. The change in the residence time affected specially

the removal of limonene (Figure 7.4C), and simultaneously the presence of α-terpinene was recorded, which eventually decreased the CME (Figure 7.5A).

Finally, the automatic infusion of nitrate was stopped at day 152 for investigating the capacity of the O_2 to act as sole electron acceptor. Limonene and toluene REs stabilized at 92 ± 1 and 98 ± 2, respectively, which was higher than the REs obtained with NO_3^- alone. The RE of hexane, D4 and D5 were maintained at similar values than those accomplished with nitrate. In this sense, the input of a 1% of O_2 in the gas matrix supported an efficient performance of the HF-MBR. These results suggest that the supplementation of NO_3^- to provide the microbial consortium with electron acceptor would not be necessary, which would eventually reduce the operating costs of the technology.
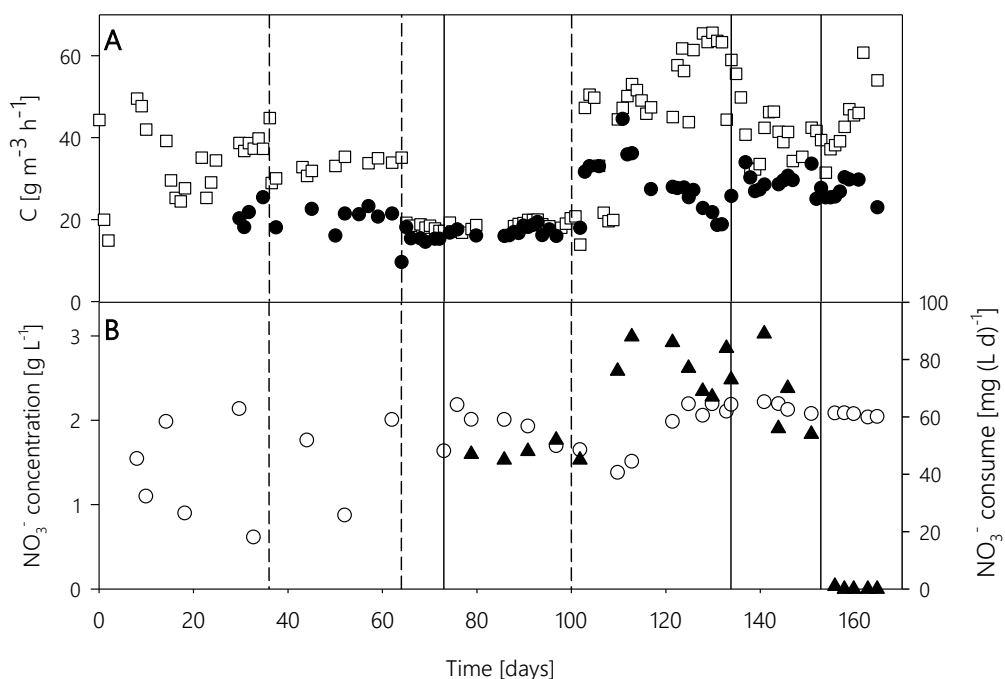
Figure 7.5 Time-course of (A) the removed pollutants in form of C (□) and the produced CO2 as C (●). And (B) the nitrate concentration in the recirculation mineral medium (O) and its consume (▲).

7.4   Final remarks

The present work confirmed the potential of PDMS membranes to separate siloxanes as well as other biogas impurities such as toluene and limonene from polluted gas towards a clean air stream. The presence of water in the other side of the membrane hindered the permeability of hexane, D4 and D5 due to their hydrophobic nature. The biofilm grown in the shell side of a HF-MBR enabled a complete transference of toluene and limonene when the gas residence time was above 31.5 s, and also a higher diffusion of hexane. The presence of CO_2 in the outlet of the HF-MBR confirmed the degradation of the pollutants and high carbon mineralization efficiencies were obtained reaching values above 90%. Several strategies regarding the final electron acceptor were performed. Supplementing the gas with a 1% of O_2 supported an efficient performance of the bioreactor, which eventually would reduce the costs of the technology since it is the common oxygen content in biogas. Moreover, byproducts from the limonene partial degradation were identified as α-terpinene in the gas emissions, and dimethylsilanediol was detected in the recirculation mineral medium from the degradation of siloxanes D4 and D5.

Chapter 8

RESULTS V

Coupling adsorption and biofiltration for siloxane removal

Redrafted from:
Beneficial aspects of coupling adsorption and biological technologies for siloxane abatement from biogas
Eric Santos-Clotas, Alba Cabrera-Codony, Maria J. Martin
Prepared for submission

8.1   Background and objectives

Activated carbon is by far the most applied technology for siloxanes abatement in biogas due to its maturity and high efficiencies [37]. However, its major disadvantage is the frequent replacements of exhausted material and disposal as waste, which leads to high operating costs [110]. Contrarily, biotechnologies are generally more convenient in terms of economic criteria and sustainability than their physic-chemical counterparts. Up to date, biotrickling filtration is the only technology that has been (scarcely) explored for siloxanes abatement. Nevertheless, as observed in Chapters 6 and 7, the efforts for removing these hydrophobic compounds by means of biological technologies has been challenged by mass transfer limitations [57,74].

The objective of the present work is to investigate the feasibility of coupling biotechnologies, particularly BTF, to adsorption onto activated carbon in pursuance of decreasing operational costs associated with carbon frequent replacement and disposal of the spent waste generated. It is well known that VOCs compete for the adsorptive sites of the activated carbon surface with siloxanes. Thus, removal of VOCs by biological technologies may extend the lifespan of adsorbent beds.

8.2   Methodology

Breakthrough curves were carried out following the concentrations in the different scenarios reported in Table 8.1. A set of three activated carbons, previously characterized in Chapter 4 was used for conducting the breakthrough experiments. AC1, AC2 and AC3 were named as SAC-2, SAC-4 and PhAC-1, respectively, in Chapter 5.

Table 8.1 Target concentrations of each compound for the different scenarios and their corresponding standard deviations.

Compound	Scenario A [mg m^{-3}]	REs reported [%]	Scenario B [mg m^{-3}]	Scenario C [mg m^{-3}]	Scenario D [mg m^{-3}]
Hexane	2520 ± 41	70[a]	714 ± 27	703 ± 16	0
Toluene	164 ± 4	99[a]	0	0	0
Limonene	1713 ± 31	99[b]	0	0	0
D4	431 ± 15	40[c]	377 ± 19	236 ± 11	430 ± 22
D5	765 ± 21	n.f.	673 ± 25	528 ± 44	765 ± 29

[a] Hexane and toluene REs at short EBRT [74] / [b] Limonene RE at short EBRT [111]
[c] D4 RE at long EBRT [57] / n.f. data not found

8.3 Results and discussion

8.3.1 Siloxane competitive adsorption

Biological abatement of siloxanes has recently proved to be a feasible technology to reduce their concentration in biogas streams while removing volatile organic compounds to further extend (as observed in Chapter 6). The efficiency of biotrickling filters was reported to depend on the EBRT of the gas with the biofilm grown in the bioreactor. Thus, the competitive adsorption of siloxanes with VOCs was evaluated considering biological pretreatment capable to reduce the concentrations of the feed gas to certain levels.

A set of experiments was performed to evaluate the performance of three ACs on the adsorption of cyclic siloxanes D4 and D5 in competition with limonene, toluene and hexane. Breakthrough curves are presented in Figure 8.1 depicting the concentration of each compound at the outlet of the adsorption column along with the bed volumes treated ($m_{gas\ treated}^3\ L_{AC}^{-1}$).

8.3.2 Scenario A: Raw biogas

Scenario A (S-A) corresponded to the raw biogas, where both siloxanes and VOCs presented the highest concentrations in comparison with the other scenarios (Table 8.1). In all the carbons tested (Figure 8.1) the first compound to break through was hexane, showing a steep profile in every case. Even being the highest concentrated molecule, the low molecular weight and size of hexane made this component the hardest to adsorb and the breakthrough curves showed an overshot, where the outlet concentration exceeded the inlet concentration, i.e. $C/C_0 > 1$. This roll-up effect demonstrated that hexane was weakly adsorbed and displaced by the other molecules in the mixture. When it comes to the rest of compounds, the lowest porous-developed AC1 (Figure 8.1A-1) behaved differently than AC2 and AC3 (Figure 8.1A-2 and A-3); breakthrough of siloxanes occurred simultaneously along with toluene and limonene when ca. 13 BVs had been treated. Complete exhaustion of the material (i.e. concentration in the outlet reached the feed concentration) did not occur until 22.5 BV had been treated. Limonene and D5 resulted the most strongly adsorbed compounds displacing both toluene and D4 as shown in competitive breakthrough curves.

In the contrary, breakthrough of target compounds in AC2 and AC3 followed the order: hexane>toluene>D4=limonene>D5, being more spaced out in AC3. Pore size distribution of these materials, where mesoporosity contribution is higher, led to stronger adsorption of the bulkiest D5 displacing the rest of compounds including limonene.
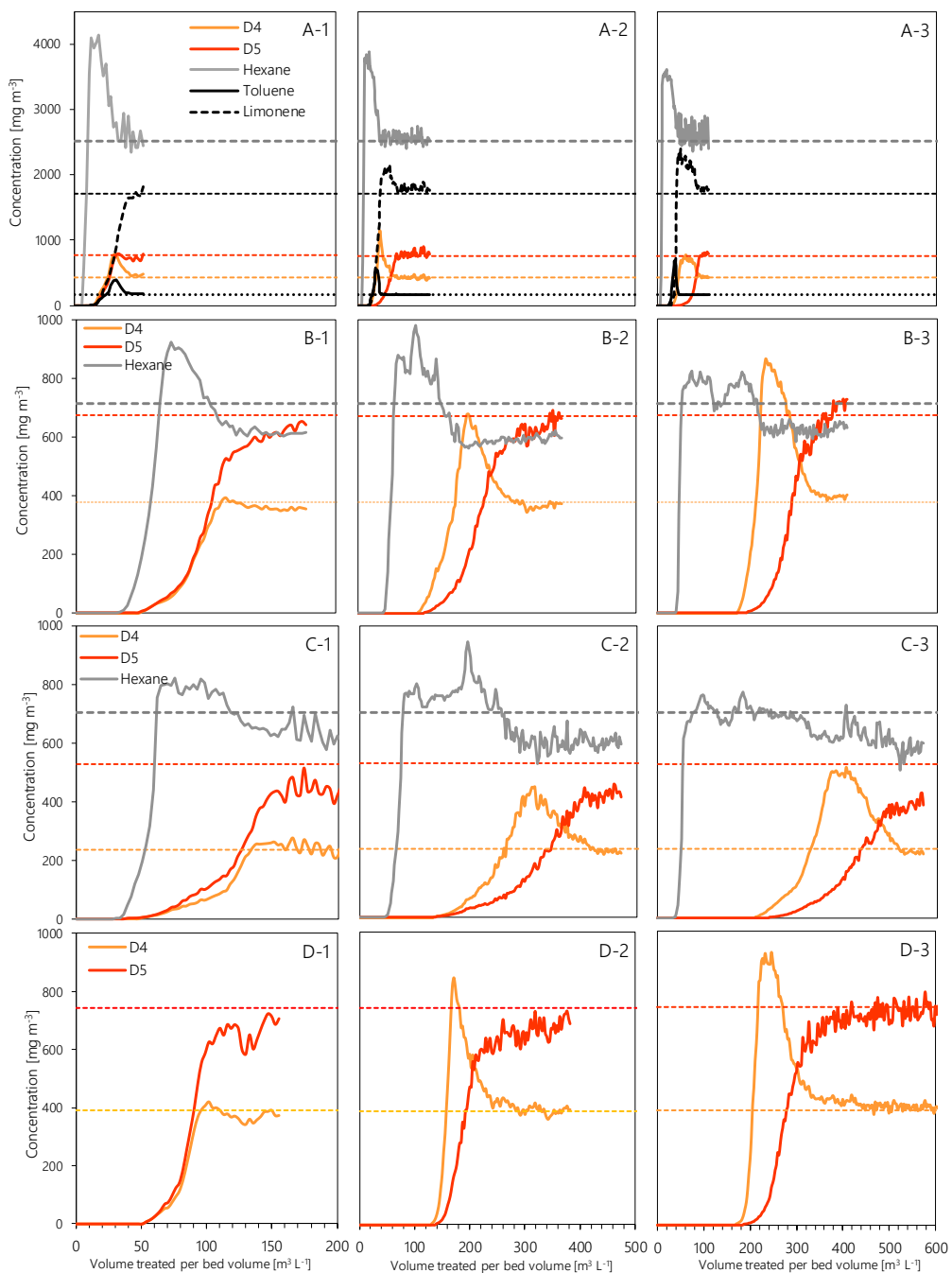
Figure 8.1 Breakthrough curves corresponding to the different scenarios (titled by its letter; A, B, C and D) and each activated carbon (denoted by the number after the scenario letter). Dashed lines correspond to the inlet concentration of each compound.

The adsorption uptake of each compound was calculated at i) D4 breakthrough (D4 BT), ii) D5 breakthrough (D5 BT), and iii) bed exhaustion (BE). In contemplation of Figure 8.2, the amounts of each compound adsorbed at different experimental points is compared. The hexane and toluene remaining at D4 breakthrough were completely displaced at bed exhaustion for all the carbons tested, while D4 uptake was successively reduced because of the displacement caused by limonene and D5. According to what is observed in the breakthrough curves, limonene was displaced by D5 only in AC2 and AC3 while the amount adsorbed increased until bed exhaustion for AC1. Thus, AC2 and AC3 are more suitable for siloxane adsorption than AC1 due to the larger pore size development. The comparative performance of these materials was evaluated by the BV treated at the time of the first siloxane breakthrough (D4 C/C_0=0.05): 23.9 and 35.5 m^3 L^{-1}, for AC2 and AC3 respectively.
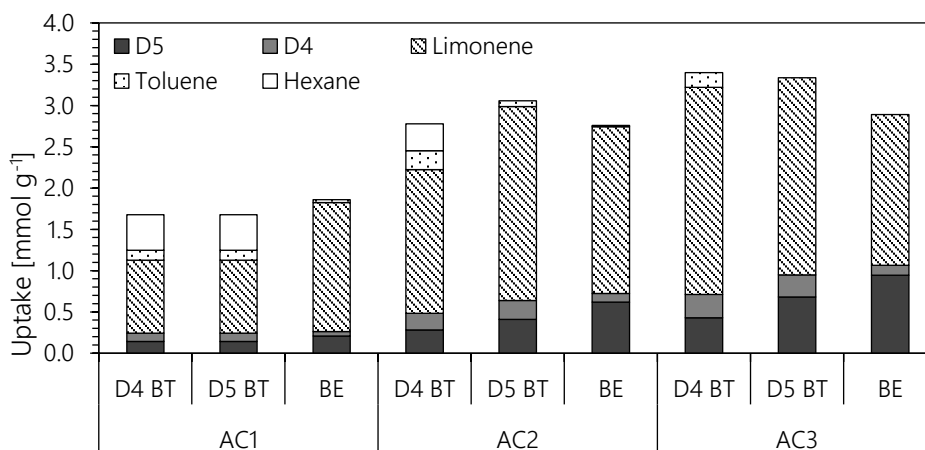

Figure 8.2 Distribution of the adsorbed target pollutants in S-A for all materials tested at D4 breakthrough (BT), D5 BT and bed exhaustion (BE).

8.3.3   Scenario B: Biological treatment

The gas in scenario B (S-B) corresponded to the biogas pretreated in a biotrickling filter operating at a short EBRT (1.5 min) where target compounds' concentration is reduced according to reported removal efficiencies in Table 8.1. Therefore, feed concentrations of siloxanes ~12% lower than in S-A, toluene and limonene were completely removed, and hexane's concentration decreased a ~70% because of the low mass transfer reported for this compounds [104]. It is important to highlight that, while toluene and hexane produced a low impact upon the siloxane adsorption capacities, as shown in Figure 8.2, the biological removal of limonene was expected to significantly increase the performance of the adsorbent beds

towards siloxane removal. Moreover, the competition of the remaining hexane with siloxanes is further discussed in Section 8.3.5.

The adsorption curves are depicted in Figure 8.1B. Overall, while the profile shape of the remaining compounds was similar to those in S-A, the absence of limonene in the test gas dramatically increased the BV treated for all the adsorbent materials; breakthrough of D4 increased up to 64.5 in AC1, 121.7 in AC2 and 181.1 m^3 L^{-1} in AC3 (Table 8.2). This corresponded to an enlargement of the adsorbent bed lifespan up to 500%. At bed exhaustion, the BV corresponded to 143.5, 305.5 and 351.2 m^3 L^{-1} for AC1, AC2 and AC3 respectively.

8.3.4   Scenario C: Extensive biological pretreatment

Further extending the EBRT in the BTF, up to 14 min, leads to a siloxane concentration decrease of ~40% as reported for D4 [57]. Thus, siloxane feed gas concentration in scenario C (S-C) were accordingly lower (Table 8.1). The curves depicted in Figure 8.1C revealed a significant decrease in the slope after the breakthrough because of the adsorption kinetics slow down due to the lowest inlet concentration. Thus, the bed exhaustion was reached at longer experimental time, reaching 450 m^3 L^{-1} of BV treated for AC3, which was 1.2 and 2.5 times higher than the BV treated in S-B and S-A, respectively.

8.3.5   Scenario D: complete VOC removal

Experiments corresponding to scenario D (S-D) were devoted to get further insights in the competence of VOCs and siloxanes for the adsorption sites in each activated carbon. Thus, adsorption tests of D4 and D5 in absence of VOCs were run to determine the maximum siloxane uptake and the performance decay caused by the presence of VOCs. BV results are gathered in Table 8.2 at different experimental points, i.e. D4 breakthrough, D5 breakthrough and bed exhaustion (D5 C/C_0 = 0.9). At the light of the breakthrough curves obtained (Figure 8.1D) it was confirmed that in AC1 both siloxanes broke through at the same time when 64.5 m^3 L^{-1} of BV had been treated without D4 roll-up while in AC2 and AC3 D5 displaced the smaller siloxane. At bed exhaustion, AC2 duplicated the performance of AC1 while AC3 triplicated it.

In general terms, results pointed out that hexane did not much interfere in siloxanes' adsorption in S-B, where the ~12% reduction on siloxanes concentration led to larger BV treated at bed exhaustion of all the carbons. Besides this, when siloxanes were previously abated ~40% using BTF with longer EBRT (S-C) the lifespan of activated carbon is further increased.

Table 8.2 Bed volumes treated at D4 and D5 breakthrough (BT) and bed exhaustion (BE).

	D4 BT			D5 BT			BE		
	AC1	AC2	AC3	AC1	AC2	AC3	AC1	AC2	AC3
S-A	12.6	23.9	35.5	12.6	35.1	56.8	22.5	66.7	88.3
S-B	64.5	121.7	181.1	64.5	140.3	221.6	143.2	305.5	351.2
S-C	78.4	181.0	245.5	78.4	194.1	302.2	185.3	397.1	450.2
S-D	64.8	139.2	186.1	64.8	152.5	218.5	113.0	255.6	353.4

8.3.6 Performance evaluation and economic approach

AC1 is currently being used in a WWTP for siloxanes removal from sewage biogas and the other materials are commercially available for other applications. Activated carbon is commonly replaced by fresh adsorbent when the carbon material is saturated in a lead-lag configuration.

In order to evaluate the performance of each activated carbon in the different scenarios explored, bed exhaustion was considered when D5 in the outlet of the column reached 90% of the feed concentration. Thus, this parameter was set for comparing the adsorption experiments in terms of total silicon uptake shown in Figure 8.3. The presence of VOCs clearly decreased the silicon adsorption capacity up to >2 times for the three materials. Furthermore, the steam-activated AC1 presented the lowest capacity (40 mg Si g^{-1}) and the phosphoric-activated AC3 displayed the highest capacity (274 mg Si g^{-1}). Contrarily, scenarios S-B and S-C presented comparable silicon adsorption capacities for each AC, but the BV treated were much higher in scenario C, where the concentration of the pollutants was reduced by a BTF operating at long EBRT.
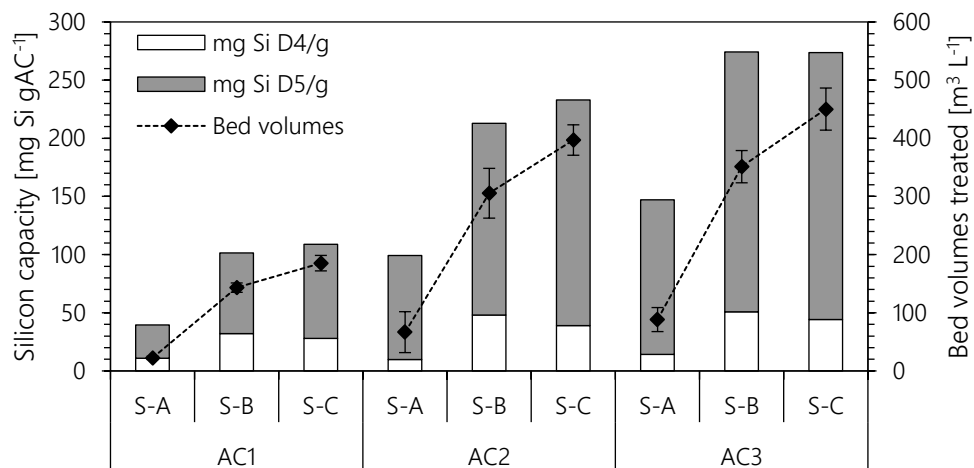
Figure 8.3 Adsorption capacities reported as silicon adsorbed from the contribution of D4 and D5 and bed volumes treated at bed exhaustion for each AC and scenario tested

In contemplation of all the scenarios, a pretreatment of biogas in a BTF at a high EBRT (S-C), clearly increased the BV treated with all the materials tested. Moreover, if biogas was pretreated and AC3 was used instead of AC1 (AC1 in S-A vs AC3 in S-C), the durability of the material would be extended up to 20 times. This remarkable lengthening of the material lifespan would induce savings in the operating costs of the adsorption technology, due to a reduced frequency in the replacement of the activated carbon as well as the exhausted material deposition.

A comparative economic evaluation of the operational costs of adsorption using each AC was carried out considering the bed volumes treated upon adsorbent exhaustion in each scenario according to the prices of the materials provided by the suppliers (ranging 2-7 € kg^{-1}). As shown in Figure 8.4, the steam-activated AC1, which is currently used in the studied WWTP, displayed the highest costs. When biological pretreatment is considered, i.e. S-B and S-D, activated carbon costs drastically decreased for the three materials up to 6 and to almost 10 times respectively. According to removal efficiency and material price, the lowest operating costs calculated were obtained by the steam-activated AC2 in S-C reaching 0.78 € (1000 m$^3_{treated}$)$^{-1}$.
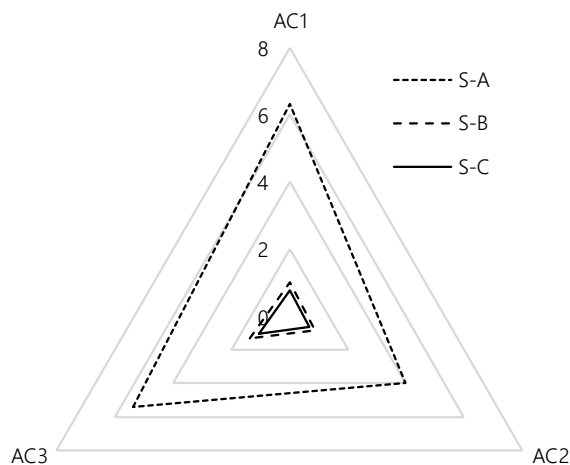
Figure 8.4 Operating costs in € $(1000m^3_{treated})^{-1}$ as a function of the biogas treated considering bed exhaustion as well as the AC market cost.

The economic feasibility of polishing the biogas in a BTF prior to the adsorption unit was also explored by taking into account not only the operating costs of the carbon filter but also the CAPEX and OPEX of the technologies involved in each scenario (Figure 8.5). Regarding the CAPEX of activated carbon technology, the adsorption unit was thought to be equal for all scenarios (~1400 € year^{-1}). The annual OPEX was calculated according to the costs shown in Figure 8.4, which ranged from >50000 € year^{-1} (in S-A with AC1) to <6000 € year^{-1} (in S-B with AC2). On the other hand, the annual capital costs associated with the BTFs was of ca. 4100 and 15600 € year^{-1} for S-B and S-C, respectively, considering a 10-year annualization. A higher residence time in the BTF leads to higher reactor volumes for treating the same flowrate, hence the greater costs obtained in S-C (EBRT = 14 min) compared to S-B (EBRT = 1.5 min). CAPEX of BTF was higher than for the adsorption unit, which is in agreement with other reports [12]. Contrarily to the OPEX of the AC filter, the BTF presented significantly lower operating costs, especially when compared with S-A. This remarkable difference is mainly due to the packing material replacement and disposal as a hazardous waste. Activated carbon filters require not only frequent replacement of the saturated material but also its disposal as hazardous waste. In contrast, the packing material in BTFs are much cheaper and have longer lifespans than porous activated carbons.

Overall, total annual costs were noticeably the highest obtained in the scenario treating a mixture of siloxanes and VOCs. The competition of VOCs and siloxanes for the porous sites of the adsorbent material led to reduced BVs and thus more frequent replacement of saturated material, which could be translated into higher operating costs. Even the costs associated with

the pre-treatment of biogas in a BTF, both in S-B and S-C, the total annual costs in these scenarios was much lower than S-A suggesting that the implementation of a BTF for polishing biogas from VOCs was economically feasible. The lowest annual costs were obtained for the steam AC2 in S-B (14315 € year^{-1}).
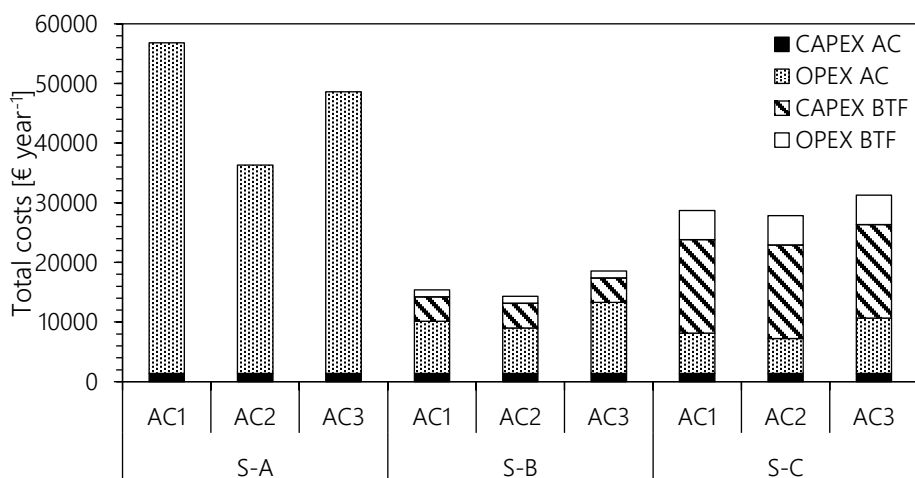

Figure 8.5 Total annual costs estimated for the treatment of biogas in all scenarios for each activated carbon.

8.4 Final remarks

The present chapter investigates the performance of three activated carbons on the adsorption of siloxanes at different concentrations in competence with VOCs aiming to evaluate the beneficial use of biological pretreatment of biogas. The abatement of limonene led to a high extension of the activated carbon lifespan, while using mesoporous carbons reduced the operational costs of the adsorption despite their higher price. Moreover, the economic approach on the technologies coupling confirmed the beneficial economic aspect of biotrickling filtration implementation to abate VOCs. The coal-based steam-AC (AC2) resulted in the material depicting the lowest operating costs, which decreased from 4.6 (in the worst-case scenario) to 0.7 € (1000 m$^3_{treated}$)$^{-1}$ in the scenario representing a pre-treated biogas in a BTF. Even contemplating both the CAPEX and OPEX of a BTF, the total annual costs were much lower when biogas was pre-polished from VOCs in a BTF. Therefore, the installation of a BTF operating at short EBRTs prior to an activated carbon filter with AC2 as the adsorbent material would imply savings in the total annual costs up to 4 times due to the lengthening of the lifespan of the adsorbent as well a less frequent disposal as hazardous waste.

Chapter 9

General discussion

General discussion

Biogas from anaerobic digesters in WWTP and landfills constitutes an alternative renewable source of energy that can be used for its conversion into heat or energy, injected to the gas grid or even used as a vehicle fuel. The energy conversion within the ECS is greatly hampered by the presence of siloxanes given their abrasive properties when exposed to combustion reactions. Therefore, its removal from biogas is a mandatory step in most of biogas applications. The most widely used technology for siloxanes abatement is non-regenerative adsorption onto activated carbon due to its major removal efficiency compared to other currently available techniques (e.g. absorption, refrigeration). Chemical interactions of carbon surfaces with siloxanes have been reported to occur, leading to polymerization reactions in which siloxanes are converted into silicon compounds of larger molecular weight that hinder thermal regeneration of spend adsorbents [112,113]. Hence the necessity to frequently replace the exhausted materials and so its disposal as a hazardous waste resulting in high operating costs and environmental impact. In this context, the elimination of siloxanes is a crucial topic of interest and there exists a pressing need to enhance the current technologies to more sustainable processes.

The present dissertation explores the abatement of siloxanes from biogas in both adsorption process and biological technologies. Since adsorption is currently applied for this issue in real facilities, the efforts within this work advance towards improving the performance of activated carbons, which is regarded in Chapters 4 and 5. Moreover, the elimination of siloxanes in a biotrickling filter (Chapter 6) and a membrane bioreactor (Chapter 7) was investigated in order to overcome the high operating costs linked to non-regenerative adsorption. Moreover, Chapter 8 analyses the benefits of coupling both technologies to overcome the limitations identified in the biological processes towards their implementation.

Adsorption of siloxanes onto activated carbons

Since adsorption is the most applied technique, it is an essential issue to screen the adequate carbon adsorbent to be integrated into biogas treatment technologies for removing siloxanes. Most of the reports on siloxane abatement found in the literature are focused on the removal of D4 or D5, correlating their uptake with textural properties such as surface area and pore volume [24,30,33]. It is also important to highlight that other biogas impurities compete for the adsorptive sites, which confers an unexplored topic in this field so far.

In the framework of Chapter 4, a set of 10 commercial ACs from different precursor materials and activations is evaluated towards the adsorption of a mixture of siloxanes (L2, D4 and D5) and VOCs (toluene and limonene). From the adsorption breakthrough curves carried out for all the materials, 3 main groups of carbons were classified according to the adsorption profiles. The competitive behavior of the adsorbates was explained by the porous features. The porosity in the H_3PO_4-ACs in group C was comprised of large pore volumes and widths and displayed higher siloxane uptakes than steam-ACs (group A and B). The carbons in group A were characterized by a distribution of small-size micropores leading to a higher uptake of VOCs than siloxanes D4 and D5. Contrarily, ACs in group B presented a greater contribution of larger pores which enabled the accessibility of D4 and D5. In most materials D5 and limonene were the most efficiently removed pollutants and were even capable of displacing the rest of compounds (i.e. roll-up).

The adsorption tests were also carried out with a relative humidity in the synthetic gas of ca. 25% (similar to real biogas). The high availability of water promoted transformation reactions of siloxanes into other cyclic siloxanes as well as α-ω-silanediols, leading to greater amounts of siloxane species, specially the phosphoric-ACs (given the higher presence of oxygen-functional groups). These species were identified in THF extractions of the spent carbon samples, but not in the outlet gas, which suggested that they were strongly retained in the carbon surface and/or the pores. The polymerization and transformation of siloxanes into silanediols enhanced the siloxane uptake. However, it need to be outlined that α-ω-silanediols condense into non-volatile polymers over the adsorbent surface thus hampering its thermal regeneration [112,114].

Seeking sustainable precursor materials

The main disadvantage of non-regenerative adsorption is the high operating costs related to the frequent replacement of the exhausted carbon and its disposal [20]. Not to mention the unsustainability derived from the constant generation of waste material and the subsequent demand of fresh adsorbent. Moreover, traditional activated carbons are commonly produced from expensive and non-renewable feedstocks such as coal, lignite, anthracite. The production of adsorbent materials from the valorization of lignocellulosic wastes as precursor materials is of great interest given the low cost associated in valorizing wastes from industrial activities [115,116]. Waste valorization not only implies the optimization of industrial production but also creates positive resources, which are some of the objectives of Circular Economy. CE is a

trending topic nowadays and it consists in an economic system that looks for minimizing waste and valorizing as much as possible the resources closing the loops of the materials.

In Chapter 5, a set of four experimental activated carbons were obtained from the valorization of lignocellulosic waste generated in a food industry. The lignocellulosic waste for two of the materials was pyrolyzed to explore the potentialities of the char residue as precursor material. The precursor materials were activated with K_2CO_3 and KOH at different activating agent/precursor weight ratios and activation temperatures, and the resulting adsorbents were characterized in terms of chemistry and texture together with three commercial ACs. Regarding their texture, all the experimental materials displayed BET surfaces above 1000 m^2 g^{-1} and total pore volumes between 0.4 and 0.7 cm^3 g^{-1}. These parameters were comparable or even higher than the commercial ACs. From the experimental materials, better textural developments were obtained within the non-pyrolyzed carbons activated with K_2CO_3.

The performance of these materials was investigated towards the adsorption of siloxanes and VOCs present in biogas. Upon adsorption equilibrium experiments, the waste-based ACs performed similarly or even better than some of the commercial samples (from non-renewable material precursors). The experimental data was fitted to the Dubinin-Astakhov model for predicting the maximum adsorption capacity for each target pollutant and AC. The highest capacity was found for the siloxane D4 in the commercial lignocellulosic-based H_3PO_4-activated carbon reaching 577 mg g^{-1}. One of the experimental carbons, K_2CO_3-activated, demonstrated the highest adsorption capacities for both toluene and limonene, up to 417 and 446 mg g^{-1}, respectively.

The relationship between the adsorption capacities (predicted by the DA model) and the textural development was explored. Ultramicropore volume did not correlate with any of the target pollutants, due to the molecule sizes being higher than the width of such porosity (0.7 nm). Microporosity was the major contributor for the adsorption of VOCs whereas for siloxanes both micro and mesoporosity played an important role.

Biogas pre-polishing in biological technologies

Non-regenerative adsorption onto activated carbon is the technology widely used for siloxane removal despite frequent exhausted material replacement and associated costs. Biological technologies are commonly superior in terms of economic and environmental sustainability criteria [54]. Emerging technologies such as biotrickling filtration and membrane separation in biogas are currently under investigation. BTF is a greatly versatile technology that can cope

with highly loaded waste gas effluents as well as low concentrations of odor-causing compounds in off-gas emissions [74,97]. Furthermore, the removal of H_2S from biogas in BTFs is a technically effective and economically feasible alternative to the physicochemical processes [7]. Regarding the biological abatement of siloxanes, some papers can be found in the literature reporting on the performance of BTFs for the treatment of a synthetic air stream spiked with D4 or D3 [57,58,60]. Most of these studies agree on a limited mass-transfer of siloxanes even operating at EBRT as high as 30 min. However, the performance of a BTF treating a synthetic biogas closer to real biogases (i.e. without O_2 and with other impurities) has not been explored up until the present dissertation. In the case of membrane processes, Ajhar *et al.*, (2012) proved siloxane permeation using PDMS membranes in gas-gas experiments [48], but the performance of membrane bioreactors has not been explored up to date. This thesis explores the potential of a BTF (Chapter 6) and an MBR (Chapter 7) for the cotreatment of VOCs and siloxanes under anoxic conditions.

The BTF was firstly inoculated with anaerobic sludge from a WWTP and operated at an EBRT of 14.5 min for the treatment of siloxane D4 reaching a RE of 14%. The microbial community analysis revealed that *Pseudomonas sp*. was one of the predominant species attached to the packing bed, so a pure inoculum of this specie was used for re-inoculating the reactor and thus boost the siloxane removal capacity. The C-source was switched from D4 to a mixture of siloxanes (D4 and D5) and VOCs (hexane, toluene and limonene) to approach real biogases, and the influence of the EBRT was evaluated (from 14.5 to 4 min). Toluene and limonene were completely removed from the influent gas regardless the EBRT. The removal of hexane and D4 did not show a significant relationship with the contact time, but D5 RE increased from 16 to 37% by increasing the EBRT from 4 to 14.5 min. The performance of the BTF towards hexane and both siloxanes was limited by mass transfer, which was enhanced by the supplementation of the packing bed with a 20% of activated carbon, especially for hexane and D5. The AC promoted hydrolysis reactions (as observed in Chapters 4 and 5) leading to water-soluble silanediols and finally biodegraded into silica.

Regarding the membrane experiments, gas-gas tests confirmed the transport of siloxanes and the VOCs up to transport efficiencies above 70% at flow ratios shell/lumen of 8. Also, in the water-gas tests high removal efficiencies (>50%) were recorded for limonene and toluene. Hexane diffusion was, in both scenarios, limited probably by a low affinity with the membrane material. When water was present in the other side, hexane and both siloxanes' transport across the membrane was challenged due to their low water solubility. The inoculation of the membrane module with anaerobic sludge enabled the complete diffusion and degradation of

toluene and limonene from gas contact times above 31.5 s. At this same contact time hexane, D4 and D5 were removed in 43, 17 and 21%, respectively.

On the whole, both biotechnologies tested were capable of eliminating completely toluene and limonene and reduce the rest of compounds' concentration to some extent. The main difference that needs to be pointed out is the gas residence time required for the different technologies, which in practical applications will define the biogas flowrate that may be treated as well as the reactor volume. In this sense, the gas residence time in the BTF was in the range 4-14.5 min whereas in the membrane was between 18 and 63 s. In terms of pollutants abatement, this was translated into a superior elimination capacity by the MBR reaching the highest EC for limonene at 33 g m^{-3} h^{-1}, which was more than 5 times higher than the highest EC accomplished by the BTF (when operated with AC at an EBRT of 2 min).

Hybrid technologies

Up to this point of the dissertation, the BTF set up in Chapter 6 proved to be capable of not only eliminating completely the VOCs but also reducing siloxanes concentration up to ca. 40%. However, the concentration of siloxanes in biogas must be decreased to really low levels in most of biogas-to-energy applications. Since accomplishing such low concentrations was not possible biologically, due to mass-transfer limitation, adsorption is still imperative for meeting the requirements for biogas applications. Furthermore, in Chapter 4 we assessed the high competitiveness of VOCs towards the porous sites of ACs, decreasing the siloxane uptake. In order to merge the knowledge acquired in these chapters, the benefits of coupling both technologies were examined in Chapter 8.

Chapter 8 explored both the technical and economic implications of coupling adsorption and biofiltration for siloxane removal as well as the use of different activated carbons, from which one of them is currently being used in a WWTP for this application. Moreover, several scenarios were suggested according to pre-treatment steps in a BTF operating at different EBRTs or mere adsorption of a raw biogas. The breakthrough curves revealed a remarkable increase in the bed volumes treated when biogas had (hypothetically) undergone a pre-polishing step in a BTF. The absence of toluene and specially limonene in the influent gas of the adsorption column led to an extended lifespan of the adsorbent up to 6 times when the BTF operated at short EBRT (i.e. 1.5 min). When the BTF operated at higher EBRT (i.e. 14 min), which permitted the reduction of siloxanes concentration up to 40%, the bed volumes treated were increased up to 8 times.

Regarding the operating costs of the adsorption process, the increased lifetime of the adsorbent drastically decreased the corresponding costs from 7 down to 0.78 € (1000 m$^3_{treated}$)$^{-1}$. In order to take a look at the big picture, not only the OPEX but also the CAPEX of both technologies was taken into account, resulting in lower total annual costs for the coupling of BTF and adsorption than treating the raw biogas (with VOCs) by adsorption alone.

Prospects for future research

Biogas is a highly attractive renewable energy and its use for energy applications is a trending market. So is the presence of silicon compounds in this methane-rich gas, given their interesting properties for many industry sectors, which leads to the undeniable necessity to remove them in an end-of-pipe technology. Biogas cleaning technologies are already capable of fulfilling the quality specifications from the combustion systems manufacturers' or legislations. However, additional work is necessary to further understand siloxanes behavior for treating them in a more sustainable and economic way. Some future prospects fueled by the present dissertation are listed below:

Non-regenerative adsorption

- Tailoring the textural properties of carbon adsorbents to improve their adsorption capacity towards siloxanes.
- Look for effective materials in siloxane adsorption that can be feasibly regenerated and avoid the huge amounts of material disposal as hazardous waste.
- Find technically effective and economically viable regeneration processes for exhausted carbon adsorbents.
- Investigate the feasibility of implementing low-cost and sustainable ACs at pilot scale and real WWTPs.

Biological technologies

- Explore the use of organic solvents (e.g. silicon oils) in order to overcome mass transfer limitations of siloxanes in biofiltration systems.
- Evaluate the co-treatment of VOCs, siloxanes and H$_2$S in one phase BTF, so the typical treatment train given to biogas (H$_2$S-water vapor-siloxanes) could be simplified.
- Study the supplementation of a HF-MBR with activated carbon in order to enhance the mass transfer of siloxanes to the biofilm.

Chapter 10

General conclusions

General conclusions

This thesis presented a step towards the evaluation of different technologies, including adsorption and biological processes, for siloxane removal from biogas. The most relevant conclusions arising from the present work are listed below:

Regarding adsorption onto activated carbons:

- Competitive adsorption:
    - VOCs impurities, commonly found in biogas, competed for porous sites of the adsorbent materials decreasing the adsorption of siloxanes.
    - Bulky siloxanes (D4 and D5) were preferentially adsorbed in the large micro and mesoporosity.
    - H_3PO_4 chemically activated carbons resulted in higher textural development as well as BET surface area, which was well positively correlated with siloxane adsorption.
    - Activated carbons promoted the ring-opening of siloxanes and so their transformation to other cyclic compounds and silanediols. This catalytic activity was superior in the H_3PO_4-ACs over the steam-ACs.

- Efficiency of the lignocellulosic-based activated carbons:
    - Lignocellulosic waste resulted to be a potential precursor material for its valorization into activated carbon.
    - Chemical activation with both KOH and K2CO3 led to good textural development in the experimental activated carbons.
    - Lignocellulosic waste-based chemically activated carbons demonstrated comparable, and even higher, adsorption capacities for both siloxanes and VOCs to commercial ACs.

Regarding the performance of biotechnologies:

- Biotrickling filter:
    - A complete removal of toluene and limonene was accomplished by an anoxic lab-scale BTF inoculated with Pseudomonas sp. regardless the EBRT.
    - The removal of hexane, D4 and D5 was correlated to their Henry's law coefficients, which indicated that mass transfer limitations challenged their abatement in the BTF.

- The supplementation of the packing bed of the BTF with AC enhanced the transference of hexane and D5 to the microbial community.
- AC supplementation enabled BTF operation at reduced EBRTs while displaying a high robustness towards interruptions in the trickling irrigation.

- Membrane bioreactor:
  - High transport efficiencies were recorded for most of the compounds at flow ratios above 1 in gas-gas tests. Hexane was the less transferred pollutant through the membrane.
  - Pollutants permeation across the membrane was challenged when clean water was circulated on the shell side, especially for the most hydrophobic compounds.
  - An anoxic lab-scale HF-MBR inoculated with anaerobic sludge was capable of diffusing and biodegrading toluene and limonene completely when gas residence times was set above 31.5 s.
  - Hexane RE was correlated with the gas residence time achieving a 42% at 63 s. Siloxanes removal did not depict a significant correlation with the residence time and was limited due to scarce mass-transfer.
  - The automatic injection of NO_3^- enhanced the stability in the elimination of siloxanes and improved the removal efficiency of the VOCs.
  - Supplementing the gas with a 1% of O_2 supported an efficient performance of the bioreactor, which eventually would reduce the costs of the technology.

Regarding the coupling of adsorption and BTF:

- The presence of VOCs in the synthetic biogas, especially limonene, reduced the capacity of activated carbons to adsorb siloxanes.
- When VOCs were hypothetically removed in a BTF prior to adsorption the BV treated were up to 8 times higher.
- A higher EBRT in the BTF led to lower concentrations of siloxanes in the BTF, which resulted into even higher BV treated in the adsorption unit.
- The pre-polishing step in a BTF led to lower operating costs of the activated carbon filter due to less frequent replacements of exhausted material.
- When CAPEX and OPEX of both technologies were regarded, the pre-treatment in a BTF at short EBRT followed by adsorption was the most feasible treatment train.
- Adsorption of raw biogas, with the presence of siloxanes as well as other impurities (i.e. VOCs), was the costliest treatment choice given the spent carbon replacement costs.

Chapter 11

References

[1]   B. Barometer, BAROMETER, (2017).

[2]   B. Deremince, S. Königsberger, Statistical Report of the European Biogas Association 2017, (2017) 20.

[3]   B. Tansel, S.C. Surita, Differences in volatile methyl siloxane (VMS) profiles in biogas from landfills and anaerobic digesters and energetics of VMS transformations, Waste Manag. 34 (2014) 2271–2277. doi:10.1016/j.wasman.2014.07.025.

[4]   S. Rasi, J. Läntelä, J. Rintala, Trace compounds affecting biogas energy utilisation - A review, Energy Convers. Manag. 52 (2011) 3369–3375. doi:10.1016/j.enconman.2011.07.005.

[5]   D. Deublein, A. Steinhauser, Biogas from Waste and Renewable Resources: An Introduction, WILEY-VCH Verlag GmbH & Co. KGaA, Weinheim, 2008.

[6]   D. Papadias, S. Ahmed, R. Kumar, Fuel Quality Issues in Stationary Fuel Cell Systems, (2011). http://www1.eere.energy.gov/hydrogenandfuelcells/pdfs/fuel_quality_stationary_fuel_cells.pdf.

[7]   A.M. Montebello, M. Mora, L.R. López, T. Bezerra, X. Gamisans, J. Lafuente, M. Baeza, D. Gabriel, Aerobic desulfurization of biogas by acidic biotrickling filtration in a randomly packed reactor, J. Hazard. Mater. 280 (2014) 200–208. doi:10.1016/j.jhazmat.2014.07.075.

[8]   G. Soreanu, M. Béland, P. Falletta, K. Edmonson, L. Svoboda, M. Al-Jamal, P. Seto, Approaches concerning siloxane removal from biogas - A review, Can. Biosyst. Eng. / Le Genie Des Biosyst. Au Canada. 53 (2011).

[9]   P.G. Aguilera, F.J. Gutiérrez Ortiz, Techno-economic assessment of biogas plant upgrading by adsorption of hydrogen sulfide on treated sewage–sludge, Energy Convers. Manag. 126 (2016) 411–420. doi:10.1016/j.enconman.2016.08.005.

[10]   A. Baldinelli, L. Barelli, G. Bidini, Upgrading versus reforming: an energy and exergy analysis of two Solid Oxide Fuel Cell-based systems for a convenient biogas-to-electricity conversion, Energy Convers. Manag. 138 (2017) 360–374. doi:10.1016/j.enconman.2017.02.002.

[11]   BOE-A-2013-185, Resolución de 21 de diciembre de 2012, de la Dirección General de Política Energética y Minas, por la que se modifica el protocolo de detalle PD-01, (2013) 889–892.

[12]   N. de Arespacochaga, C. Valderrama, J. Raich-Montiu, M. Crest, S. Mehta, J.L. Cortina, Understanding the effects of the origin, occurrence, monitoring, control, fate and removal of siloxanes on the energetic valorization of sewage biogas—A review, Renew. Sustain. Energy Rev. 52 (2015) 366–381. doi:10.1016/j.rser.2015.07.106.

[13]   Z. Zhang, H. Qi, N. Ren, Y. Li, D. Gao, K. Kannan, Survey of cyclic and linear siloxanes in sediment from the Songhua River and in sewage sludge from wastewater treatment plants, Northeastern China, Arch. Environ. Contam. Toxicol. 60 (2011) 204–211. doi:10.1007/s00244-010-9619-x.

[14]   A.L. Quinn, J.M. Regan, J.M. Tobin, B.J. Marinik, J.M. McMahon, D.A. McNett, C.M. Sushynski, S.D. Crofoot, P.A. Jean, K.P. Plotzke, In vitro and in vivo evaluation of the estrogenic, androgenic, and progestagenic potential of two cyclic siloxanes, Toxicol. Sci. 96 (2007) 145–153. doi:10.1093/toxsci/kfl185.

[15]   R. Dewil, L. Appels, J. Baeyens, Energy use of biogas hampered by the presence of siloxanes, Energy Convers. Manag. 47 (2006) 1711–1722. doi:10.1016/j.enconman.2005.10.016.

[16]   E. Wheless, J. Pierce, Siloxanes in landfill and digester gas update, SCS Eng. Environ. Consult. Contract. (2004) 1–10. http://mercmail.scsengineers.com/Papers/Pierce_2004Siloxanes_Update_Paper.pdf.

[17]   L. Xu, Y. Shi, Y. Cai, Occurrence and fate of volatile siloxanes in a municipal Wastewater Treatment Plant of Beijing, China, Water Res. 47 (2013) 715–724. doi:10.1016/j.watres.2012.10.046.

[18]   M. Ajhar, M. Travesset, S. Yüce, T. Melin, Siloxane removal from landfill and digester gas - A technology overview, Bioresour. Technol. 101 (2010) 2913–2923. doi:10.1016/j.biortech.2009.12.018.

[19]   F. Deng, X.-B. Luo, L. Ding, S.-L. Luo, Application of Nanomaterials and Nanotechnology in the Reutilization of Metal Ion From Wastewater, Nanomater. Remov. Pollut. Resour. Reutil. (2019) 149–178. doi:https://doi.org/10.1016/B978-0-12-814837-2.00005-6.

[20]   A. Cabrera-Codony, M.A. Montes-Morán, M. Sánchez-Polo, M.J. Martín, R. Gonzalez-Olmos, Biogas upgrading: Optimal activated carbon properties for siloxane removal, Environ. Sci. Technol. 48 (2014). doi:10.1021/es501274a.

[21]   E. Finocchio, T. Montanari, G. Garuti, C. Pistarino, F. Federici, M. Cugino, G. Busca, Purification of Biogases from Siloxanes by Adsorption : On the Regenerability of Activated Carbon Sorbents, (2009) 4156–4159.

[22]   S. Giraudet, B. Boulinguiez, P. Le Cloirec, Adsorption and electrothermal desorption of volatile organic compounds and siloxanes onto an activated carbon fiber cloth for biogas purification, Energy and Fuels. 28 (2014) 3924–3932. doi:10.1021/ef500600b.

[23]   A. Cabrera-Codony, R. Gonzalez-Olmos, M.J.J. Martín, Regeneration of siloxane-exhausted activated carbon by advanced oxidation processes, J. Hazard. Mater. 285 (2015). doi:10.1016/j.jhazmat.2014.11.053.

[24]   M. Schweigkofler, R. Niessner, Removal of siloxanes in biogases, 83 (2001) 183–196.

[25]   L. Sigot, G. Ducom, B. Benadda, C. Labouré, Adsorption of octamethylcyclotetrasiloxane on silica gel for biogas purification, Fuel. 135 (2014) 205–209. doi:10.1016/j.fuel.2014.06.058.

[26]   C.A. Hepburn, B.D. Martin, N. Simms, E.J. McAdam, Characterization of full-scale carbon contactors for siloxane removal from biogas using online Fourier transform infrared spectroscopy, Environ. Technol. (United Kingdom). 36 (2015) 178–187. doi:10.1080/09593330.2014.941310.

[27]   W. Urban, H. Lohmann, J.I.S. Gómez, Catalytically upgraded landfill gas as a cost-effective alternative for fuel cells, 193 (2009) 359–366. doi:10.1016/j.jpowsour.2008.12.029.

[28]   R. Huppmann, H. Werner, H. Friederich, Cyclic siloxanes in the biological waste water treatment process – Determination, quantification and possibilities of elimination, Fresenius. J. Anal. Chem. 354 (1999) 66–71. doi:10.1007/s002169600011.

[29]   M. Schweigkofler, R. Niessner, Determination of siloxanes and VOC in landfill gas and sewage gas by canister sampling and GC-MS/AES analysis, Environ. Sci. Technol. 33 (1999) 3680–3685. doi:10.1021/es9902569.

[30]   D.R. Ortega, A. Subrenat, Siloxane treatment by adsorption into porous materials, Environ. Technol. 30 (2009) 1073–1083. doi:10.1080/09593330903057540.

[31]   B. Boulinguiez, P. Le Cloirec, Biogas pre-upgrading by adsorption of trace compounds onto granular activated carbons and an activated carbon fiber-cloth, Water Sci. Technol. 59 (2009) 935–944. doi:10.2166/wst.2009.070.

[32]   T. Matsui, S. Imamura, Removal of siloxane from digestion gas of sewage sludge, Bioresour. Technol. 101 (2010) S29–S32. doi:10.1016/j.biortech.2009.05.037.

[33]   K. Oshita, Y. Ishihara, M. Takaoka, N. Takeda, T. Matsumoto, S. Morisawa, A. Kitayama, Behaviour and adsorptive removal of siloxanes in sewage sludge biogas, Water Sci. Technol. 61 (2010) 2003–2012. doi:10.2166/wst.2010.101.

[34]   S. Nam, W. Namkoong, J.H. Kang, J.K. Park, N. Lee, Adsorption characteristics of siloxanes in landfill gas by the adsorption equilibrium test, Waste Manag. 33 (2013) 2091–2098. doi:10.1016/j.wasman.2013.03.024.

[35]   M. Yu, H. Gong, Z. Chen, M. Zhang, Adsorption characteristics of activated carbon for siloxanes, J. Environ. Chem. Eng. 1 (2013) 1182–1187. doi:10.1016/j.jece.2013.09.003.

[36]   P. Gislon, S. Galli, G. Monteleone, Siloxanes removal from biogas by high surface area adsorbents, Waste Manag. 33 (2013) 2687–2693. doi:10.1016/j.wasman.2013.08.023.

[37]   A. Cabrera-Codony, M.A.M.A. Montes-Morán, M. Sánchez-Polo, M.J.M.J. Martín, R. Gonzalez-Olmos, Biogas upgrading: Optimal activated carbon properties for siloxane removal, Environ. Sci. Technol. 48 (2014). doi:10.1021/es501274a.

[38]   T. Jafari, I. Noshadi, N. Khakpash, S.L. Suib, Superhydrophobic and stable mesoporous polymeric adsorbent for siloxane removal: D4 super-adsorbent, J. Mater. Chem. A. 3 (2015) 5023–5030. doi:10.1039/c4ta06593j.

[39]   T. Kajolinna, P. Aakko-Saksa, J. Roine, L. Kåll, Efficiency testing of three biogas siloxane removal systems in the presence of D5, D6, limonene and toluene, Fuel Process. Technol. 139 (2015) 242–247. doi:10.1016/j.fuproc.2015.06.042.

[40]   T. Jafari, T. Jiang, W. Zhong, N. Khakpash, B. Deljoo, M. Aindow, P. Singh, S.L. Suib, Modified Mesoporous Silica for Efficient Siloxane Capture, Langmuir. 32 (2016) 2369–2377. doi:10.1021/acs.langmuir.5b04357.

[41]   T. Jiang, W. Zhong, T. Jafari, S. Du, J. He, Y.J. Fu, P. Singh, S.L. Suib, Siloxane D4 adsorption by mesoporous aluminosilicates, Chem. Eng. J. 289 (2016) 356–364. doi:10.1016/j.cej.2015.12.094.

[42]   A. Cabrera-Codony, A. Georgi, R. Gonzalez-Olmos, H. Valdés, M.J. Martín, Zeolites as recyclable adsorbents/catalysts for biogas upgrading: Removal of octamethylcyclotetrasiloxane, Chem. Eng. J. 307 (2017). doi:10.1016/j.cej.2016.09.017.

[43]   W. Zhong, T. Jiang, T. Jafari, A.S. Poyraz, W. Wu, D.A. Kriz, S. Du, S. Biswas, M. Thompson Pettes, S.L. Suib, Modified inverse micelle synthesis for mesoporous alumina with a high D4 siloxane adsorption capacity, Microporous Mesoporous Mater. 239 (2017) 328–335. doi:10.1016/j.micromeso.2016.10.028.

[44]   S. Rasi, J. La, A. Veijanen, J. Rintala, Landfill gas upgrading with countercurrent water wash, 28 (2008) 1528–1534. doi:10.1016/j.wasman.2007.03.032.

[45]   M. Ajhar, T. Melin, Siloxane removal with gas permeation membranes, Desalination. 200 (2006) 234–235. doi:10.1016/j.desal.2006.03.308.

[46]   P. Pandey, R.S. Chauhan, Membranes for gas separation, Prog. Polym. Sci. 26 (2001) 853–893. doi:10.1016/S0079-6700(01)00009-0.

[47]   A. Petersson, A. Wellinger, Biogas upgrading technologies–developments and innovations, IEA Bioenergy. (2009) 20. doi:10.1016/j.wasman.2011.09.003.

[48]   M. Ajhar, S. Bannwarth, K.H. Stollenwerk, G. Spalding, S. Yüce, M. Wessling, T. Melin, Siloxane removal using silicone-rubber membranes, Sep. Purif. Technol. 89 (2012) 234–244. doi:10.1016/j.seppur.2012.01.003.

[49]   S.J. Ergas, L. Shumway, M.W. Fitch, J.J. Neemann, Membrane process for biological treatment of contaminated gas streams, Biotechnol. Bioeng. (1999). doi:10.1002/(SICI)1097-0290(19990520)63:4<431::AID-BIT6>3.0.CO;2-G.

[50]   A. Kumar, J. Dewulf, H. Van Langenhove, Membrane-based biological waste gas treatment, Chem. Eng. J. 136 (2008) 82–91. doi:10.1016/j.cej.2007.06.006.

[51]   P. Habil, J. Lukasiak, A. Dorosz, Biodegradation of Silicones (Organosiloxanes), Biodegradation. (n.d.) 539–543. doi:10.1002/3527600035.bpol9024.

[52]   J.C. Carpenter, J.A. Cella, S.B. Dorn, Study of the Degradation of Potydimethyfsiiexanes on Soil, Environ. Sci. Technol. 29 (1995) 864–868. doi:10.1021/es00004a005.

[53]   R.G. Lehmann, S. Varaprath, R.B. Annelin, J.L. Arndt, Degradation of silicone polymer in a variety of soils, Environ. Toxicol. Chem. 14 (1995) 1299–1305. doi:10.1002/etc.5620140806.

[54]   R. Muñoz, L. Meier, I. Diaz, D. Jeison, A review on the state-of-the-art of physical/chemical and biological technologies for biogas upgrading, Rev. Environ. Sci. Biotechnol. 14 (2015) 727–759. doi:10.1007/s11157-015-9379-1.

[55]   H.H.J. Cox, M.A. Deshusses, Co-treatment of H2S and toluene in a biotrickling filter, Chem. Eng. J. 87 (2002) 101–110. doi:10.1016/S1385-8947(01)00222-4.

[56]   S. Ahmed, D. Papadias, R. Kumar, Fuel Quality in Fuel Cell Systems, Energy. (2010).

[57]   S.C. Popat, M. a. Deshusses, Biological removal of siloxanes from landfill and digester gases: Opportunities and challenges, Environ. Sci. Technol. 42 (2008) 8510–8515. doi:10.1021/es801320w.

[58]   F. Accettola, G.M. Guebitz, R. Schoeftner, Siloxane removal from biogas by biofiltration: Biodegradation studies, Clean Technol. Environ. Policy. 10 (2008) 211–218. doi:10.1007/s10098-007-0141-4.

[59]   Y. Li, W. Zhang, J. Xu, Siloxanes removal from biogas by a lab-scale biotrickling filter inoculated with Pseudomonas aeruginosa S240, J. Hazard. Mater. 275 (2014) 175–184. doi:10.1016/j.jhazmat.2014.05.008.

[60]   J. Wang, W. Zhang, J. Xu, Y. Li, X. Xu, Octamethylcyclotetrasiloxane removal using an isolated bacterial strain in the biotrickling filter, Biochem. Eng. J. 91 (2014) 46–52. doi:10.1016/j.bej.2014.07.003.

[61]   N. Ferrera-Lorenzo, E. Fuente, I. Suárez-Ruiz, B. Ruiz, Sustainable activated carbons of macroalgae waste from the Agar-Agar industry. Prospects as adsorbent for gas storage at high pressures, Chem. Eng. J. 250 (2014) 128–136. doi:10.1016/j.cej.2014.03.119.

[62]   R.R. Gil, R.P. Girón, M.S. Lozano, B. Ruiz, E. Fuente, Pyrolysis of biocollagenic wastes of vegetable tanning. Optimization and kinetic study, J. Anal. Appl. Pyrolysis. 98 (2012) 129–136. doi:10.1016/J.JAAP.2012.08.010.

[63]   J.. Figueiredo, M.F.. Pereira, M.M.. Freitas, J.J.. Órfão, Modification of the surface

chemistry of activated carbons, Carbon N. Y. 37 (1999) 1379–1389. doi:10.1016/S0008-6223(98)00333-9.

[64] S. Brunauer, L.S. Deming, W.E. Deming, E. Teller, On a Theory of the van der Waals Adsorption of Gases, J. Am. Chem. Soc. 62 (1940) 1723–1732. doi:10.1021/ja01864a025.

[65] S. Brunauer, P.H. Emmett, E. Teller, Adsorption of Gases in Multimolecular Layers, J. Am. Chem. Soc. 60 (1938) 309–319. doi:10.1021/ja01269a023.

[66] J.P. Olivier, W.B. Conklin, M. v. Szombathely, Determination of Pore Size Distribution from Density Functional Theory: A Comparison of Nitrogen and Argon Results, Stud. Surf. Sci. Catal. 87 (1994) 81–89. doi:10.1016/S0167-2991(08)63067-0.

[67] F. Stoeckli, L. Ballerini, Evolution of microporosity during activation of carbon, Fuel. 70 (1991) 557–559. doi:10.1016/0016-2361(91)90036-A.

[68] J. Jae, G.A. Tompsett, A.J. Foster, K.D. Hammond, S.M. Auerbach, R.F. Lobo, G.W. Huber, Investigation into the shape selectivity of zeolite catalysts for biomass conversion, J. Catal. 279 (2011) 257–268. doi:10.1016/j.jcat.2011.01.019.

[69] J.F. Richardson, Chemical Engineering Volume 2, Fifth Edition, (2002) 1232. http://www.amazon.com/Chemical-Engineering-Volume-Fifth-Edition/dp/0750644451.

[70] S. Varaprath, R.G. Lehmann, Speciation and Quantitation of Degradation Products of Silicones (Silane/Siloxane Diols) by Gas Chromatography-Mass Spectrometry and Stability of Dimethylsilanediol, J. Environ. Polym. Degrad. 5 (1997). https://link.springer.com/content/pdf/10.1007%252FBF02763565.pdf (accessed February 9, 2018).

[71] J.M. Estrada, N.J.R. (Bart) Kraakman, R. Lebrero, R. Muñoz, A sensitivity analysis of process design parameters, commodity prices and robustness on the economics of odour abatement technologies, Biotechnol. Adv. 30 (2012) 1354–1363. doi:10.1016/j.biotechadv.2012.02.010.

[72] J.M. Estrada, N.J.R.B. Kraakman, R. Muñoz, R. Lebrero, A comparative analysis of odour treatment technologies in wastewater treatment plants., Environ. Sci. Technol. 45 (2011) 1100–1106. doi:10.1021/es103478j.

[73] M.A. Tribe, R.L.W. Alpine, Scale economies and the "0.6 rule," Eng. Costs Prod. Econ. 10 (1986) 271–278. doi:10.1016/0167-188X(86)90053-4.

[74] R. Lebrero, A.C. Gondim, R. Pérez, P.A. García-Encina, R. Muñoz, Comparative assessment of a biofilter, a biotrickling filter and a hollow fiber membrane bioreactor for odor treatment in wastewater treatment plants, Water Res. 49 (2014) 339–350. doi:10.1016/j.watres.2013.09.055.

[75] M. Thommes, K. Kaneko, A. V. Neimark, J.P. Olivier, F. Rodriguez-Reinoso, J.

Rouquerol, K.S.W. Sing, Physisorption of gases, with special reference to the evaluation of surface area and pore size distribution (IUPAC Technical Report), Pure Appl. Chem. 87 (2015) 1051–1069. doi:10.1515/pac-2014-1117.

[76]   A.M. Puziy, J.M.D. Tascón, Adsorption by Phosphorus-Containing Carbons, in: Nov. Carbon Adsorbents, 2012: pp. 245–267. doi:10.1016/B978-0-08-097744-7.00008-9.

[77]   T.J. Bandosz, C.O. Ania, Surface chemistry of activated carbons and its characterization, in: Elsevier Ltd, 2006: pp. 159–229. doi:10.1016/S1573-4285(06)80013-X.

[78]   S. Haydar, C. Moreno-Castilla, M.A. Ferro-García, F. Carrasco-Marín, J. Rivera-Utrilla, A. Perrard, J.P. Joly, Regularities in the temperature-programmed desorption spectra of CO2 and CO from activated carbons, Carbon N. Y. 38 (2000) 1297–1308. doi:10.1016/S0008-6223(99)00256-0.

[79]   R. Krishna, Diffusion of binary mixtures in microporous materials: Overshoot and roll-up phenomena, Int. Commun. Heat Mass Transf. 27 (2000) 893–902. doi:10.1016/S0735-1933(00)00169-X.

[80]   H. Marsh, F. Rodríguez-Reinoso, Activated Carbon, 2006. doi:10.1016/B978-0-08-044463-5.X5013-4.

[81]   L. Li, P.A. Quinlivan, D.R.U. Knappe, Effects of activated carbon surface chemistry and pore structure on the adsorption of organic contaminants from aqueous solution, Carbon N. Y. 40 (2002) 2085–2100. doi:10.1016/S0008-6223(02)00069-6.

[82]   T. Karanfil, S.A. Dastgheib, Trichloroethylene adsorption by fibrous and granular activated carbons: Aqueous phase, gas phase, and water vapor adsorption studies, Environ. Sci. Technol. 38 (2004) 5834–5841. doi:10.1021/es0497936.

[83]   X. fei Tan, S. bo Liu, Y. guo Liu, Y. ling Gu, G. ming Zeng, X. jiang Hu, X. Wang, S. heng Liu, L. hua Jiang, Biochar as potential sustainable precursors for activated carbon production: Multiple applications in environmental protection and energy storage, Bioresour. Technol. 227 (2017) 359–372. doi:10.1016/j.biortech.2016.12.083.

[84]   B. Ruiz, N. Ferrera-Lorenzo, E. Fuente, Valorisation of lignocellulosic wastes from the candied chestnut industry. Sustainable activated carbons for environmental applications, J. Environ. Chem. Eng. 5 (2017) 1504–1515. doi:10.1016/j.jece.2017.02.028.

[85]   A. V. Bridgwater, Review of fast pyrolysis of biomass and product upgrading, Biomass and Bioenergy. 38 (2012) 68–94. doi:10.1016/j.biombioe.2011.01.048.

[86]   B. Ruiz, E. Ruisánchez, R.R. Gil, N. Ferrera-Lorenzo, M.S. Lozano, E. Fuente, Sustainable porous carbons from lignocellulosic wastes obtained from the extraction of tannins, Microporous Mesoporous Mater. 209 (2015) 23–29. doi:10.1016/j.micromeso.2014.09.004.

[87]   N. Ferrera-Lorenzo, E. Fuente, I. Suárez-Ruiz, B. Ruiz, KOH activated carbon from conventional and microwave heating system of a macroalgae waste from the Agar-Agar industry, Fuel Process. Technol. 121 (2014) 25–31. doi:10.1016/j.fuproc.2013.12.017.

[88]   F.R.-R. Harry Marsh, Activated Carbon, 1st ed., Elsevier, 2006. doi:10.1016/B978-0-08-044463-5.X5013-4.

[89]   S.A. Dastgheib, T. Karanfil, The effect of the physical and chemical characteristics of activated carbons on the adsorption energy and affinity coefficient of Dubinin equation, J. Colloid Interface Sci. 292 (2005) 312–321. doi:10.1016/j.jcis.2005.06.017.

[90]   J. Rodríguez-Mirasol, J. Bedia, T. Cordero, J. Rodríguez, Influence of water vapor on the adsorption of VOCs on lignin-based activated carbons, Sep. Sci. Technol. 40 (2005) 3113–3135. doi:10.1080/01496390500385277.

[91]   X. Yang, H. Yi, X. Tang, S. Zhao, Z. Yang, Y. Ma, T. Feng, X. Cui, Behaviors and kinetics of toluene adsorption-desorption on activated carbons with varying pore structure, J. Environ. Sci. (China). 67 (2018) 104–114. doi:10.1016/j.jes.2017.06.032.

[92]   M.A. Lillo-Ródenas, D. Cazorla-Amorós, A. Linares-Solano, Behaviour of activated carbons with different pore size distributions and surface oxygen groups for benzene and toluene adsorption at low concentrations, Carbon N. Y. 43 (2005) 1758–1767. doi:10.1016/j.carbon.2005.02.023.

[93]   Q. Qian, C. Gong, Z. Zhang, G. Yuan, Removal of VOCs by activated carbon microspheres derived from polymer: a comparative study, Adsorption. 21 (2015) 333–341. doi:10.1007/s10450-015-9673-9.

[94]   A. Cabrera-Codony, E. Santos-Clotas, C.O. Ania, M.J. Martín, Competitive siloxane adsorption in multicomponent gas streams for biogas upgrading, Chem. Eng. J. 344 (2018). doi:10.1016/j.cej.2018.03.131.

[95]   L. Malhautier, G. Quijano, M. Avezac, J. Rocher, J.L. Fanlo, Kinetic characterization of toluene biodegradation by Rhodococcus erythropolis: Towards a rationale for microflora enhancement in bioreactors devoted to air treatment, Chem. Eng. J. 247 (2014) 199–204. doi:10.1016/j.cej.2014.02.099.

[96]   G. Soreanu, Insights into siloxane removal from biogas in biotrickling filters via process mapping-based analysis, Chemosphere. 146 (2016) 539–546. doi:10.1016/j.chemosphere.2015.11.121.

[97]   R. Muñoz, T.S.O. Souza, L. Glittmann, R. Pérez, G. Quijano, Biological anoxic treatment of O2-free VOC emissions from the petrochemical industry: A proof of concept study, J. Hazard. Mater. 260 (2013) 442–450. doi:10.1016/j.jhazmat.2013.05.051.

[98]   I. Akmirza, C. Pascual, A. Carvajal, R. Pérez, R. Muñoz, R. Lebrero, Anoxic

biodegradation of BTEX in a biotrickling filter, Sci. Total Environ. 587–588 (2017) 457–465. doi:10.1016/j.scitotenv.2017.02.130.

[99]   F. Almenglo, M. Ramírez, J.M. Gómez, D. Cantero, Operational conditions for start-up and nitrate-feeding in an anoxic biotrickling filtration process at pilot scale, Chem. Eng. J. 285 (2016) 83–91. doi:10.1016/j.cej.2015.09.094.

[100]   E. Boada, E. Santos-Clotas, A. Cabrera-Codony, M.J. Martin, L. Bañeras, F. Gich, Isolation of bacterial species with potential capacity siloxane removal in biogas upgrading, in: 2nd Int. Conf. Bioresour. Technol. Bioenergy, Bioprod. Environ. Sustain., Sitges, Spain, 2018.

[101]   P. Rościszewski, J. Łukasiak, A. Dorosz, J. Galiński, M. Szponar, Biodegradation of polyorganosiloxanes, Macromol. Symp. 130 (1998) 337–346. doi:10.1002/masy.19981300129.

[102]   K.S.M. Rahman, T.J. Rahman, S. McClean, R. Marchant, I.M. Banat, Rhamnolipid biosurfactant production by strains of Pseudomonas aeruginosa using low-cost raw materials, Biotechnol. Prog. 18 (2002) 1277–1281. doi:10.1021/bp020071x.

[103]   E. Santos-Clotas, A. Cabrera-Codony, B. Ruiz, E. Fuente, M.J. Martín, Sewage biogas efficient purification by means of lignocellulosic waste-based activated carbons, Bioresour. Technol. 275 (2019) 207–215. doi:10.1016/j.biortech.2018.12.060.

[104]   R. Muñoz, S. Arriaga, S. Hernández, B. Guieysse, S. Revah, Enhanced hexane biodegradation in a two phase partitioning bioreactor: Overcoming pollutant transport limitations, Process Biochem. 41 (2006) 1614–1619. doi:10.1016/j.procbio.2006.03.007.

[105]   Ç. Kalkan, K. Yapsakli, B. Mertoglu, D. Tufan, A. Saatci, Evaluation of Biological Activated Carbon (BAC) process in wastewater treatment secondary ef fl uent for reclamation purposes, DES. 265 (2011) 266–273. doi:10.1016/j.desal.2010.07.060.

[106]   M.W. Reij, J.T.F. Keurentjes, S. Hartmans, Membrane bioreactors for waste gas treatment, J. Biotechnol. 59 (1998) 155–167.

[107]   K. Barbusinski, K. Kalemba, D. Kasperczyk, K. Urbaniec, V. Kozik, Biological methods for odor treatment e A review costs Thermal oxidation Catalytic oxidation Chemical scrubbing Adsorption Bioscrubbing Chemical neutralisation Biofiltration, J. Clean. Prod. 152 (2017) 223–241. doi:10.1016/j.jclepro.2017.03.093.

[108]   A. Kumar, J. Dewulf, M. Luvsanjamba, H. Van Langenhove, Continuous operation of membrane bioreactor treating toluene vapors by Burkholderia vietnamiensis G4, Chem. Eng. J. (2008). doi:10.1016/j.cej.2007.09.039.

[109]   S. Rasi, A. Veijanen, J. Rintala, Trace compounds of biogas from different biogas production plants, Energy. 32 (2007) 1375–1380. doi:10.1016/j.energy.2006.10.018.

[110]   E. Santos-Clotas, A. Cabrera-Codony, A. Castillo, M.J. Martín, M. Poch, H. Monclús,

Environmental Decision Support System for Biogas Upgrading to Feasible Fuel, Energies. 12 (2019) 1546. doi:10.3390/en12081546.

[111]   F. Hosoglu, M.W. Fitch, Abatement of synthetic landfill gas including limonene by biotrickling filter and membrane biofiltration, J. Environ. Sci. Heal. - Part A Toxic/Hazardous Subst. Environ. Eng. 47 (2012) 1065–1072. doi:10.1080/10934529.2012.667338.

[112]   A. Cabrera-Codony, R. Gonzalez-Olmos, M.J. Martín, Regeneration of siloxane-exhausted activated carbon by advanced oxidation processes, J. Hazard. Mater. (2015). doi:10.1016/j.jhazmat.2014.11.053.

[113]   A. Cabrera-Codony, M.A. Montes-Morán, M. Sánchez-Polo, M.J. Martín, R. Gonzalez-Olmos, Biogas upgrading: Optimal activated carbon properties for siloxane removal, Environ. Sci. Technol. 48 (2014). doi:10.1021/es501274a.

[114]   A. Cabrera-Codony, A. Georgi, R. Gonzalez-Olmos, H. Valdés, M.J. Martín, Zeolites as recyclable adsorbents/catalysts for biogas upgrading: Removal of octamethylcyclotetrasiloxane, Chem. Eng. J. 307 (2017) 820–827. doi:10.1016/j.cej.2016.09.017.

[115]   Suhas, P.J.M. Carrott, M.M.L. Ribeiro Carrott, Lignin - from natural adsorbent to activated carbon: A review, Bioresour. Technol. 98 (2007) 2301–2312. doi:10.1016/j.biortech.2006.08.008.

[116]   B. Cagnon, X. Py, A. Guillot, F. Stoeckli, G. Chambat, Contributions of hemicellulose, cellulose and lignin to the mass and the porous properties of chars and steam activated carbons from various lignocellulosic precursors, Bioresour. Technol. 100 (2009) 292–298. doi:10.1016/j.biortech.2008.06.009.

Chapter 12

Appendices

Molecular structure of the target VOCs and siloxanes
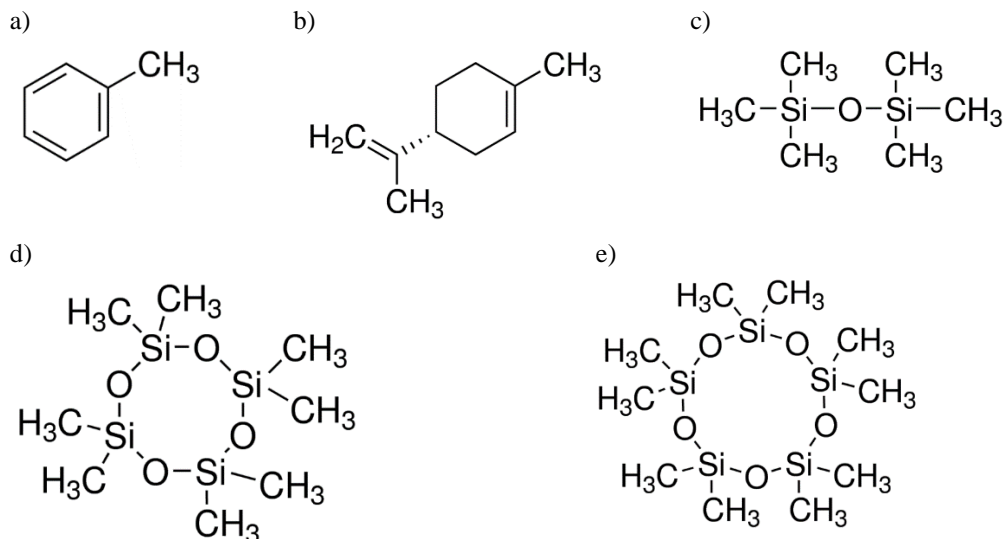
Figure 12.1 2D molecular structure of a) toluene, b) limonene, c) L2, d) D4 and e) D5
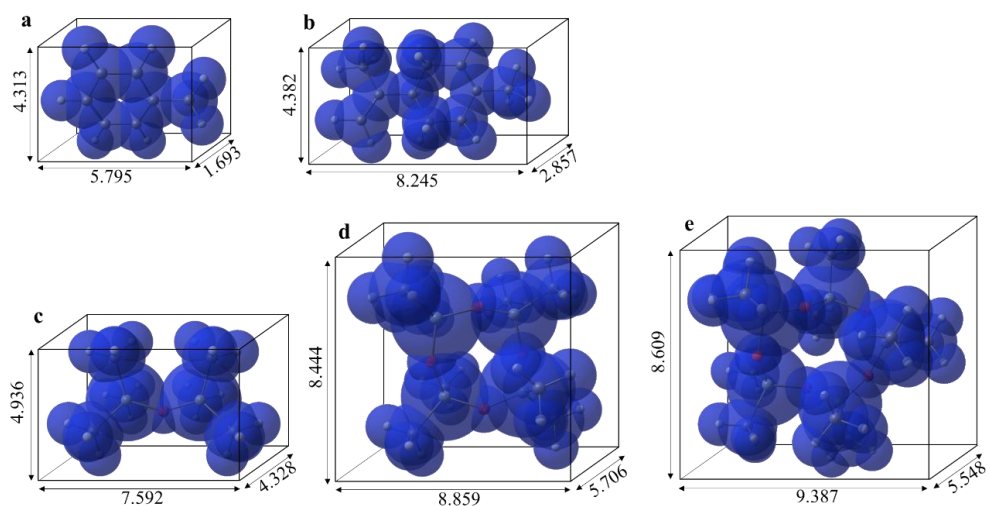
Figure 12.2 3D molecular structure of a) toluene, b) limonene, c) L2, d) D4 and e) D5. Length measurements expressed in Å (1.2 Å corresponding to hydrogen van der Waals radium must be added in each extreme).

Textural characterization of the ACs in Chapter 5
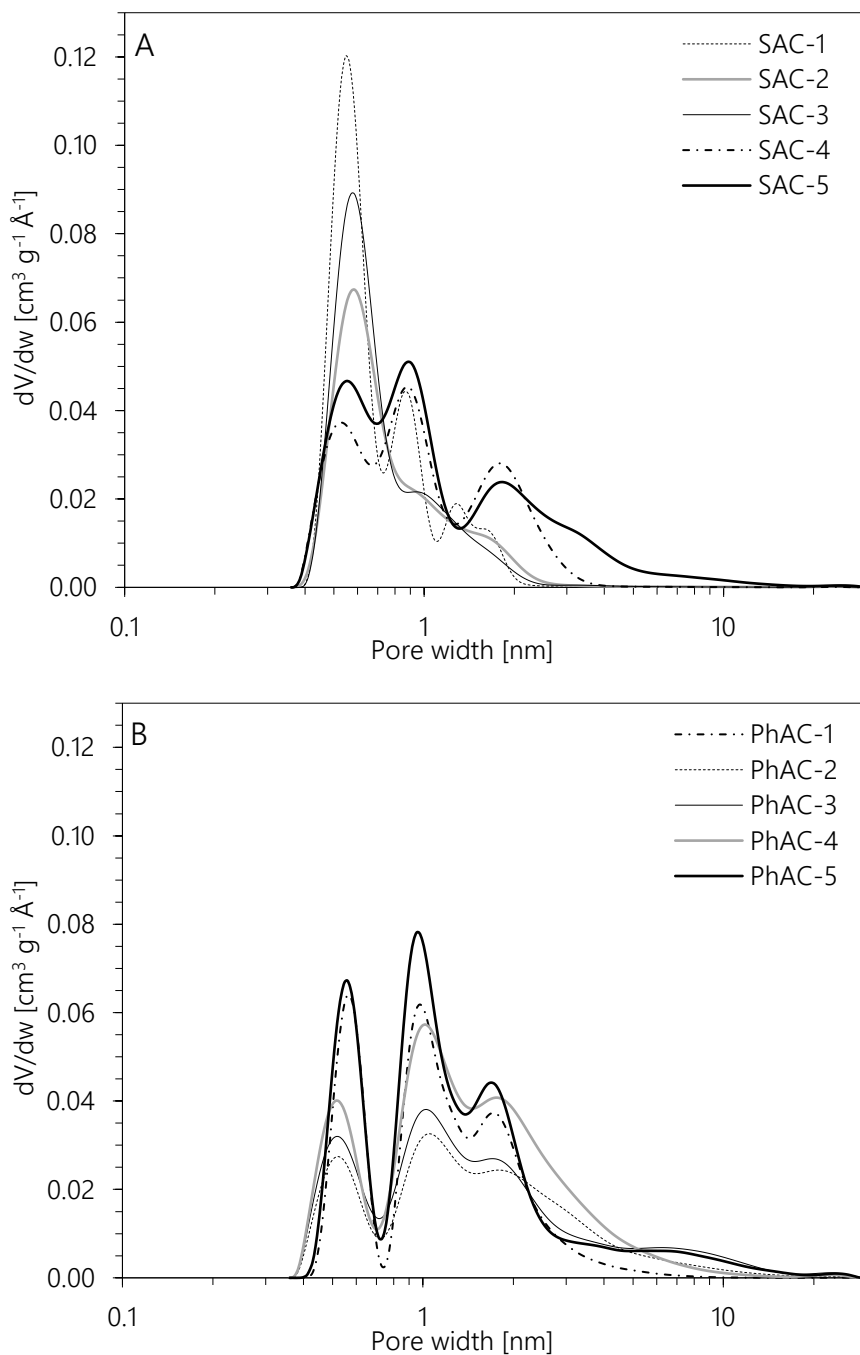
Figure 12.3 Pore size distribution: a) steam-AC, and b) H_3PO_4-AC
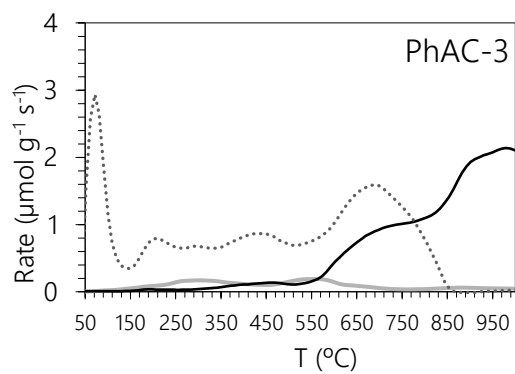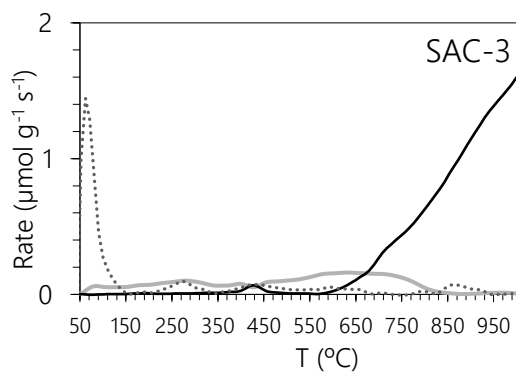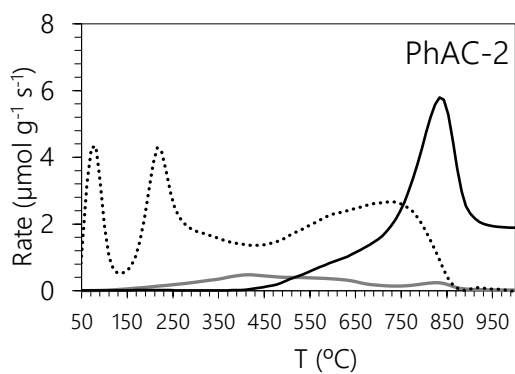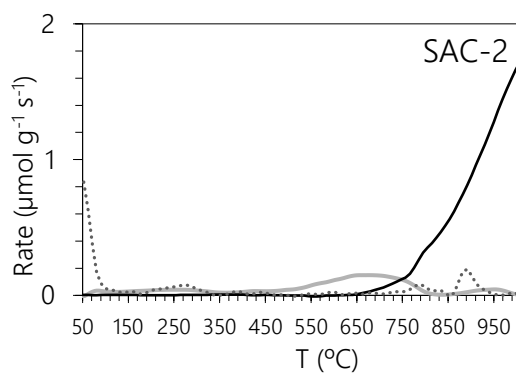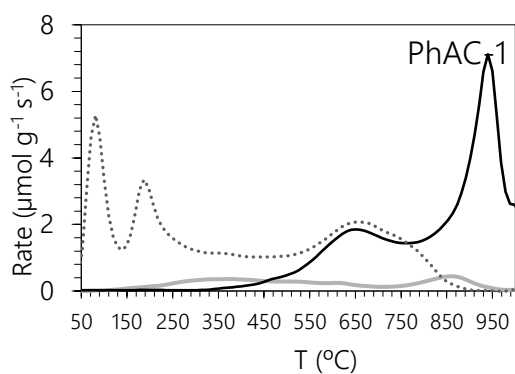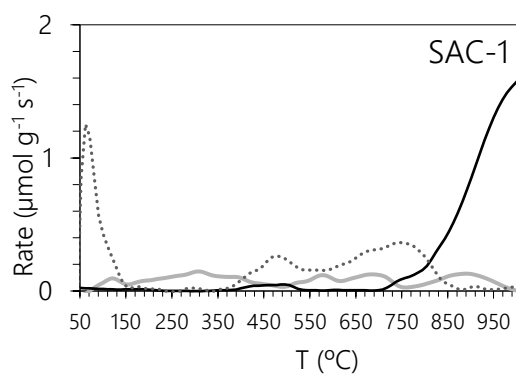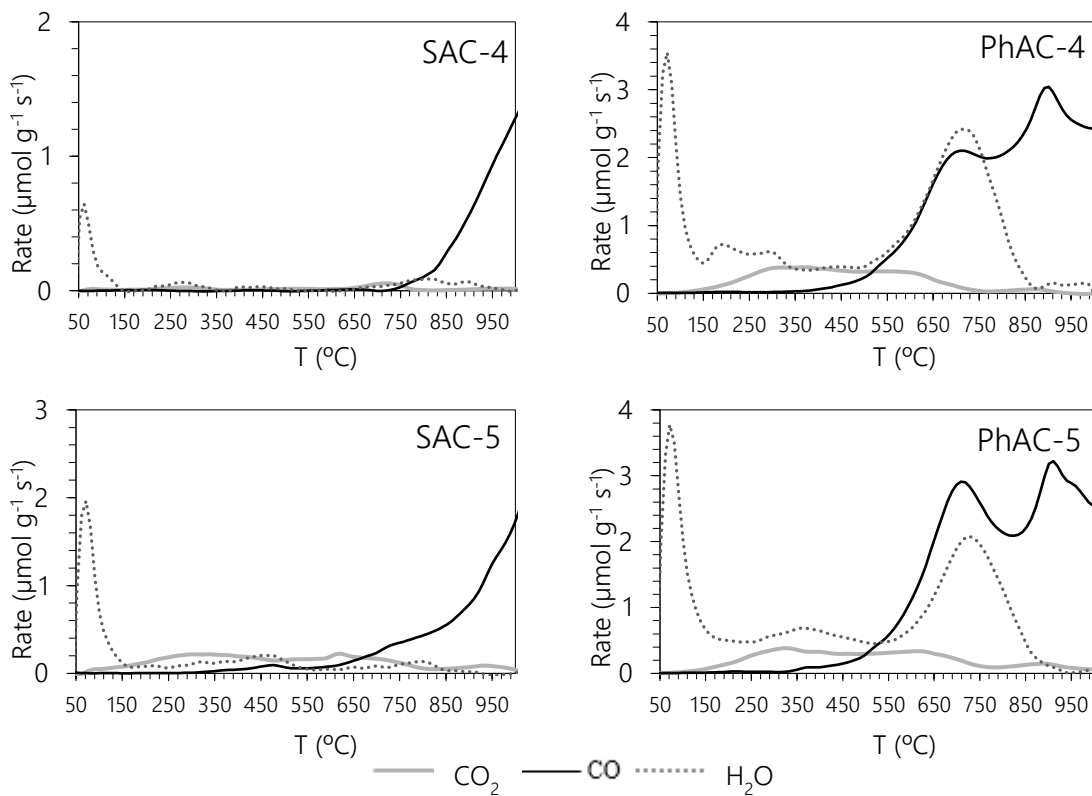
Figure 12.4 TG-MS desorption profiles of CO_2, CO and H_2O

Adsorption breakthrough curves
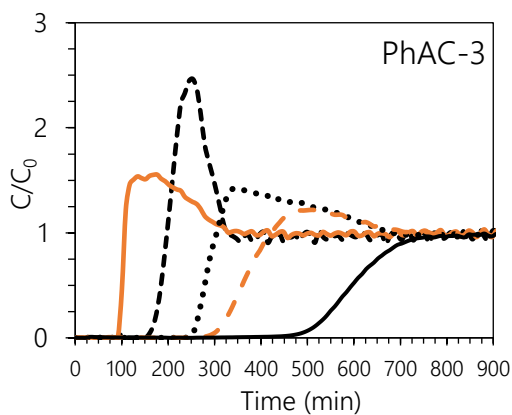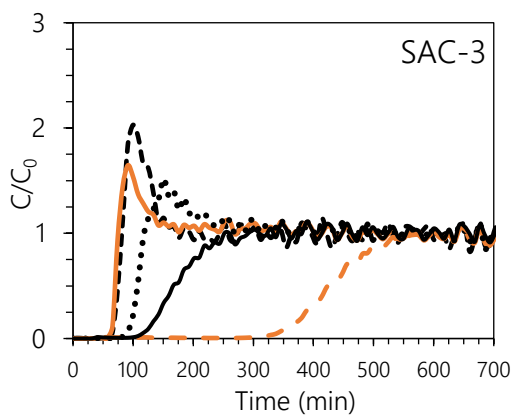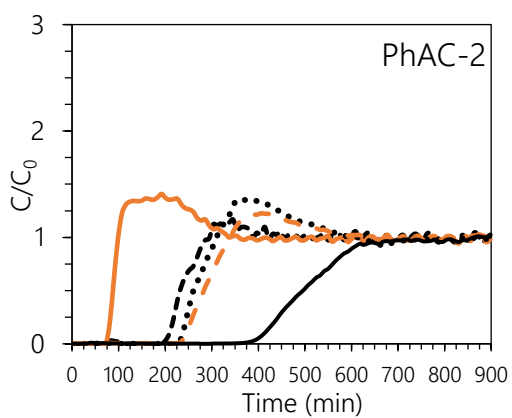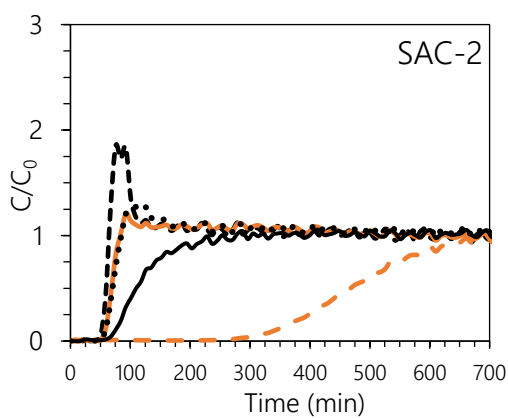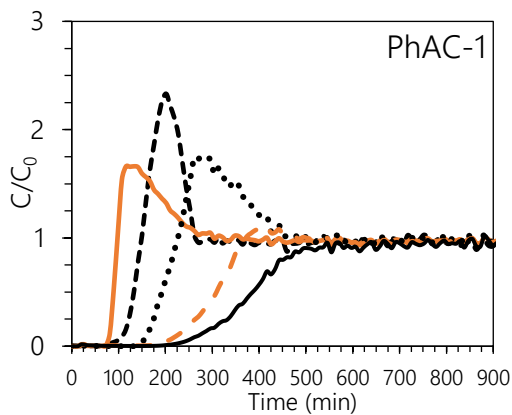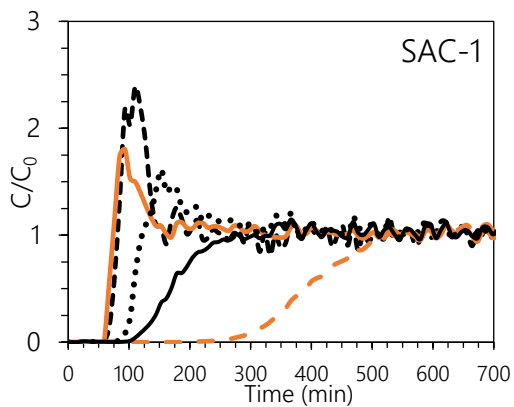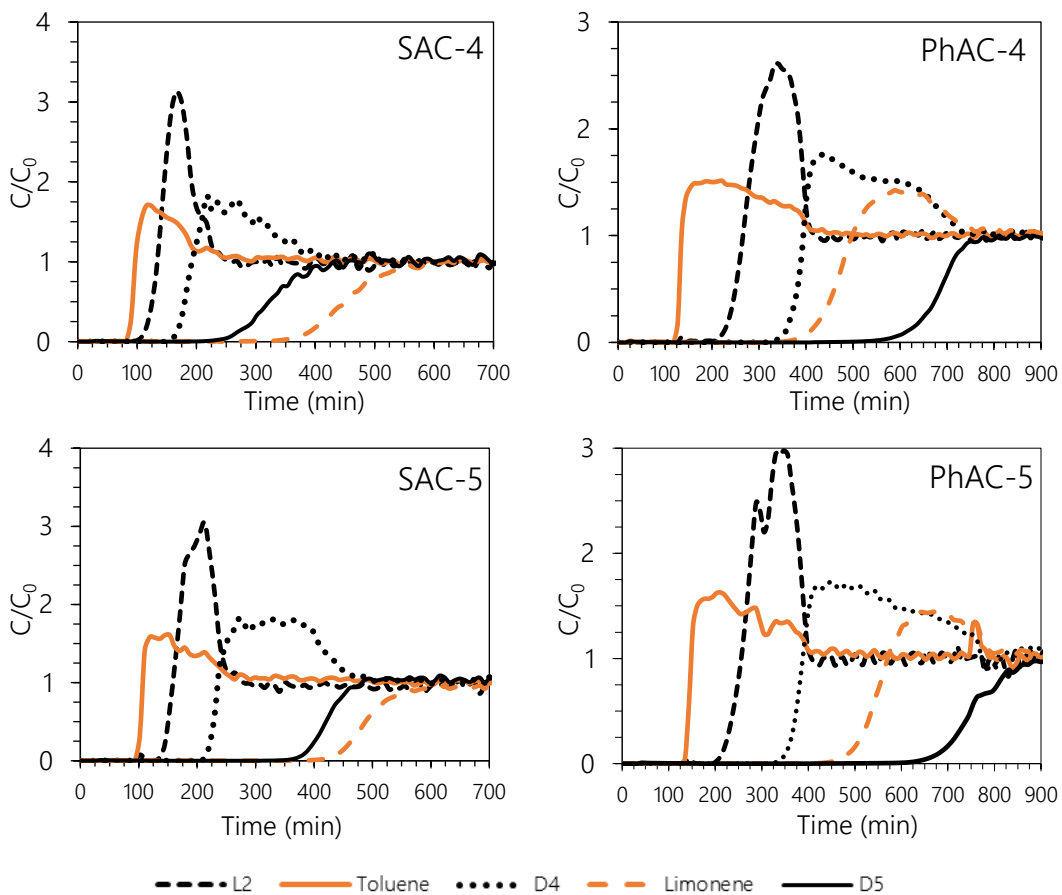
Figure 12.5 Multicomponent dynamic adsorption breakthrough curves obtained for the set of activated carbons (dry gas matrix).
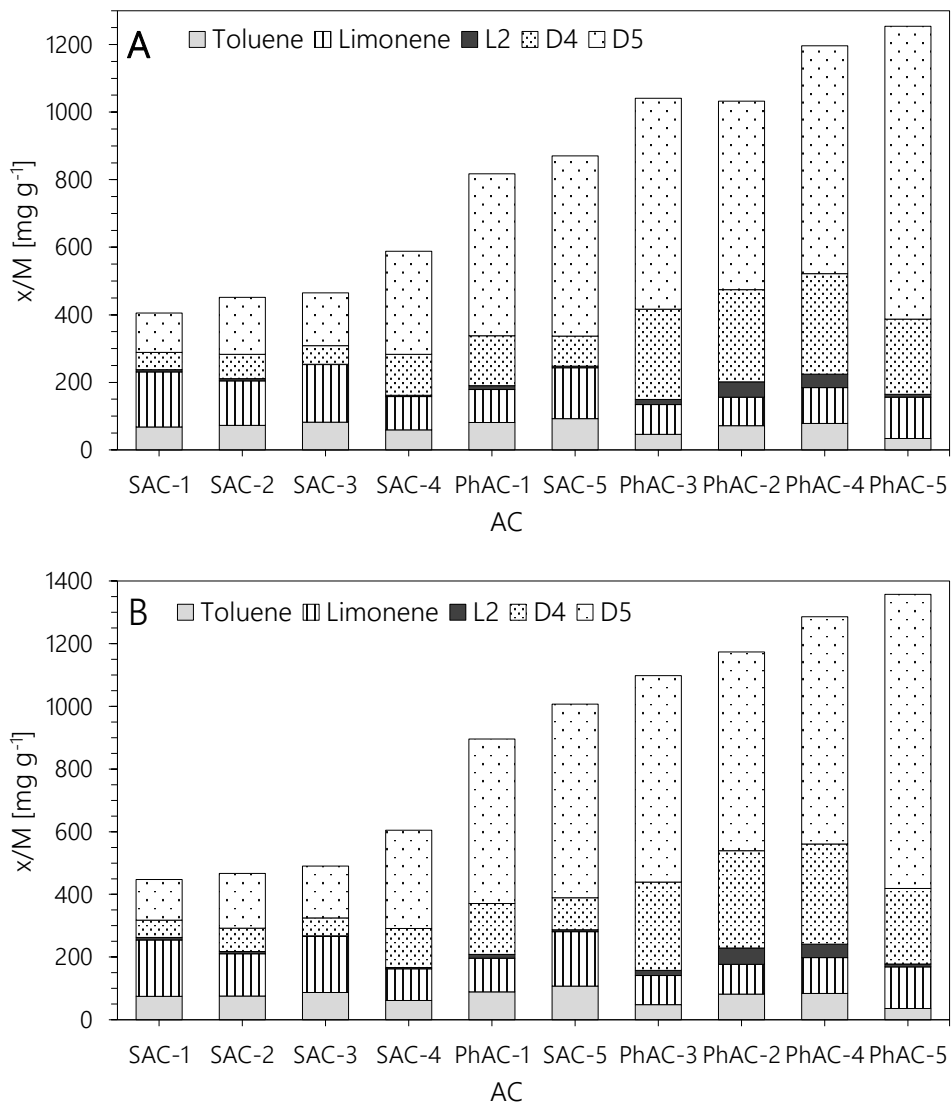
Figure 12.6 Adsorption capacities reported in multicomponent dynamic adsorption tests in dry matrix gas test for the 10 ACs considered, A) Mass of AC considered as received and B) AC mass normalized on dry-basis.
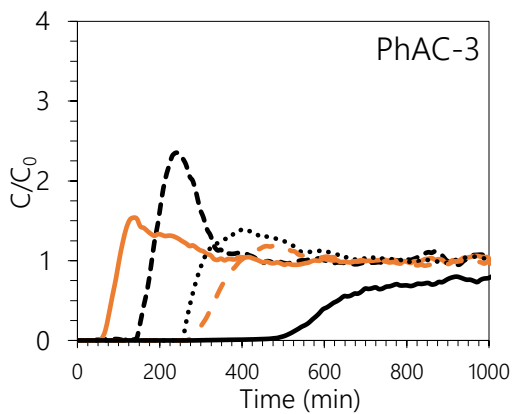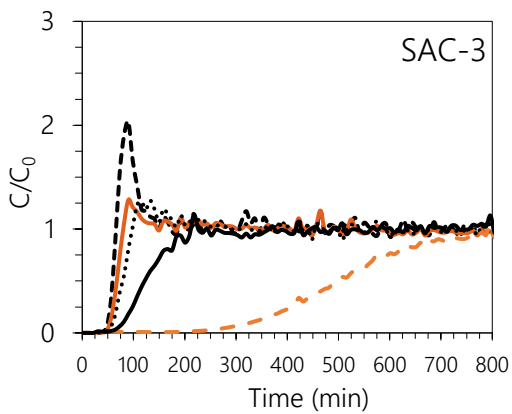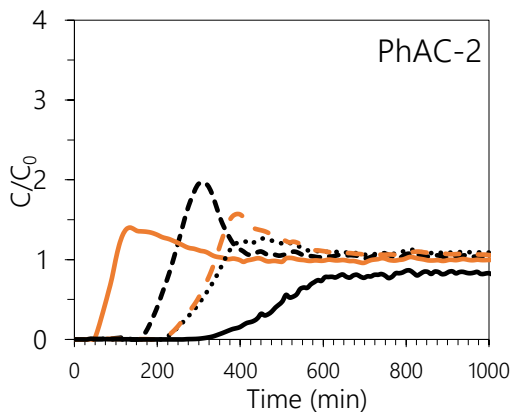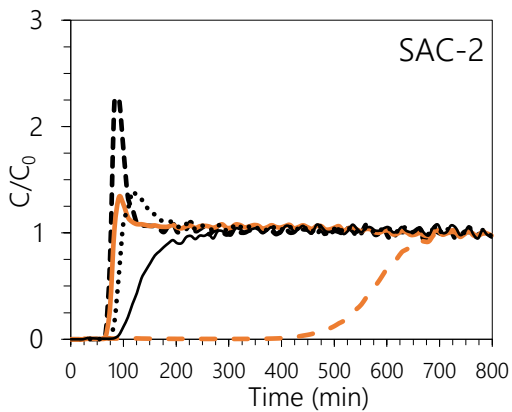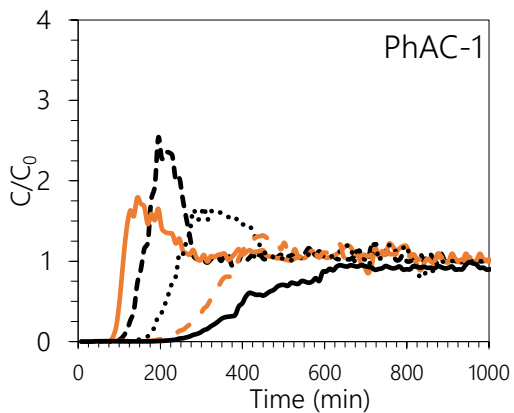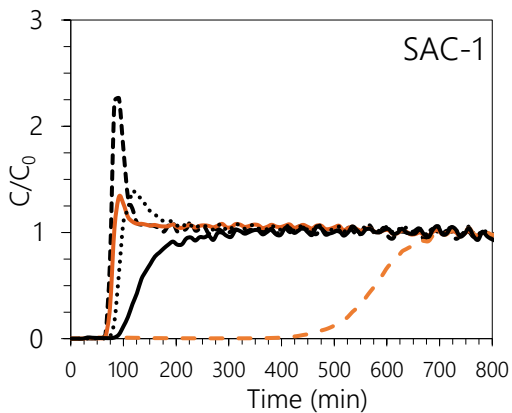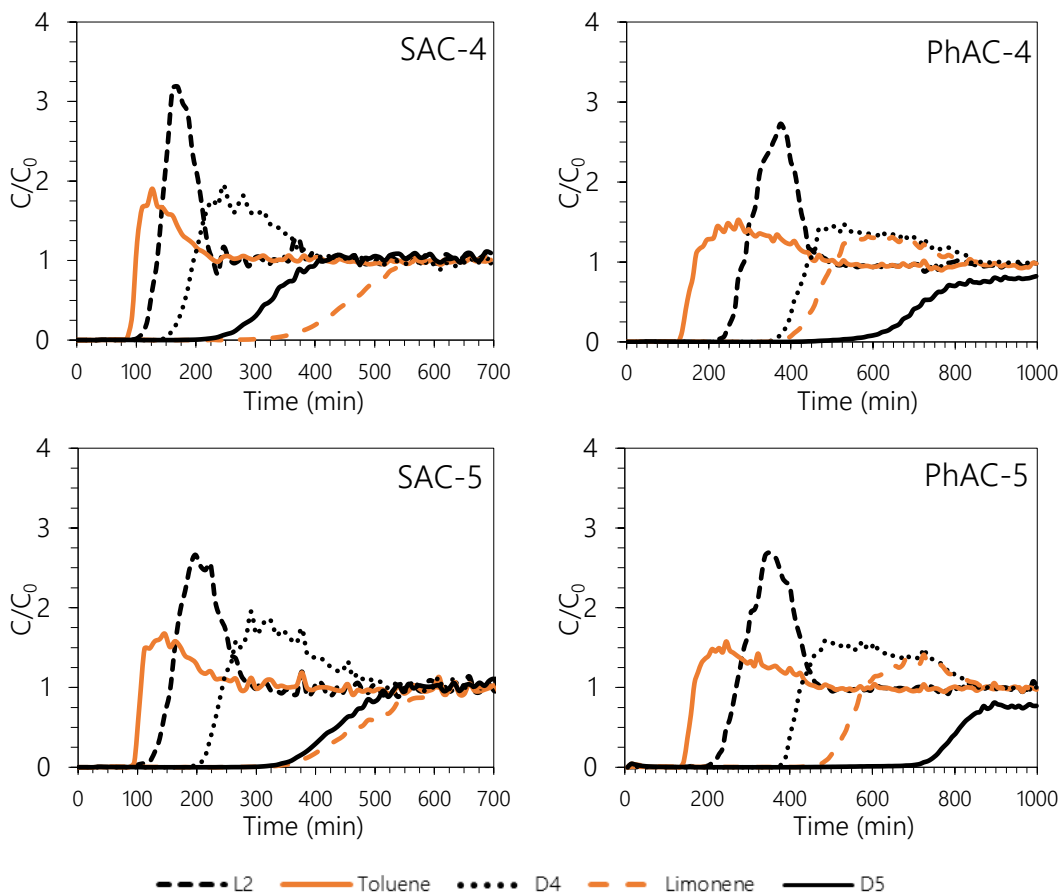
Figure 12.7 Multicomponent dynamic adsorption breakthrough curves obtained for the set ACs (wet gas matrix).
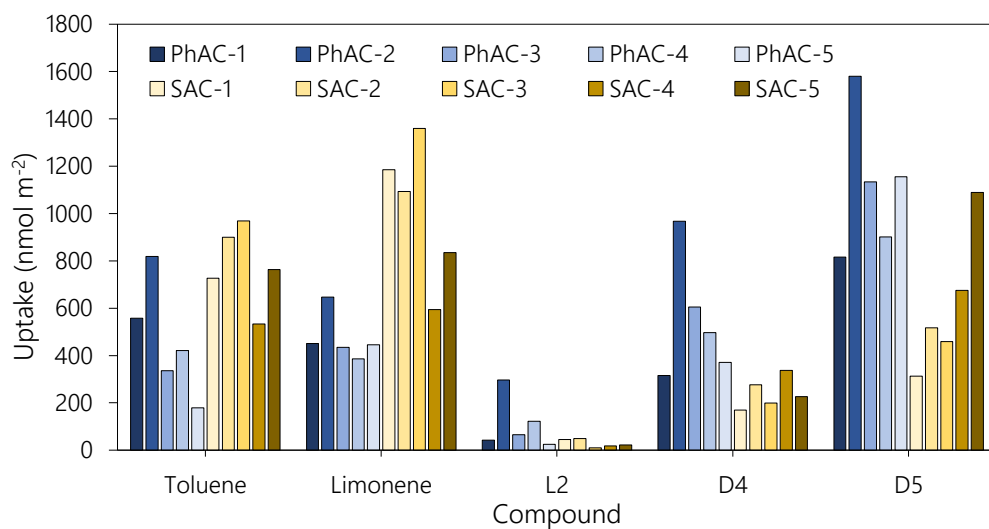
Figure 12.8 Amount adsorbed in each AC at bed exhaustion, expressed as nmols per m^2 of surface considering the BET-specific surface area determined (Dry condition adsorption tests, considering AC net mass).

Relationship between siloxanes adsorption and textural parameters
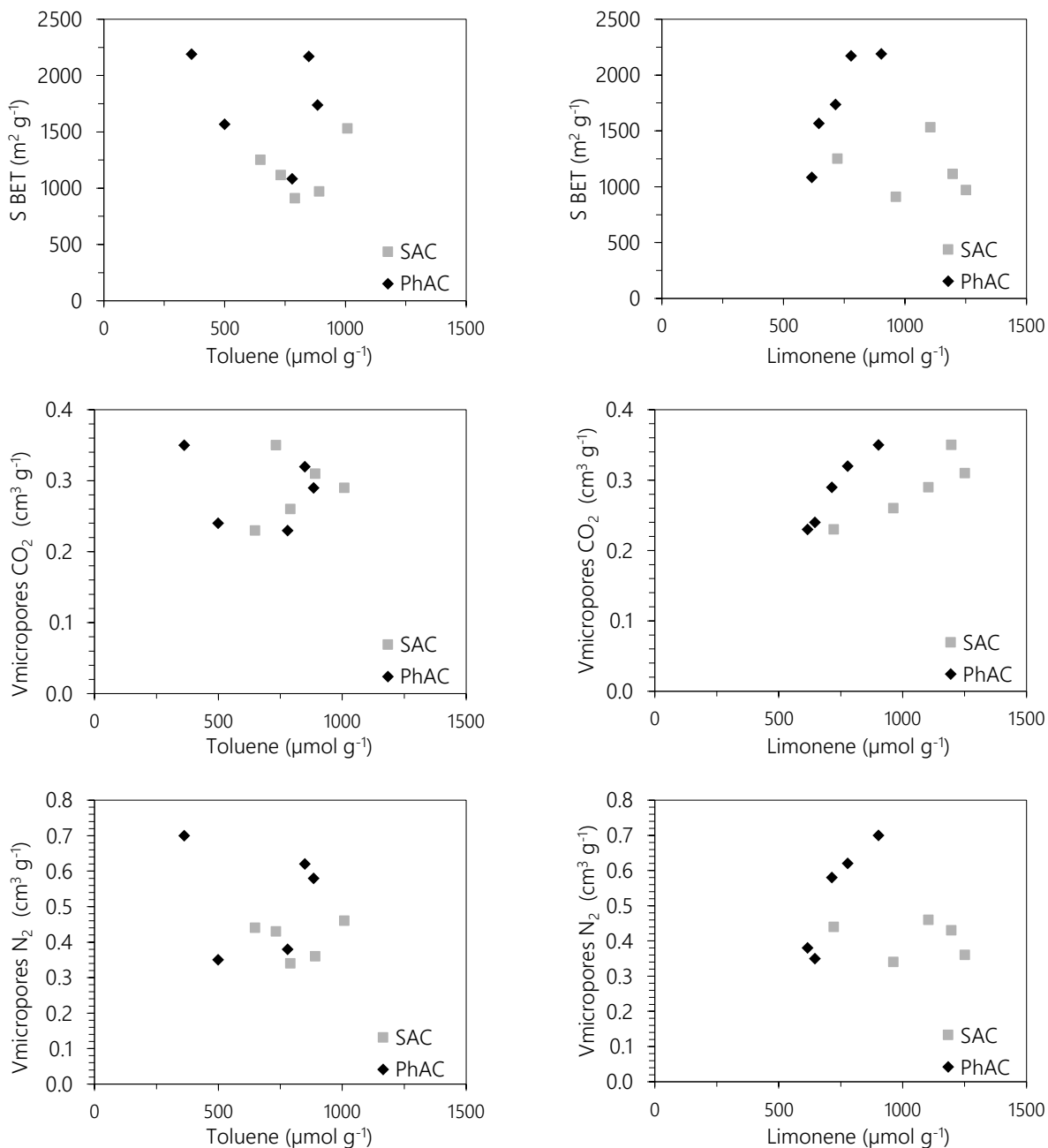
Figure 12.9 Continues
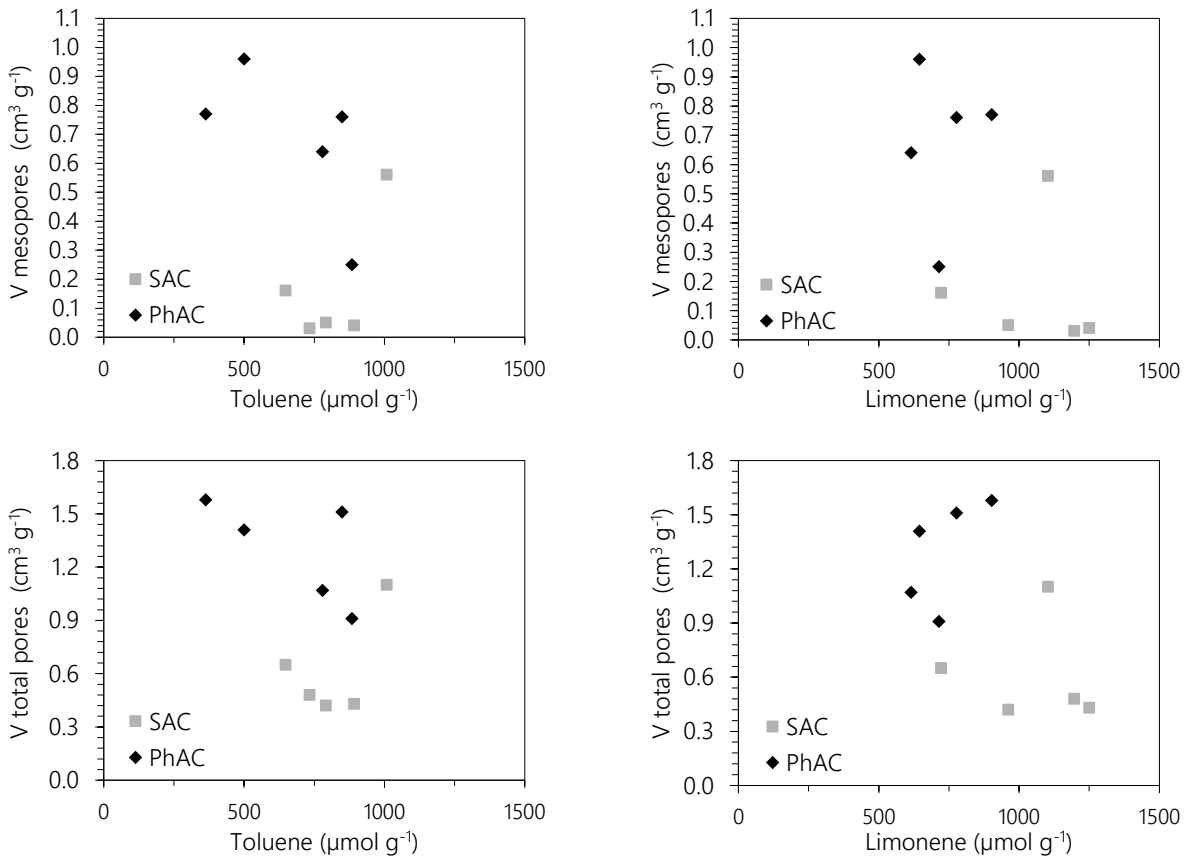
Figure 12.9 Relation between adsorption capacity of toluene and limonene (reported at bed exhaustion) with the textural properties of the ACs
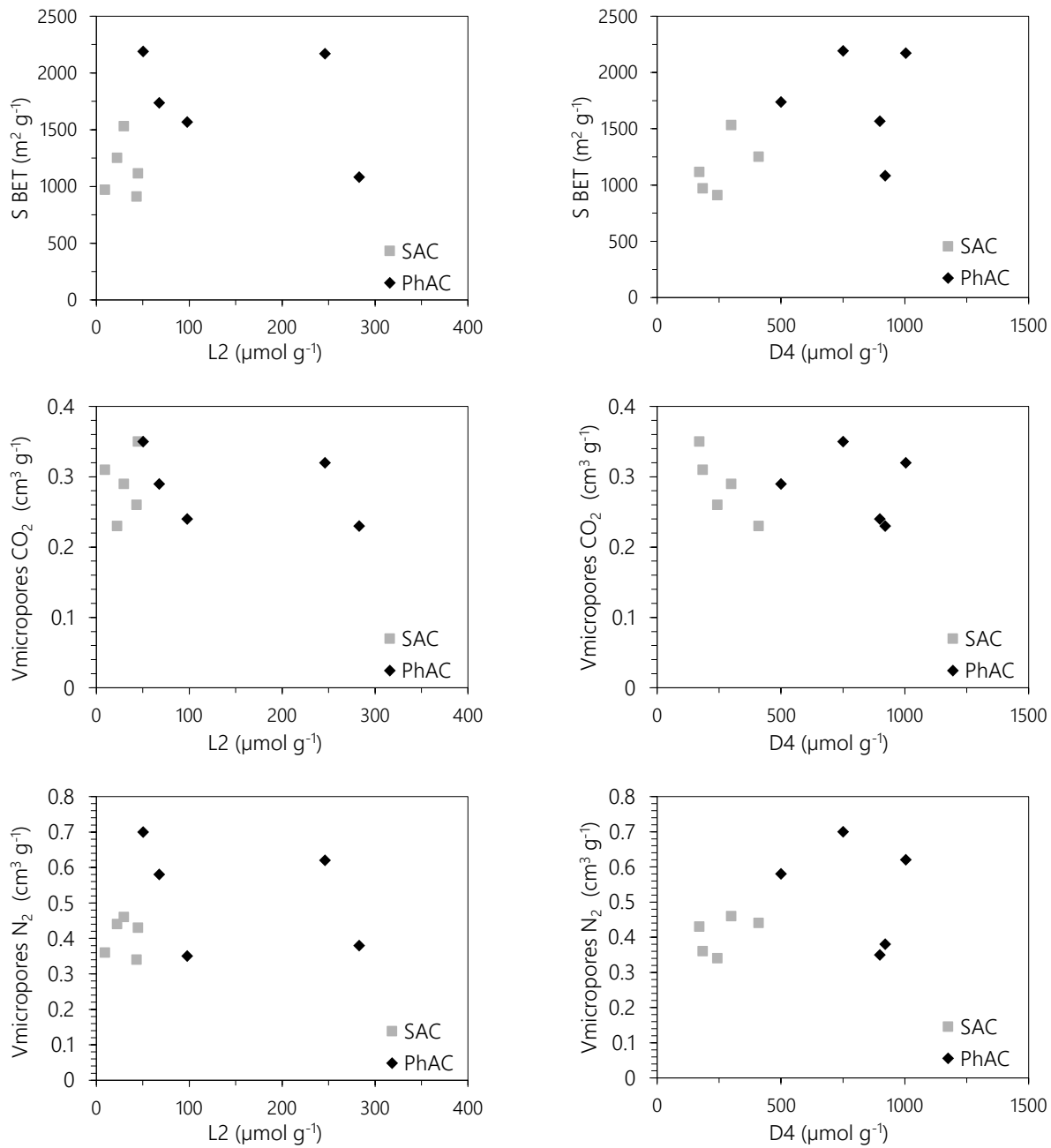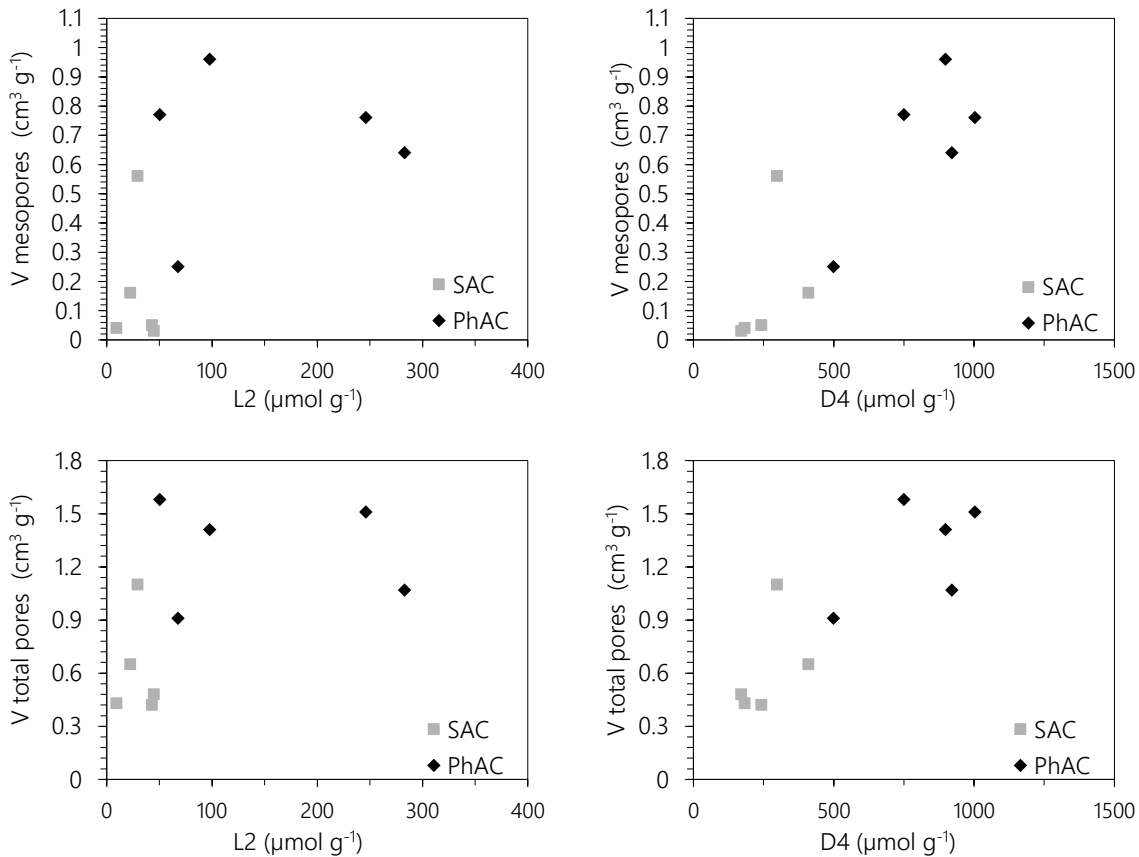
Figure 12.10 Continues

Figure 12.10 Relation between adsorption capacity of L2 and D4 (reported at bed exhaustion) with the textural properties of the ACs
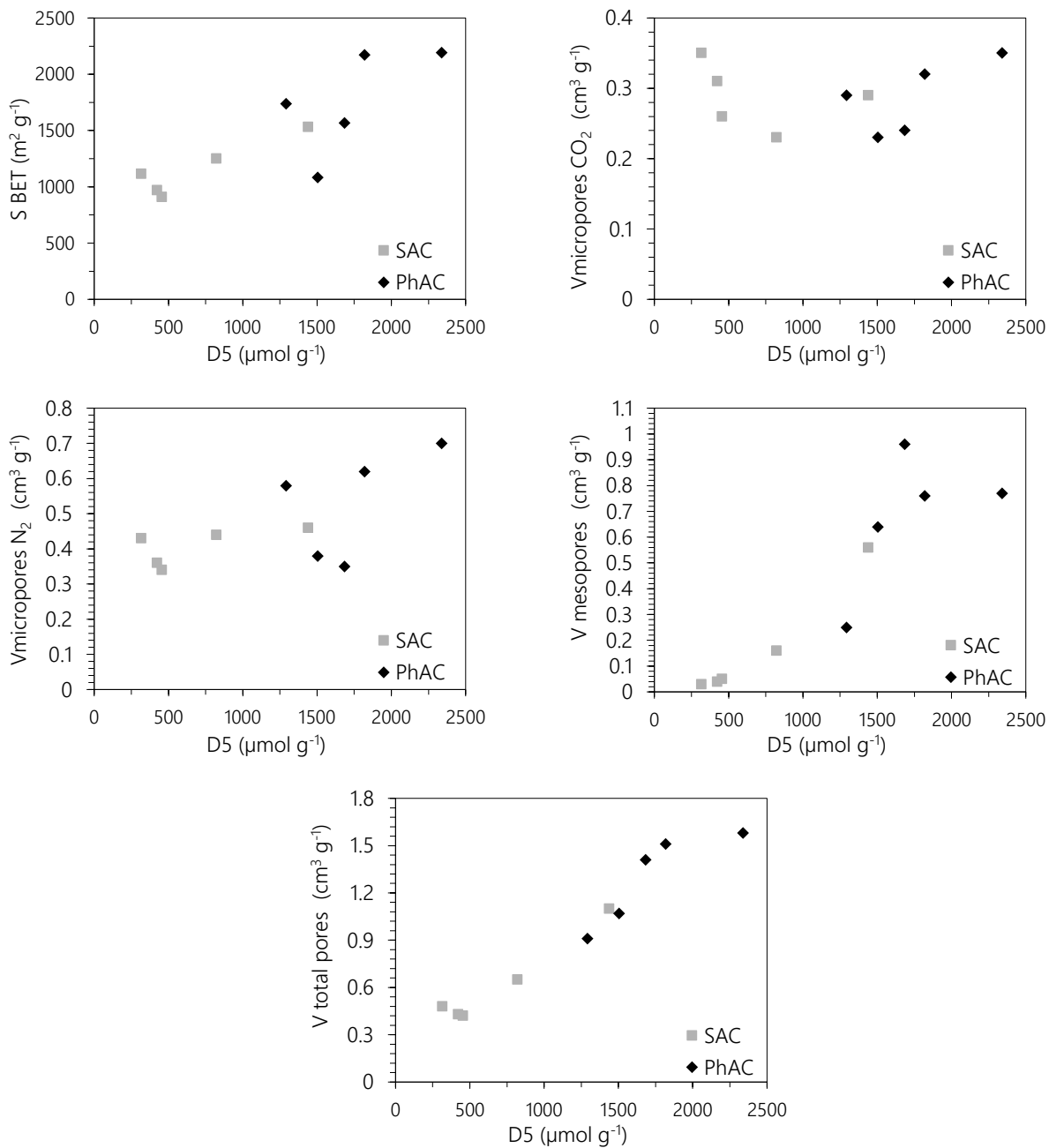
Figure 12.11 Relation between adsorption capacity of D5 (reported at bed exhaustion) with the textural properties of the ACs
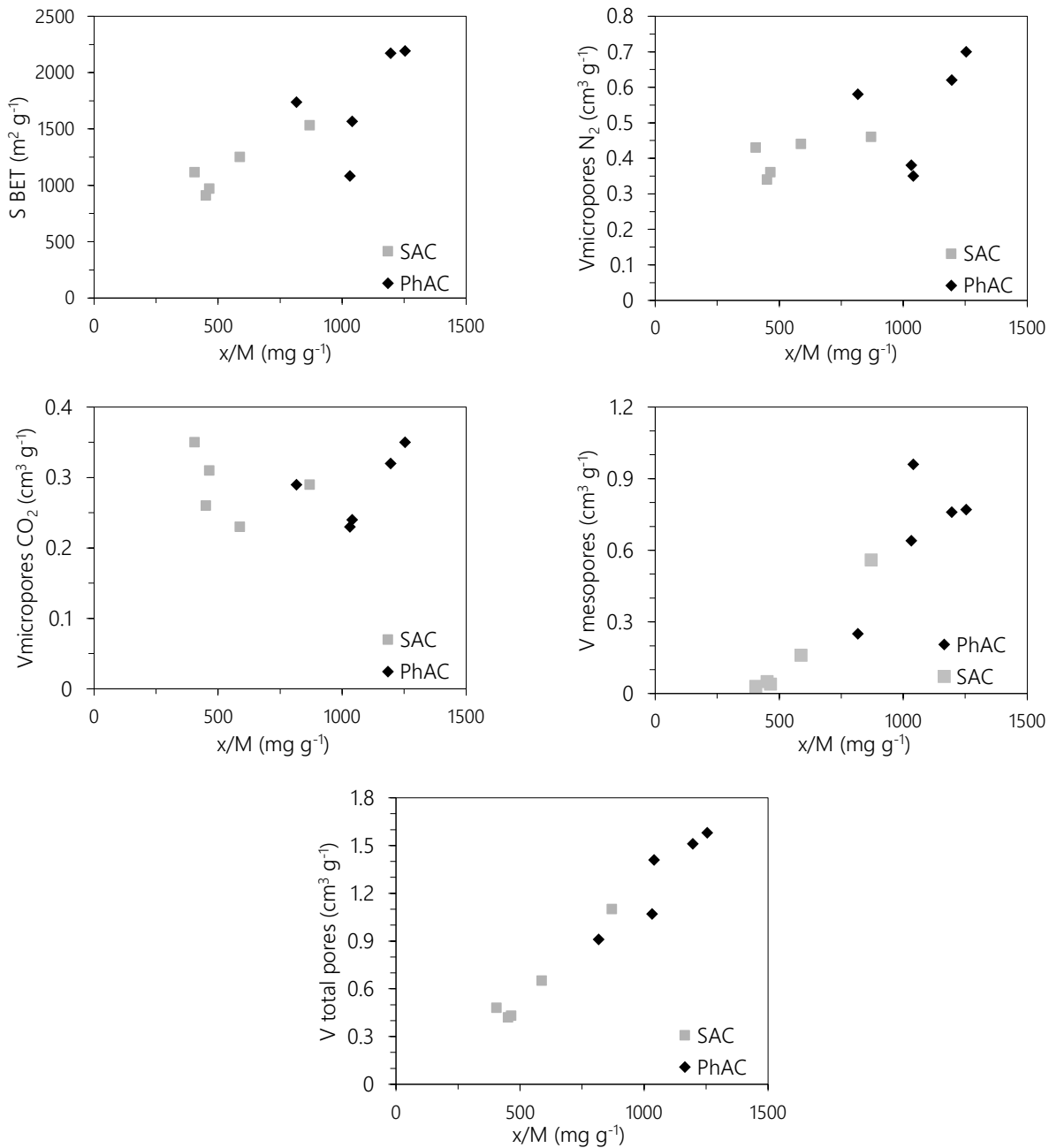
Figure 12.12 Relation between adsorption capacity (totality of compounds reported at bed exhaustion) with the textural properties of the ACs.